Natti S. Rao Günter Schumacher

Design Formulas for Plastics Engineers

2nd Edition

The Authors:

Dr.-Ing. Natti S. Rao, 327 Route 216, Ghent, NY 12075, USA

Dr. Günter Schumacher, Am Bollerweg 6, 75045 Walzbachtal-Jöhlingen, Germany

Distributed in the USA and in Canada by Hanser Gardner Publications, Inc.

6915 Valley Avenue, Cincinnati, Ohio 45244-3029, USA

Fax: (513) 527-8801

Phone: (513) 527-8977 or 1-800-950-8977

Internet: http://www.hansergardner.com

Distributed in all other countries by Carl Hanser Verlag

Call Hallsel Vellag

Postfach 86 04 20, 81631 München, Germany

Fax: +49 (89) 98 48 09

Internet: http://www.hanser.de

The use of general descriptive names, trademarks, etc., in this publication, even if the former are not especially identified, is not to be taken as a sign that such names, as understood by the Trade Marks and Merchandise Marks Act, may accordingly be used freely by anyone.

While the advice and information in this book are believed to be true and accurate at the date of going to press, neither the authors nor the editors nor the publisher can accept any legal responsibility for any errors or omissions that may be made. The publisher makes no warranty, express or implied, with respect to the material contained herein.

Library of Congress Cataloging-in-Publication Data

Rao, Natti S.

Design formulas for plastics engineers.-- 2nd ed. / Natti S. Rao, Günter Schumacher.

p. cm.

Includes bibliographical references and index.

ISBN 1-56990-370-0 (pbk.)

1. Plastics. I. Schumacher, Günter. II. Title.

TP1140.R36 2004

668.4--dc22

2004017192

Bibliografische Information Der Deutschen Bibliothek

Die Deutsche Bibliothek verzeichnet diese Publikation in der DeutschenNationalbibliografie;

detaillierte bibliografische Daten sind im Internetüber < http://dnb.ddb.de> abrufbar.

ISBN 3-446-22674-5

All rights reserved. No part of this book may be reproduced or transmitted in any form or by any means, electronic or mechanical, including photocopying or by any information storage and retrieval system, without permission in wirting from the publisher.

© Carl Hanser Verlag, Munich 2004
Production Management: Oswald Immel
Typeset by Manuela Treindl, Laaber, Germany
Coverconcept: Marc Müller-Bremer, Rebranding, München, Germany

Coverdesign: MCP · Susanne Kraus GbR, Holzkirchen, Germany

Printed and bound by Druckhaus "Thomas Müntzer", Bad Langensalza, Germany

Preface

Today, designing of machines and dies is done to a large extent with the help of computer programs. However, the predictions of theses programs do not always agree with the practical results, so that there is a need to improve the underlying mathematical models. Therefore, knowledge of the formulas, on which the models are based and the limits of their applicability is necessary if one wants to develop a new program or improve one already in use.

Often the plastics engineer has to deal with different fields of engineering. The search for the appropriate equations in the various fields concerned can be time-consuming. A collection of formulas from the relevant fields and their applications, as given in this book, make it easier to write one's own program or to make changes in an existing program to obtain a better fit with the experiments.

It is often the case that different equations are given in the literature on plastics technology for one and the same target quantity. The practicing engineer is sometimes at a loss judging the validity of the equations he encounters in the literature.

During his long years of activity as an R&D engineer in the polymer field at the BASF AG and other companies, Natti Rao tested many formulas published while solving practical problems. This book presents a summary of the important formulas and their applications, which Natti Rao, in cooperation with the well-known resin and machine manufacturers, successfully applied to solve design and processing problems.

The formulas are classified according to the fields, rheology, thermodynamics, heat transfer, and part design. Each chapter covers the relevant relations with worked-out examples. A separate chapter is devoted to the practical equations for designing extrusion and injection molding equipment with detailed examples in metric units.

In addition, this work contains new, straightforward, practical relationships that have been developed and tested in recent years in solving design problems in the area of extrusion and injection molding.

The topic of polymer machine design has been dealt with in several books. However, in these books the know-how was presented in a way that the vast majority of plastics engineers cannot easily apply it to the problems in their day-to-day work. By means of thoroughly worked-out, practical examples this book elucidates the computational background of designing polymer machinery in a manner which every engineer can understand and easily apply in daily practice.

We wish to express our thanks to our colleagues at the University of Massachusetts at Lowell, USA, for fruitful discussions. Our thanks are also due to Faculty Innovation Center of the University of Austin, Texas, USA, for help in preparing the manuscript.

Austin, USA Karlsruhe, Germany Natti S. Rao, Ph. D. Günter Schumacher, Ph. D.

Contents

Pre	etac	e		V
1.	For	mulas	s of Rheology	1
	1.1	Ideal	Solids	1
		1.1.1	Hooke's Law	3
	1.2	Newto	onian Fluids	3
	1.3	Form	ulas for Viscous Shear Flow of Polymer Melts	4
		1.3.1	Apparent Shear Rate	5
		1.3.2	Entrance Loss	5
		1.3.3	True Shear Stress	6
		1.3.4	Apparent Viscosity	7
		1.3.5	True Shear Rate	7
		1.3.6	True Viscosity	8
		1.3.7	Empirical Formulas for Apparent Viscosity	8
			1.3.7.1 Hyperbolic Function of Prandtl and Eyring	8
			1.3.7.2 Power Law of Ostwald and de Waele	9
			1.3.7.3 Muenstedt's Polynomial	11
			1.3.7.4 Carreau's Viscosity Equation	14
			1.3.7.5 Klein's Viscosity Formula	16
			1.3.7.6 Effect of Pressure on Viscosity	16
			1.3.7.7 Dependence of Viscosity on Molecular	
			Weight	17
			1.3.7.8 Viscosity of Two Component Mixtures	18

viii Contents

	1.4	Visco	elastic Behavior of Polymers	18
		1.4.1	Shear	19
			1.4.1.1 Linear Viscoelastic Behavior	19
			1.4.1.2 Nonlinear Viscoelastic Behavior	23
		1.4.2	Uniaxial Tension	25
			1.4.2.1 Linear Viscoelastic Behavior	25
			1.4.2.2 Nonlinear Viscoelastic Behavior	28
		1.4.3	Maxwell Model	29
		1.4.4	Practical Formulas for Die Swell and Extensional	
			Flow	31
2.	The	ermod	lynamic Properties of Polymers	35
	2.1	Speci	fic Volume	35
	2.2	Speci	fic Heat	36
	2.3	Entha	ılpy	38
	2.4	Thern	nal Conductivity	40
3.	For	mulas	s of Heat Transfer	43
	3.1	Stead	ly State Conduction	43
		3.1.1	Plane Wall	43
		3.1.2	Cylinder	44
		3.1.3	Hollow Sphere	45
		3.1.4	Sphere	45
		3.1.5	Heat Conduction in Composite Walls	46
			Overall Heat Transfer through Composite	
			Walls	49
	3.2	Trans	ient State Conduction	50
		3.2.1	Temperature Distribution in One-Dimensional Solids	51
		3 2 2	Thermal Contact Temperature	57
		J.Z.Z	THETHIAL COHIACI TEHIPELATULE	<i>31</i>

				Co	ontents	İX
	3.3	Heat (Conducti	on with Dissipation		59
	3.4	Dimer	nsionless	Groups		60
		3.4.1	Physica	al Meaning of Dimensionless Groups		61
	3.5	Heat [*]	Transfer	by Convection		62
	3.6	Heat ⁷	Transfer	by Radiation		64
	3.7	Dielec	ctric Hea	ting		67
	3.8	Fick's	Law of [Diffusion		69
		3.8.1	Permea	ability		69
		3.8.2	Absorp	tion and Desorption		70
4.	Des	signin	g Plast	ics Parts		73
	4.1	Stren	gth of Po	lymers		73
	4.2	Part F	ailure			74
	4.3	Time-	Depende	ent Deformational Behavior		76
		4.3.1	Short-T	erm Stress-Strain Behavior		76
		4.3.2	Long-T	erm Stress-Strain Behavior		77
5.	For	mulas	s for De	signing Extrusion and Injection		
	Мо	lding	Equipm	nent		81
	5.1	Extrus	sion Dies	·		81
		5.1.1	Calcula	tion of Pressure Drop		81
			5.1.1.1	Effect of Die Geometry on Pressure Drop		81
			5.1.1.2	Shear Rate in Die Channels		83
			5.1.1.3	General Relation for Pressure Drop in Any	y	
				Given Channel Geometry		83
			5.1.1.4	Examples		84
				Temperature Rise and Residence Time .		94
			5.1.1.6	Adapting Die Design to Avoid Melt		
			5 4 4 7	Fracture		95
			511/	Designing Screen Packs for Extruders		102

x Contents

5.2	Extrus	sion Screws	105
	5.2.1	Solids Conveying	105
	5.2.2	Melt Conveying	109
		5.2.2.1 Correction Factors	111
		5.2.2.2 Screw Power	111
		5.2.2.3 Heat Transfer between the Melt and the	
		Barrel	114
		5.2.2.4 Melt Temperature	115
		5.2.2.5 Melt Pressure	116
	5.2.3	Melting of Solids	118
		5.2.3.1 Thickness of Melt Film	118
		5.2.3.2 Melting Rate	121
		5.2.3.3 Dimensionless Melting Parameter	121
		5.2.3.4 Melting Profile	122
	5.2.4	Temperature Fluctuation of Melt	125
	5.2.5	Scale-up of Screw Extruders	126
	5.2.6	Mechanical Design of Extrusion Screws	131
		5.2.6.1 Torsion	131
		5.2.6.2 Deflection	131
5.3	Injecti	ion Molding	133
	5.3.1	Pressure Drop in Runner	134
	5.3.2	Mold Filling	137
		5.3.2.1 Injection Pressure and Clamp	
		Force	137
	5.3.3	Flowability of Injection Molding Resins	139
	5.3.4	Cooling of Melt in Mold	142
		5.3.4.1 Crystalline Polymers	142
		5.3.4.2 Amorphous Polymers	145
	5.3.5	Design of Cooling Channels	145
		5.3.5.1 Thermal Design	145
		5.3.5.2 Mechanical Design	149

	Contents	ΧI
5.3.6	Melting in Injection Molding Screws	150
	5.3.6.1 Melting by Heat Conduction	150
	5.3.6.2 Melting during Screw Rotation	151
5.3.7	Predicting Flow Length of Spiral Melt Flows	156
A Final Wor	d	163
Biography		164
Index		165

1 Formulas of Rheology

One of the most important steps in processing polymers is melting the resin, which is initially in the solid state, and forcing the melt through a die of a given shape. During this operation, the melt, whose structure plays a key role in determining the quality of the product to be manufactured, undergoes different flow and deformation processes.

The plastics engineer has therefore to deal with the melt rheology, which describes the flow behavior and deformation of the melt. The theory of elasticity and hydromechanics can be considered the frontier field of rheology, because the former describes the behavior of ideal elastic solids, whereas the latter is concerned with the behavior of ideal viscous fluids.

Ideal elastic solids deform according to Hooke's Law and ideal viscous fluids obey the laws of Newtonian flow. The latter are also denoted as Newtonian fluids. Plastic melts exhibit both viscous and elastic properties.

Thus, the design of machines and dies for polymer processing requires quantitative description of the properties related to polymer melt flow. Starting from the relationships for Hookean solids, formulas describing viscous shear flow of the melt are treated first, as far as they are of practical use in designing polymer machinery. This is followed by a summary of expressions for steady and time-dependent viscoelastic behavior of melts.

1.1 Ideal Solids

The behavior of a polymer subjected to shear or tension can be described by comparing its reaction to external force with that of an ideal elastic solid under load. To characterize ideal solids, first of all it is necessary to define certain quantities as follows [1]:

The axial force F_n in Figure 1.1 causes an elongation Δl of the sample of diameter d_0 and length l_0 that is fixed at one end. Following equations apply for this case:

Engineering strain:

$$\varepsilon' = \frac{\Delta l}{l_0} \tag{1.1}$$

Hencky strain:

$$\varepsilon = \ln\left(\frac{l}{l_0}\right) \tag{1.2}$$

Tensile stress:

$$\sigma_{\rm Z} = \frac{F_{\rm n}}{A_{\rm o}} \tag{1.3}$$

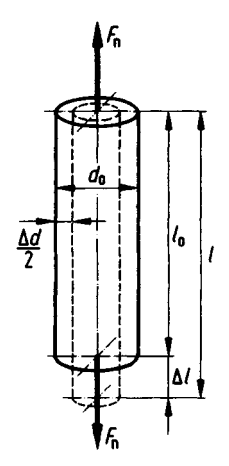


Figure 1.1 Deformation of a Hookean solid by a tensile stress [1]

Reference area:

$$A_0 = \frac{\pi \, d_0^2}{4} \tag{1.4}$$

Poisson's ratio:

$$\mu = -\frac{\Delta d/d_0}{\Delta I/l_0} \tag{1.5}$$

Figure 1.2 shows the influence of a shear force F_v , acting on the area A of a rectangular sample causing the displacement ΔU . The valid expressions are defined by:

Shear strain:

$$\gamma = \frac{\Delta U}{I} \tag{1.6}$$

Shear stress:

$$\tau = \frac{F_{\rm t}}{A} \tag{1.7}$$

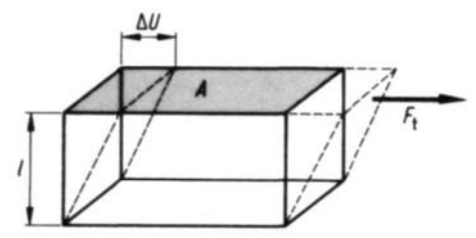


Figure 1.2 Deformation of a Hookean solid by shearing stress [1]

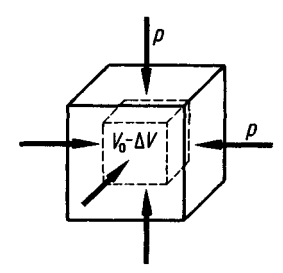


Figure 1.3 Hookean solid under compression [1]

The isotropic compression due to the pressure acting on all sides of the cube shown in Figure 1.3 is given by the engineering compression ratio κ .

$$\kappa = \frac{\Delta V}{V_0} \tag{1.8}$$

where ΔV is the reduction of volume of a body with the original volume V_0 due to deformation.

1.1.1 Hooke's Law

The linear relationships between stress and strain of a Hookean solid are given by [1].

$$\sigma_{\rm Z} = E \cdot \varepsilon' \tag{1.9}$$

$$\tau = G \cdot \gamma \tag{1.10}$$

$$p = -K \cdot \kappa \tag{1.11}$$

Where E is the modulus of elasticity, G is the shear modulus, and K is the bulk modulus. These moduli are constant for a Hookean solid. In addition, the relationship existing between E, G and K is expressed as [1]

$$E = 2 G (1 + \mu) = 3 K (1 - 2 \mu)$$
 (1.12)

For an incompressible solid this leads $(K \to \infty, \mu \to 0.5)$ to [1]

$$E = 3G \tag{1.13}$$

1.2 Newtonian Fluids

There is a linear relationship between stress and strain in the case of Newtonian fluids similar to the one for ideal elastic solids.

The fluid between the upper plate in Figure 1.4 is moving at a constant velocity U_x and the lower stationary plate experiences a shear stress τ (see also Figure 1.2).

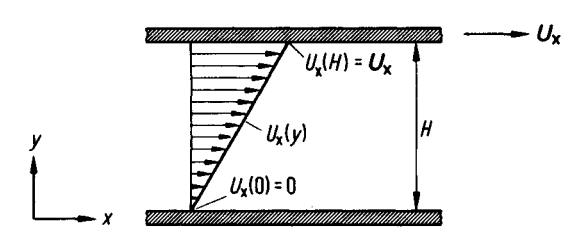


Figure 1.4 Shear flow

$$\tau = \frac{F_{\rm t}}{A} \tag{1.14}$$

The shear or deformation rate of the fluid is equal to

$$\dot{\gamma} = \frac{U_{x}}{H} = \frac{\mathrm{d}u}{\mathrm{d}y} \tag{1.15}$$

The shear viscosity is defined as

$$\eta = \frac{\tau}{\dot{\gamma}} \tag{1.16}$$

For an extensional flow, which corresponds to the tension test of a Hookean solid, we get

$$\sigma_7 = \lambda \cdot \dot{\varepsilon} \tag{1.17}$$

where

 $\sigma_{\rm Z}$ = normal stress

 λ = Trouton viscosity

 $\dot{\varepsilon}$ = strain rate

Analogously to Equation 1.13 one obtains

$$\lambda = 3\,\eta\tag{1.18}$$

1.3 Formulas for Viscous Shear Flow of Polymer Melts

Macromolecular fluids such as thermoplastic melts exhibit significant non-Newtonian behavior. This can be seen in the marked decrease of melt viscosity when the melt is subjected to shear or tension as shown in Figure 1.5. The plastic melt in the channels of polymer processing machinery is subjected mainly to shear flow. Therefore, knowledge of the laws of shear flow is necessary when designing machines and dies for polymer processing. For practical applications, the following summary of the relationships was found to be useful.

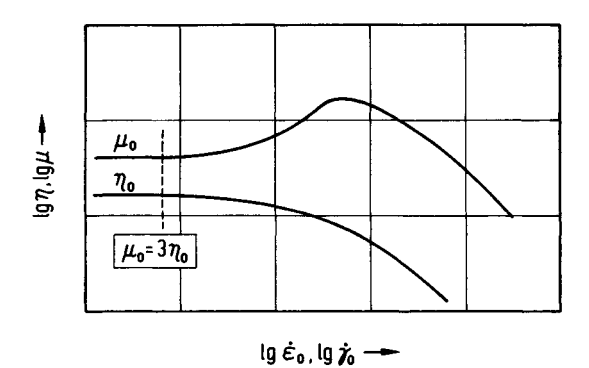


Figure 1.5 Tensile viscosity and shear rate viscosity of a polymer melt as a function of strain rate [21]

1.3.1 Apparent Shear Rate

The apparent shear rate for a melt flowing through a capillary is defined as

$$\dot{\gamma}_{\rm a} = \frac{4\,\dot{Q}}{\pi\,R^3} \tag{1.19}$$

where \dot{Q} is the volume flow rate per second and R is the radius of the capillary.

1.3.2 Entrance Loss

Another rheological quantity of practical importance is the entrance loss p_c , representing the loss of energy of flow at the entrance to a round nozzle. This is empirically correlated by the relation [2]

$$p_{c} = c \cdot \tau^{m} \tag{1.20}$$

Table 1.1 Resin-Dependent Constants c and m in Equation 1.20 [2]

Polymer	С	m	
Polypropylene (Novolen 1120 H)	2.551 · 10 ⁻⁵	2.116	
Polypropylene (Novolen 1120 L)	$1.463 \cdot 10^{-4}$	1.976	
Polypropylene (Novolen 1320 L)	$2.871 \cdot 10^{-7}$	2.469	
LDPE (Lupolen 1800 M)	$1.176 \cdot 10^{-1}$	1.434	
LDPE (Lupolen 1800 S)	$6.984\cdot 10^{\circ}$	1.072	
LDPE (Lupolen 1810 D)	$5.688 \cdot 10^{-4}$	1.905	
HDPE (Lupolen 6011 L)	$3.940 \cdot 10^{-2}$	1.399	
HDPE (Lupolen 6041 D)	$1.778\cdot 10^{\scriptscriptstyle 0}$	1.187	
Polyisobutylene (Oppanol B 10)	$6.401 \cdot 10^{-3}$	1.575	
Polyisobutylene (Oppanol B 15)	$1.021 \cdot 10^{-7}$	2.614	

where c and m are empirical constants and τ is the shear stress. These constants can be determined from the well-known Bagley-curves as shown in Figure 1.7. The values of these constants are given in Table 1.1 for some thermoplastic materials. Shear stress and entrance loss are measured in Pa in the calculation of c and m.

1.3.3 True Shear Stress

The flow curves of a particular LDPE measured with a capillary rheometer are given in Figure 1.6. The plot shows the apparent shear rate $\dot{\gamma}_a$ as a function of the true shear stress τ at the capillary wall with the melt temperature as a parameter. The entrance loss p_c was obtained from the Bagley plot shown in Figure 1.7.

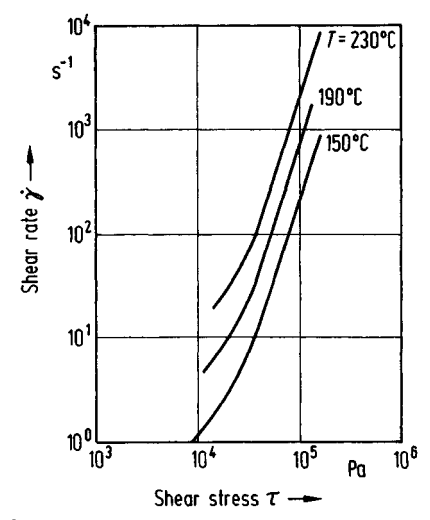


Figure 1.6 Flow curves of a LDPE [8]

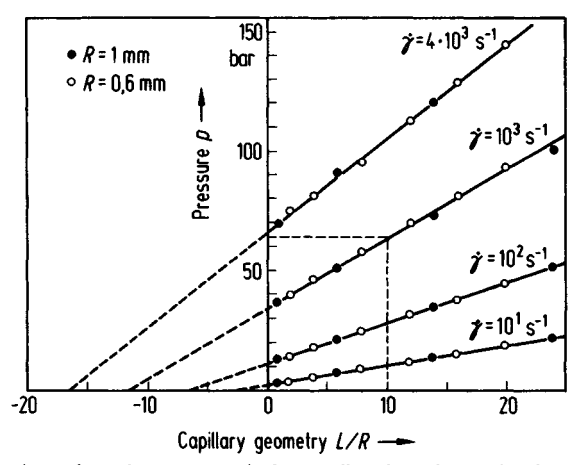


Figure 1.7 Bagley plots of a polystyrene with the capillary length L and radius R [3]

Thus, the true shear stress τ is given by

$$\tau = \frac{p - p_c}{2(L/R)} \tag{1.21}$$

where

L =length of the capillary

R = radius of the capillary

p = pressure of the melt (see Figure 1.39).

1.3.4 Apparent Viscosity

The apparent viscosity η_a is defined as

$$\eta_{a} = \frac{\tau}{\dot{\gamma}_{a}} \tag{1.22}$$

and is shown in Figure 1.8 as a function of shear rate and temperature for a LDPE.

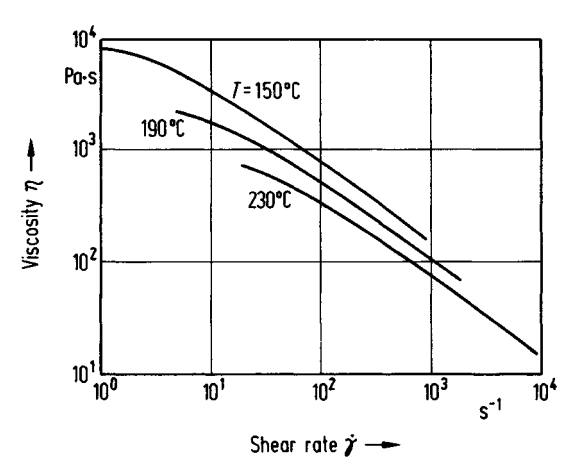


Figure 1.8 Viscosity functions of a LDPE [8]

1.3.5 True Shear Rate

The true shear rate $\dot{\gamma}_t$ is obtained from the apparent shear rate by applying the correction for the non Newtonian behavior of the melt according to Rabinowitsch

$$\dot{\gamma}_{t} = \left(\frac{n+3}{4}\right) \cdot \dot{\gamma}_{a} \tag{1.23}$$

The meaning of the power law exponent n is explained in the Section 1.3.7.2.

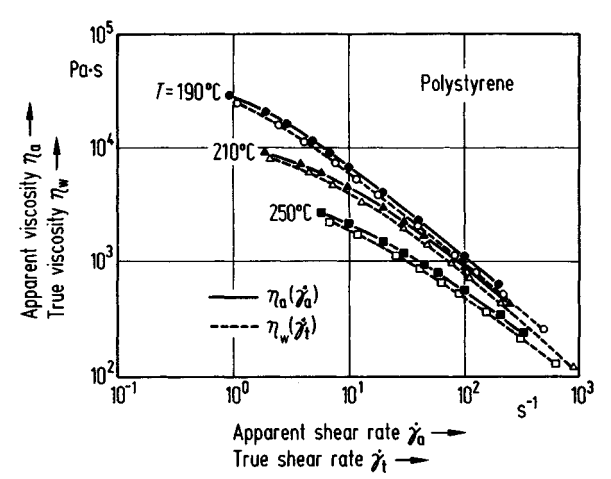


Figure 1.9 True and apparent viscosity functions of a polystyrene at different temperatures [2]

1.3.6 True Viscosity

The true viscosity η_w is given by

$$\eta_{\rm w} = \frac{\tau}{\dot{\gamma}_{\rm t}} \tag{1.24}$$

In Figure 1.9, the true and apparent viscosities are plotted as functions of the corresponding shear rates at different temperatures for a polystyrene. As can be seen, the apparent viscosity function is a good approximation for engineering calculations.

1.3.7 Empirical Formulas for Apparent Viscosity

Various fluid models have been developed to calculate the apparent shear viscosity η_a [9]. The following sections deal with some important relationships frequently used in design calculations.

1.3.7.1 Hyperbolic Function of Prandtl and Eyring

The relation between shear rate $\dot{\gamma}_a$ and shear stress τ according to the fluid model of Eyring [4] and Prandtl [5] can be written as

$$\dot{\gamma}_a = C \sinh(\tau/A) \tag{1.25}$$

where C and A are temperature-dependent material constants.

The evaluation of the constants C and A for the flow curve of LDPE at 190 °C in Figure 1.10 leads to $C = 4 \text{ s}^{-1}$ and $A = 3 \cdot 10^4 \text{ N/m}^2$. It can be seen from Figure 1.10 that the hyperbolic function of Eyring and Prandtl holds good at low shear rates.

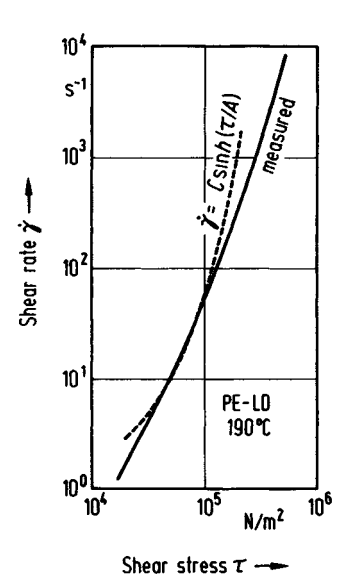


Figure 1.10 Comparison between measurements and values calculated with Equation 1.25 [8]

1.3.7.2 Power Law of Ostwald and de Waele

The power law of Ostwald [6] and DE WAELE [7] is easy to use, hence widely employed in design work [10]. This relation can be expressed as

$$\dot{\gamma}_{\mathbf{a}} = K \, \tau^n \tag{1.26}$$

or

$$\dot{\gamma}_{a} = K \mid \tau^{n-1} \mid \tau \tag{1.27}$$

where K denotes a factor of proportionality and n the power law exponent. Another form of power law often used is

$$\tau = K_{\rm R} \ \dot{\gamma}_{\rm a}^{n_{\rm R}} \tag{1.28}$$

or

$$\tau = K_{\rm R} \mid \dot{\gamma}_a^{n_{\rm R}-1} \mid \dot{\gamma}_a \tag{1.29}$$

In this case, n_R is the reciprocal of n and $K_R = K^{-n_R}$. From Equation 1.26 the exponent n can be expressed as

$$n = \frac{\mathrm{d}\lg\dot{\gamma}_a}{\mathrm{d}\lg\tau} \tag{1.30}$$

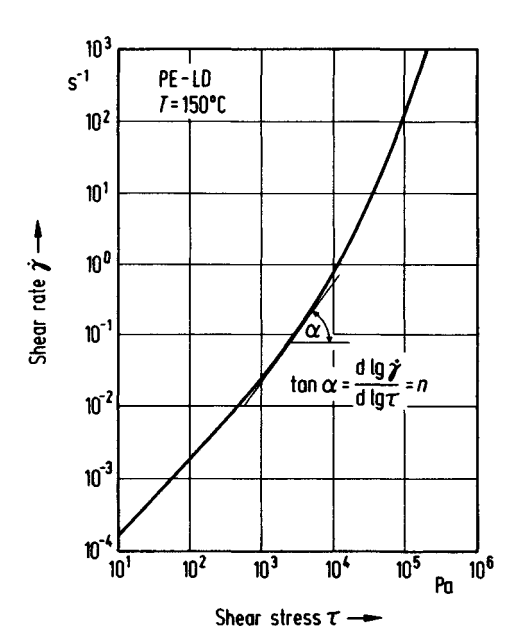


Figure 1.11 Determination of the power law exponent n in Equation 1.30

As shown in Figure 1.11, in a double log plot the exponent n represents the local gradient of the curve $\dot{\gamma}_a$ vs. τ .

Furthermore

$$\frac{1}{n} = \frac{\mathrm{dlg}\,\tau}{\mathrm{dlg}\,\dot{\gamma}_{\mathrm{a}}} = \frac{\mathrm{dlg}\,\eta_{\mathrm{a}} + \mathrm{dlg}\,\dot{\gamma}_{\mathrm{a}}}{\mathrm{dlg}\,\dot{\gamma}_{\mathrm{a}}} = \frac{\mathrm{dlg}\,\eta_{\mathrm{a}}}{\mathrm{dlg}\,\dot{\gamma}_{\mathrm{a}}} + 1\tag{1.31}$$

The values of K and n determined from the flow curve of LDPE at 190 °C shown in Figure 1.12 were found to be $K = 1.06 \cdot 10^{-11}$ and n = 2.57 [8]. As can be seen from Figure 1.12, the power law fits the measured values much better than the hyperbolic function of Eyring [4] and Prandtl [5]. The deviation between the results from the power law and from the experiment is a result of the assumption that the exponent n is constant throughout the range of shear rates considered, whereas in fact n varies with the shear rate. The power law can be extended to consider the effect of temperature on the viscosity as follows:

$$\eta_{\mathbf{a}} = K_{\mathrm{OR}} \cdot \exp(-\boldsymbol{\beta} \cdot T) \cdot \dot{\gamma}_{\mathbf{a}}^{n_{\mathrm{R}} - 1} \tag{1.32}$$

where

 K_{OR} = consistency index β = temperature coefficient

= temperature of melt.

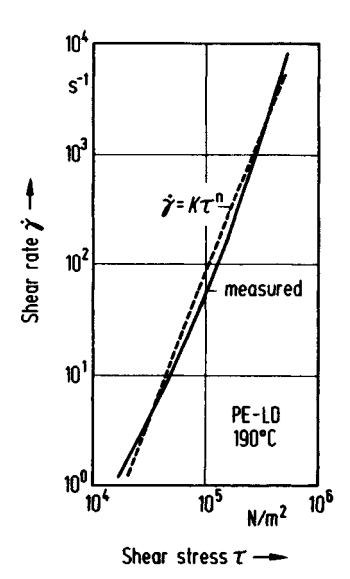


Figure 1.12 Comparison between measured values and power law

Example

Following values are given for a LDPE:

$$n_{\rm R} = 0.3286$$

 $\beta = 0.00863 \,(^{\circ}\text{C}^{-1})$
 $K_{\rm OR} = 135990 \,(\text{N} \cdot \text{s}^{n_{\rm R}} \cdot \text{m}^{-2})$

The viscosity η_a at T = 200 °C and $\dot{\gamma}_a = 500$ s⁻¹ is calculated from Equation 1.32

$$\eta_a = 373.1 \,\mathrm{Pa} \cdot \mathrm{s}$$

1.3.7.3 Muenstedt's Polynomial

The fourth degree polynomial of MUENSTEDT [2] provides a good fit for the measured values of viscosity. For a specific temperature this is expressed as

$$\lg \eta_a = A_0 + A_1 \lg \dot{\gamma}_a + A_2 (\lg \dot{\gamma}_a)^2 + A_3 (\lg \dot{\gamma}_a)^3 + A_4 (\lg \dot{\gamma}_a)^4$$
 (1.33)

where A_0 , A_1 , A_2 , A_3 , A_4 represent resin-dependent constants. These constants can be determined with the help of the program of RAO [10], which is based on multiple linear regressions.

This program in its general form fits an equation of the type

$$y = a_0 + a_1 x_1 + a_2 x_2 + \dots + a_n x_n$$

and prints out the coefficients a_0 , a_1 and so on for the best fit.

Shift Factor for Crystalline Polymers

The influence of temperature on viscosity can be taken into account by the shift factor a_T [2].

For crystalline polymers this can be expressed as

$$a_{\rm T} = b_1(T_0) \exp(b_2/T)$$
 (1.34)

where

 b_1, b_2 = resin dependent constants T = melt temperature (K) T_0 = reference temperature (K)

Shift Factor for Amorphous Polymers

The shift factor a_T for amorphous polymers is derived from the WLF equation and can be written as

$$\lg a_{\rm T} = \frac{-c_1(T - T_0)}{c_2 + (T - T_0)} \tag{1.35}$$

where

 c_1, c_2 = resin dependent constants T = melt temperature (°C) T_0 = reference temperature (°C)

The expression for calculating both the effect of temperature and shear rate on viscosity follows from Equation 1.33.

$$\lg \eta_{a} = \lg a_{T} + A_{0} + A_{1} \lg(a_{T} \dot{\gamma}_{a}) + A_{2} [\lg(a_{T} \dot{\gamma}_{a})]^{2}
+ A_{3} [\lg(a_{T} \dot{\gamma}_{a})]^{3} + A_{4} [\lg(a_{T} \dot{\gamma}_{a})]^{4}$$
(1.36)

With Equation 1.31 we get

$$\frac{1}{n} = 1 + A_1 + 2 A_2 \lg(a_T \dot{\gamma}_a) + 3 A_3 [\lg(a_T \dot{\gamma}_a)]^2 + 4 A_4 [\lg(a_T \dot{\gamma}_a)]^3$$
 (1.37)

The power law exponent is often required in the design work as a function of shear rate and temperature. Figure 1.13 illustrates this relationship for a specific LDPE. The curves shown are computed with Equation 1.34 and Equation 1.37. As can be inferred from Figure 1.13, the assumption of a constant value for the power law exponent holds good for a wide range of shear rates.

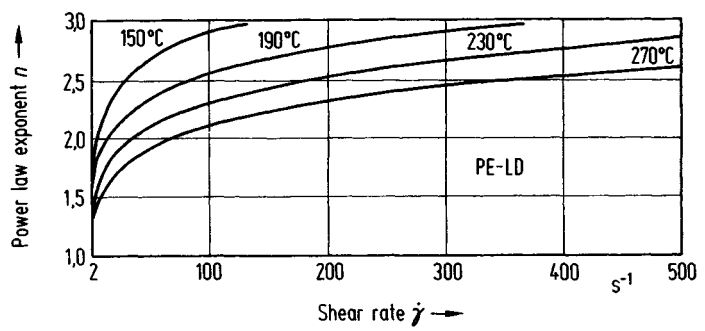


Figure 1.13 Power law exponent of a LDPE as a function of shear rate and temperature

Example

The viscosity for a LDPE is to be calculated with the following constants:

$$A = 4.2541$$

$$A1 = -0.4978$$

$$A2 = -0.0731$$

$$A3 = 0.0133$$

$$A4 = -0.0011$$

$$B = 5.13 \cdot 10^{-6}$$

$$B2 = 5640 \text{ K}$$

at
$$\dot{\gamma}_a = 500 \text{ s}^{-1}$$
 and $T = 200 \text{ °C}$.

Solution

 $a_{\rm T}$ from Equation 1.34

$$a_{\rm T} = 5.13 \cdot 10^{-6} \cdot \exp\left(\frac{5640}{473}\right) = 0.774$$

With

$$X = \lg(a_{\text{T}} \cdot \dot{\gamma}_{\text{a}})$$

 $X = \lg(0.774 \cdot 500) = 2.588$

 $\eta_{\rm a}$ from Equation 1.36

$$n_a = 10 (\lg a_{\rm T} + A_0 + A_1 X + A_2 X^2 + A_3 X^3 + A_4 X^4)$$

Substituting the values of A_0 , A_1 , and so on yields

$$\eta_a = 351.78 \, \mathrm{Pa} \cdot \mathrm{s}$$

The power law exponent is obtained from Equation 1.37

$$n = (1 + A_1 + 2 A_2 X + 3 A_3 X^2 + 4 A_4 X^3)^{-1}$$

Using the values for A_0 , A_1 , and so on

$$n = 3.196$$

1.3.7.4 Carreau's Viscosity Equation [11]

As shown in Figure 1.14 [12], the Carreau equation provides the best fit for the viscosity function, reproducing the asymptotic form of the plot at high and low shear rates correctly.

The equation is expressed as

$$\eta_{\mathbf{a}} = \frac{A}{(1 + B \cdot \dot{\gamma}_{\mathbf{a}})^C},\tag{1.38}$$

where A, B, C are resin-dependent constants. By introducing the shift factor a_T into Equation 1.38, the temperature-invariant form of the Carreau equation can be given as

$$\eta_{\rm a} = \frac{A \, a_{\rm T}}{(1 + B \, a_{\rm T} \, \dot{\gamma}_{\rm a})^C} \tag{1.39}$$

For a number of resins the shift factor can be calculated as a function of temperature from the following equation with good approximation [9, 10]

$$\lg a_{\rm T}(T_1, T_2) = \frac{8.86 (T_1 - T_{\rm ST})}{101.6 + (T_1 - T_{\rm ST})} - \frac{8.86 (T_2 - T_{\rm ST})}{101.6 + (T_2 - T_{\rm ST})}$$
(1.40)

where T_1 (°C) is the temperature at which the viscosity is given and T_2 (°C) the temperature at which the viscosity is calculated.

The standard temperature T_{ST} is given by [9]

$$T_{\rm ST} = T_{\rm g} + 50 \,{}^{\circ}{\rm C}$$
 (1.41)

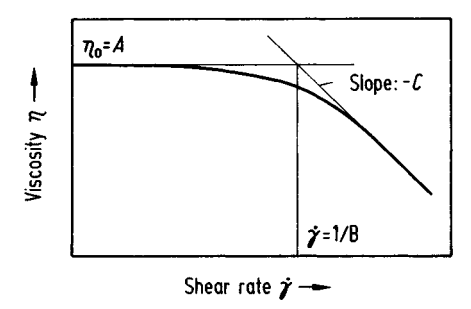


Figure 1.14 Determination of Carreau-parameters from a viscosity function [12]

Data on typical glass transition temperatures of polymers are given in Table 3.1 [9].

The power law exponent n can be obtained from Equation 1.39:

$$\frac{1}{n} = -C \cdot \frac{B \cdot a_{\mathrm{T}}}{1 + B \cdot a_{\mathrm{T}} \cdot \dot{\gamma}_{\mathrm{a}}} \cdot \dot{\gamma}_{\mathrm{a}} + 1 \tag{1.42}$$

For high shear rates n becomes [12]

$$n = \frac{1}{1 - C}$$

Example

Following constants are given for a specific LDPE:

 $= 32400 \text{ Pa} \cdot \text{s}$

В = 3.1 s

C = 0.62

 $T_{\text{ST}} = -133 \,^{\circ}\text{C}$ $T_{1} = 190 \,^{\circ}\text{C}$

The viscosity is to be calculated at

$$T_2 = 200 \, ^{\circ}\text{C} \text{ and } \dot{\gamma}_a = 500 \, \text{s}^{-1}.$$

Solution

From Equation 1.40 one obtains

$$X = \frac{8.86 (T_1 - T_{ST})}{101.6 + (T_1 - T_{ST})} = \frac{8.86 [190 - (-133)]}{101.6 + [190 - (-133)]} = 6.74$$

and

$$Y = \frac{8.86 (T_2 - T_{ST})}{101.6 + (T_2 - T_{ST})} = \frac{8.86 [200 - (-133)]}{101.6 + [200 - (-133)]} = 6.79$$

$$a_T = 10^{x-y} = 10^{-0.05} = 0.89$$

The power law exponent is calculated from Equation 1.42

$$n = \left(\frac{-C \cdot Z}{1 + Z} + 1\right)^{-1} = \left(\frac{-0.62 \cdot 1379.5}{1 + 1379.5} + 1\right)^{-1} = 2.63$$

where $Z = B \cdot a_{\rm T} \cdot \dot{\gamma}_{\rm a} = 3.1 \cdot 0.89 \cdot 500 = 1379.5$.

1.3.7.5 Klein's Viscosity Formula [14]

The regression equation of Klein et al. [14] is given by

$$\ln \eta_{\mathbf{a}} = a_0 + a_1 \ln \dot{\gamma}_{\mathbf{a}} + a_{11} (\ln \dot{\gamma}_{\mathbf{a}})^2 + a_2 T + a_{22} T^2 + a_{12} T \cdot \ln \dot{\gamma}_{\mathbf{a}}$$
 (1.43)

T = temperature of the melt (°F) $\eta_a = \text{viscosity (lb}_f \cdot \text{s/in}^2)$

The resin-dependent constants a_0 to a_{22} can be determined with the help of the computer program given in [10], as in the case of the A-coefficients in Equation 1.33.

Example

Following constants are valid for a specific type of LDPE. What is the viscosity η_a at $\dot{\gamma}_a = 500 \text{ s}^{-1}$ and $T = 200 \text{ }^{\circ}\text{C}$?

$$a_0 = 3.388$$

 $a_1 = -6.351 \cdot 10^{-1}$
 $a_{11} = -1.815 \cdot 10^{-2}$
 $a_2 = -5.975 \cdot 10^{-3}$
 $a_{22} = -2.51 \cdot 10^{-6}$ and
 $a_{12} = 5.187 \cdot 10^{-4}$

Solution

$$T$$
 (°F) = 1.8 · T (°C)+32 = 1.8 · 200 + 32 = 392

With the constants above and Equation 1.43 one gets

$$\eta_a = 0.066 \text{ lb}_f \cdot \text{s/in}^2$$

and in SI-units

$$\eta_a = 6857 \cdot 0.066 = 452.56 \text{ Pa} \cdot \text{s}$$

The expression for the power law exponent n can be derived from Equation 1.31 and Equation 1.43. The exponent n is given by

$$\frac{1}{n} = 1 + a_1 + 2 a_{11} \ln \dot{\gamma}_a + a_{12} \cdot T \tag{1.44}$$

Putting the constants $a_1 \dots a_{12}$ into this equation obtains

$$n = 2.919$$

1.3.7.6 Effect of Pressure on Viscosity

Compared to the influence of temperature, the effect of pressure on viscosity is of minor significance.

<i>p</i> bar	η_{\cdot}
30	1.03 η ₀
100	1.105 $\eta_{_0}$
200	1.221 $\eta_{\scriptscriptstyle 0}$
300	1.35 η_0
500	1.65 η_0
1000	$2.72 \stackrel{\circ}{\eta_{\scriptscriptstyle 0}}$
3000	$20 \qquad \eta_{_0}$

Table 1.2 Effect of Pressure on Viscosity for Polystyrene, Equation 1.46

However, the relative measure of viscosity can be obtained from [9, 15, 16]

$$\eta_{\rm p} = \eta_0 \, \exp(\alpha_{\rm p} \cdot p) \tag{1.45}$$

where

 $\eta_{\rm p} = {\rm viscosity} \text{ at pressure } p \text{ and constant shear stress } \tau_0$ $\eta_0 = {\rm viscosity} \text{ at constant shear stress } \tau_0$

 $\alpha_{\rm p}$ = pressure coefficient

For styrene polymers η_p is calculated from [14]

$$\eta_{\rm p} = \eta_0 \, \exp\left(\frac{p}{1000}\right) \tag{1.46}$$

where p = pressure in bar.

Thus the change of viscosity with pressure can be obtained from Equation 1.46. Table 1.2 shows the values of viscosity calculated according to Equation 1.46 for a polystyrene of average molecular weight. It can be seen that a pressure of 200 bar causes an increase of viscosity of 22% compared to the value at 1 bar. The pressure coefficient of LDPE is less than that of PS by a factor of 3-4 and the value of HDPE is again smaller by a factor of 2 compared to LDPE. This means that in the case of polyethylene an increase of pressure by 200 bar would enhance the viscosity only by 3 to 4%. Consequently, the effect of pressure on viscosity can be neglected in the case of extrusion processes which generally use low pressure. However, in injection molding with its high pressures, typically the dependence of viscosity on pressure has to be considered.

1.3.7.7 Dependence of Viscosity on Molecular Weight

The relationship between viscosity and molecular weight can be described by [12]

$$\eta_{\rm a} = K' \, \overline{M}_{\rm w}^{3.5} \tag{1.47}$$

where

 $M_{\rm w} = {\rm molecular \ weight}$

K' = resin dependent constant

The approximate value of K' for LDPE is

$$K' = 2.28 \cdot 10^{-4}$$

and for polyamide 6

$$K' = 5.21 \cdot 10^{-14}$$

according to the measurements of Laun [21].

These values are based on zero viscosity.

1.3.7.8 Viscosity of Two Component Mixtures

The viscosity of a mixture consisting of a component A and a component B can be obtained from [17]

$$\lg \eta_{\rm M} = C_{\rm A} \lg \eta_{\rm A} + C_{\rm B} \lg \eta_{\rm B} \tag{1.48}$$

where

 η = viscosity

C = weight per cent

Indices:

M: mixture

A, B: components

1.4 Viscoelastic Behavior of Polymers

Polymer machinery can be designed sufficiently accurately on the basis of the relationships for viscous shear flow alone. However, a complete analysis of melt flow should include both viscous and elastic effects, although the design of machines and dies is rather difficult when considering melt elasticity and therefore rarely used. WAGNER [18] and FISCHER [19] made attempts to dimension dies taking elastic effects into account.

For a more complete picture of melt theology the following expressions for the viscoelastic quantities according to Laun [20, 21] are presented. The calculation of the deformation of the bubble in film blowing is referred to as an example of the application of Maxwell's model.

1.4.1 Shear

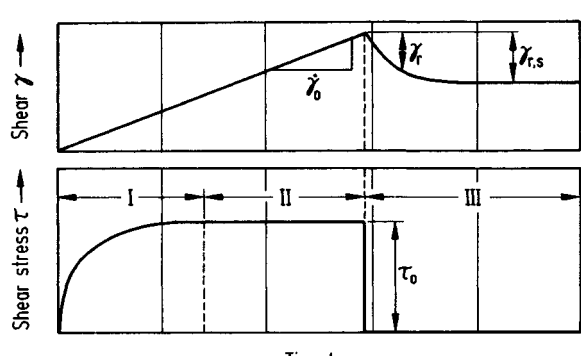
1.4.1.1 Linear Viscoelastic Behavior

The linear viscoelastic behavior occurs at low shear rates or small shear.

Steady Shear Flow

Zero viscosity η_0 as a material function for the viscous behavior (Figure 1.15 and 1.16):

$$\eta_0 = \frac{\tau_0}{\dot{\gamma}_0} \tag{1.49}$$



Time t --

Figure 1.15 Time dependence of shear strain and shear stress in a stress test at constant shear rate $\dot{\gamma}_0$ and subsequent recoil due to unloading (shear stress $\tau = 0$) with $\gamma_{r,s}$ as recoverable shear strain [21]

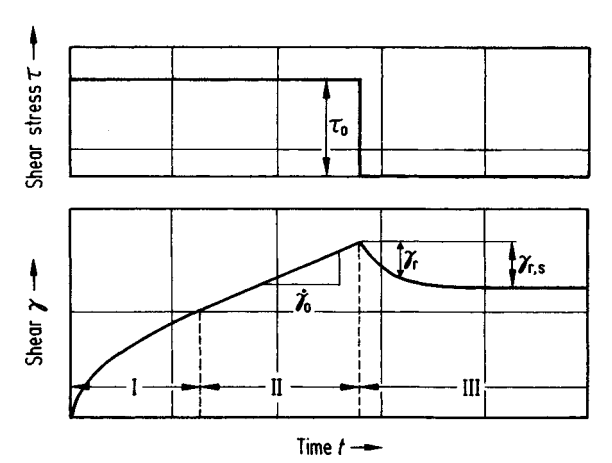


Figure 1.16 Creep test at constant shear stress τ_0 and subsequent retardation after unloading (shear stress $\tau=0$) [20].

 $\gamma_{r,s}$ = recoverable shear strain; I = initial state; II = steady state; III = retardation

Steady state shear compliance J_e^0 (Figure 1.15 and Figure 1.16) as a characteristic parameter for the elastic behavior:

$$J_{\rm e}^0 = \frac{\gamma_{\rm r,s}}{\tau_0} \tag{1.50}$$

Time-dependent Behavior

Viscosity $\eta(t)$ (Figure 1.17):

$$\overset{\circ}{\eta}(t) = \frac{\tau(t)}{\dot{\gamma}_0} \tag{1.51}$$

Shear compliance J(t) (Figure 1.18):

$$\overset{\circ}{J}(t) = \frac{\gamma(t)}{\tau_0} \tag{1.52}$$

Maximum time of retardation τ_{max} as a rheological quantity for the transient behavior (Figure 1.19):

$$\gamma_{\rm r}(t) \approx \gamma_{\rm r,s} \left[1 - \exp(-t/\tau_{\rm max})\right] \tag{1.53}$$

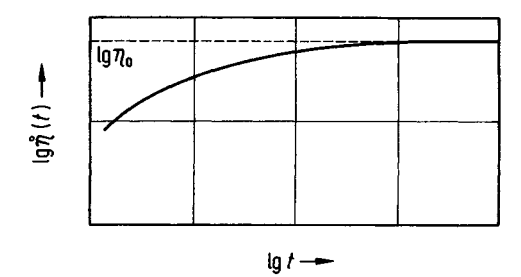


Figure 1.17 Initial state in a stress test under linear shear flow [21]

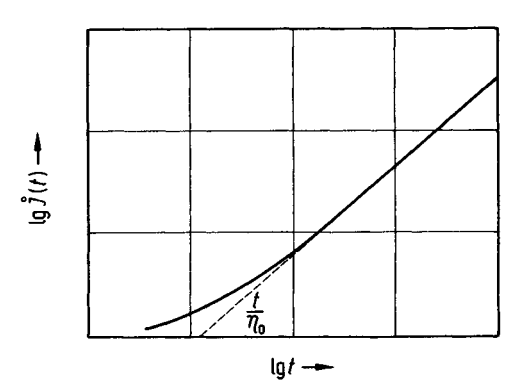


Figure 1.18 Initial state in creep under linear shear flow [21]

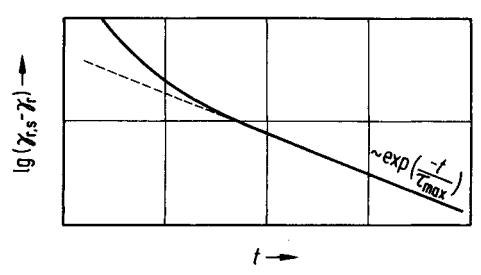


Figure 1.19 Retardation from steady shear flow [21] (shear stress $\tau = 0$ at time t = 0)

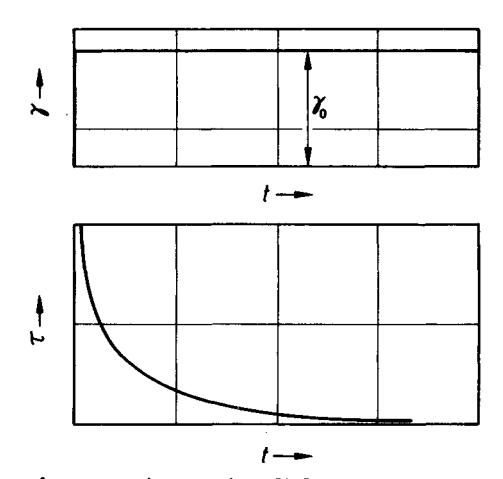


Figure 1.20 Relaxation after a step shear strain γ_0 [21]

Shear stress relaxation modulus $\overset{\circ}{G}(t)$ (Figure 1.20 and Figure 1.21):

$$\overset{o}{G}(t) = \frac{\tau(t)}{\gamma_0} \tag{1.54}$$

Dependence of storage modulus G' and loss modulus G'' on frequency (Figure 1.22) with sinusoidal shear strain γ .

$$\gamma = \hat{\gamma} \sin \omega t \tag{1.55}$$

Sinusoidal and out-of-phase shear stress τ :

$$\tau = \hat{\gamma}(G'\sin\omega t + G''\cos\omega t) \tag{1.56}$$

where

 $\hat{\gamma}$ = amplitude of shear ω = angular frequency

The storage modulus $G'(\omega)$ characterizes the elastic behavior, whereas the loss modulus G'' depicts the viscous behavior of the melt subjected to periodic shear deformation.

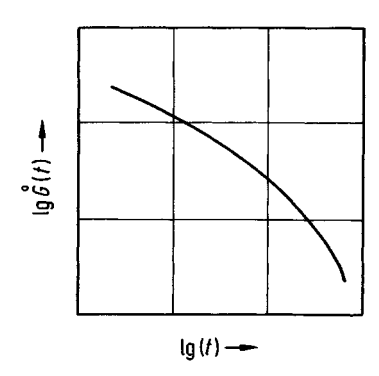


Figure 1.21 Relaxation modulus of linear shear flow [21]

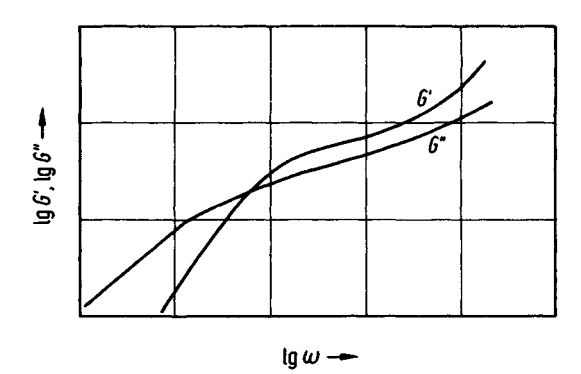


Figure 1.22 Storage modulus G' and loss modulus G'' as functions of frequency

Expressions for conversion:

Determination of zero viscosity and shear compliance from relaxation modulus [21]:

$$\eta_0 = \int_0^t G(t) \, \mathrm{d}t \tag{1.57}$$

$$J_{\rm e}^0 = \frac{1}{\eta_0^2} \int_0^t t \, G(t) \, \mathrm{d}t \tag{1.58}$$

Determination of zero viscosity and shear compliance from storage and loss moduli [21]:

$$\eta_0 = \lim_{\omega \to 0} \frac{G''}{\omega} \tag{1.59}$$

$$J_{\rm e}^0 = \frac{1}{\eta_0^2} \lim_{\omega \to 0} \frac{G'}{\omega^2} \tag{1.60}$$

1.4.1.2 Nonlinear Viscoelastic Behavior

Steady Shear Flow

The viscosity

$$\eta = \frac{\tau_0}{\dot{\gamma}_0}$$

and the shear compliance

$$J_{\rm e} = \frac{\gamma_{\rm r,s}}{\tau_0}$$

are dependent on the shear rate and shear stress respectively in the nonlinear case. Their limiting values for small shear rates or shear stresses are η_0 and J_e^0 (Figure 1.23). Another material function in addition to the shear compliance characterizing the elastic behavior is the primary normal stress coefficient Θ with N_1 as the normal stress difference:

$$\Theta = \frac{N_1}{\dot{\gamma}_0^2} \tag{1.61}$$

The limiting value of the normal stress function $\Theta(\dot{\gamma}_0)$ (Figure 1.23) at low shear rates is given by

$$\Theta_0 = \lim_{\dot{\gamma}_0 \to 0} \Theta(\dot{\gamma}_0) \tag{1.62}$$

In addition, we have:

$$J_{\rm e} = \frac{\Theta}{2\,n^2} \tag{1.63}$$

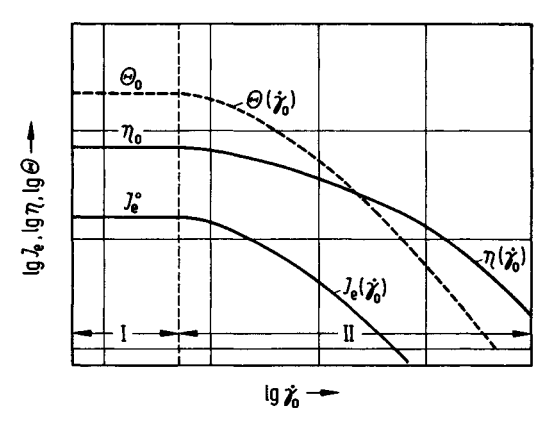


Figure 1.23 Parameters for steady shear flow [21]. I = linear region; II = nonlinear region

Characterization of the Transient State

Initial state in a stress test (Figure 1.24)

$$\eta(t) \le \stackrel{\circ}{\eta}(t) \tag{1.64}$$

 $\eta(t)$ is the asymptote.

Plots of starting state in creep test (Figure 1.25)

$$J(t) \ge \overset{\circ}{J}(t) \tag{1.65}$$

J(t) is the asymptote.

Relaxation modulus (Figure 1.26):

$$G(t) = h(\gamma_0) \overset{\circ}{G}(t) \tag{1.66}$$

The time-dependent behavior remains unchanged in the nonlinear case. The entire function plot will be displaced by the factor $h(\gamma_0)$.

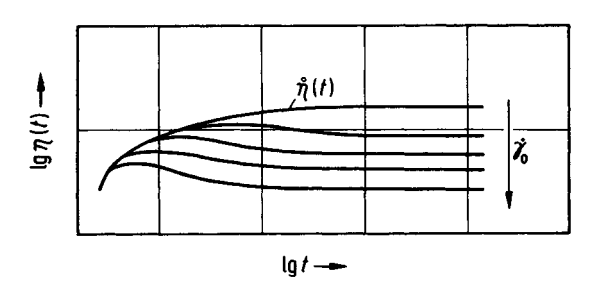


Figure 1.24 Initial state in a stress test of nonlinear shear flow [21]

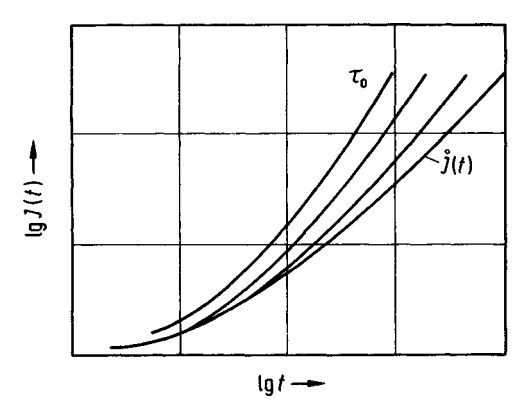


Figure 1.25 Initial state in creep test of nonlinear shear flow [21]

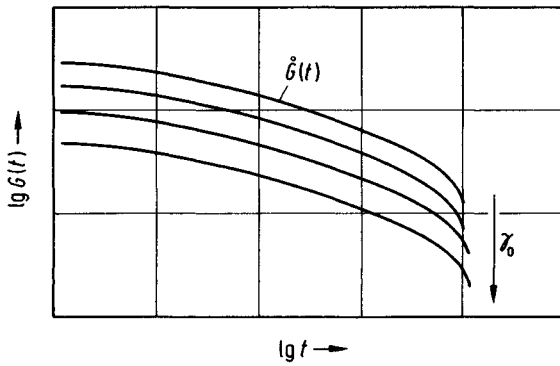


Figure 1.26 Relaxation modulus of nonlinear shear flow [21]

1.4.2 Uniaxial Tension

1.4.2.1 Linear Viscoelastic Behavior

Steady Tensile Extensional Flow

Tensile zero viscosity μ_0 as a material function for the viscous behavior (Figure 1.27 and Figure 1.28)

$$\mu_0 = \frac{\sigma_0}{\dot{\varepsilon}_0} \tag{1.67}$$

Steady state tensile compliance D_e^0 as a material function for elastic behavior:

$$D_{\rm e}^0 = \frac{\varepsilon_{\rm r,s}}{\sigma_0} \tag{1.68}$$

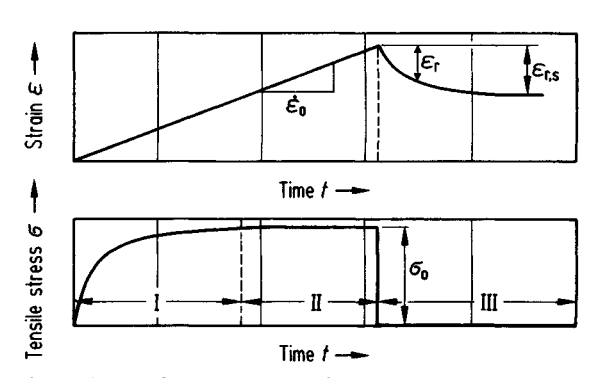


Figure 1.27 Time dependence of tensile strain and tensile stress at constant tensile strain rate $\dot{\varepsilon}_0$ and subsequent retardation after unloading (tensile stress τ = 0) [2]. $\varepsilon_{r,s}$ = recoverable tensile strain; I = initial state; II = steady state; III = retardation

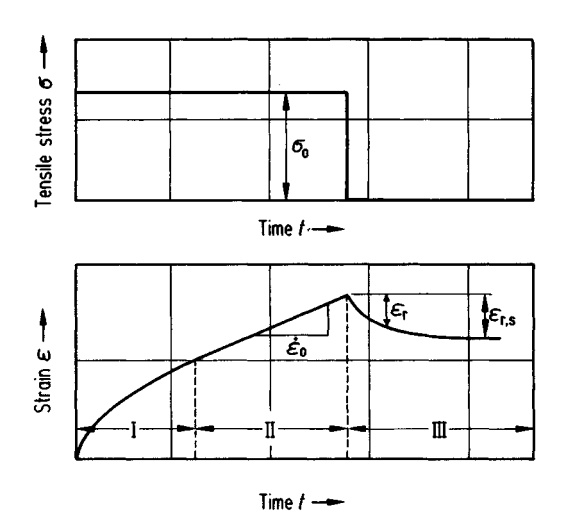


Figure 1.28 Tensile creep at constant tensile stress τ_0 and subsequent retardation after unloading (tensile stress τ = 0) [21]

Transient Behavior

Tensile viscosity $\mu(t)$ (Figure 1.29)

$$\stackrel{o}{\mu}(t) = \frac{\sigma(t)}{\dot{\varepsilon}_0} \tag{1.69}$$

$$\mu(t) = 3 \, \eta(t) \tag{1.70}$$

$$\mu_0 = 3\,\eta_0$$

The tensile viscosity is three times the shear viscosity.

Tensile creep compliance D(t) (Figure 1.30):

$$\overset{o}{D}(t) = \frac{\varepsilon(t)}{\sigma_0} \tag{1.71}$$

$$\overset{\circ}{D}(t) = \frac{1}{3} \cdot \overset{\circ}{J}(t) \tag{1.72}$$

Maximum retardation time τ_{max} (Figure 1.31)

$$\varepsilon_{\rm r}(t) \approx \varepsilon_{\rm r.s} \left[1 - \exp(-t/\tau_{\rm max})\right]$$
 (1.73)

Relaxation after a step strain of ε_0 :

Tensile relaxation modulus E(t) (Figure 1.32):

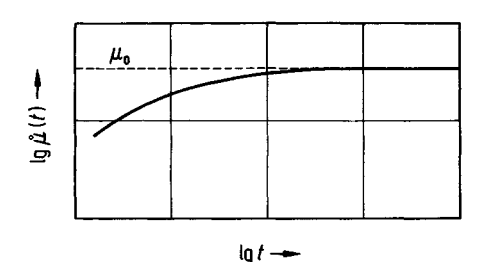


Figure 1.29 Initial state of linear tensile extension [21]

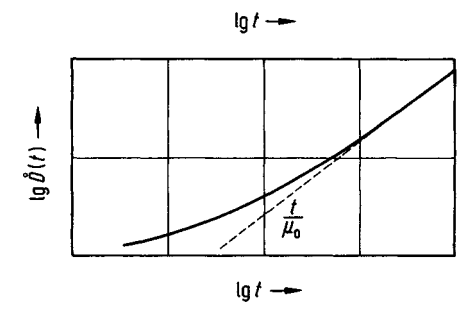
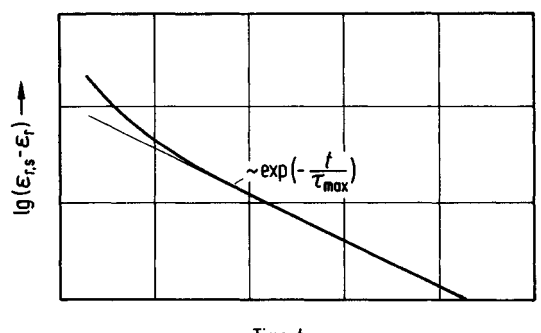


Figure 1.30 Initial state in tensile creep under linear tensile extension [21]



Time t —

Figure 1.31 Retardation from steady state tensile extension [21]

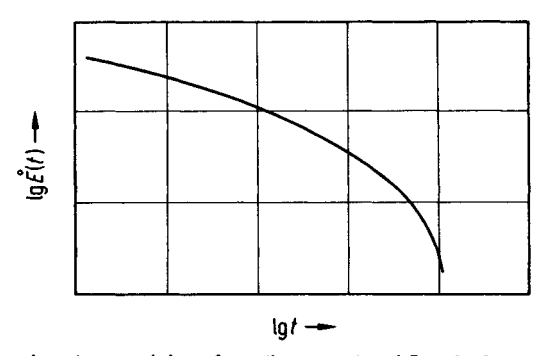


Figure 1.32 Tensile relaxation modulus of tensile extensional flow [21]

$$\stackrel{o}{E}(t) = \frac{\sigma(t)}{\varepsilon_0} \tag{1.74}$$

$$\overset{o}{E}(t) = 3 \cdot \overset{o}{G}(t) \tag{1.75}$$

1.4.2.2 Nonlinear Viscoelastic Behavior

Steady Tensile Extensional Flow

As shown in Figure 1.5, the tensile viscosity μ is given by

$$\mu_0 = \frac{\sigma_0}{\dot{\varepsilon}_0}$$

Tensile compliance D_e (Figure 1.33)

$$D_{\rm e} = \frac{\varepsilon_{\rm r,s}}{\sigma_0}$$

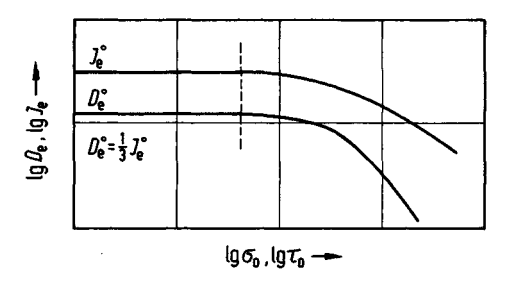


Figure 1.33 Plot of tensile compliance D_e and shear compliance J_e [21]

Time-dependent Behavior

Plots of starting state in tension test (Figure 1.34) [21]

$$\mu(t) \ge \stackrel{\circ}{\mu}(t) \tag{1.76}$$

 $\mu(t)$ is an asymptote.

Start-up curves in a tensile creep test (Figure 1.35) [21]

$$D(t) \le \overset{\circ}{D}(t) \tag{1.77}$$

D(t) is an asymptote.

Tensile relaxation modulus (Figure 1.36)

$$E(t, \varepsilon_0) \le g(\varepsilon_0) \cdot \stackrel{\circ}{E}(t) \tag{1.78}$$

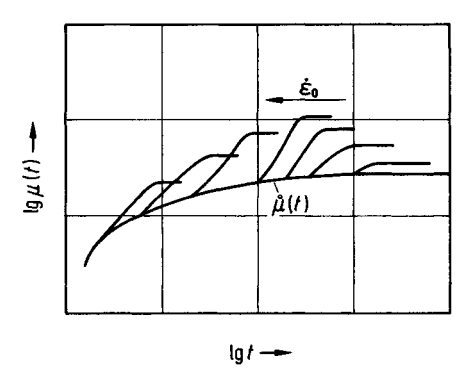


Figure 1.34 Initial state of nonlinear tensile extension [21]

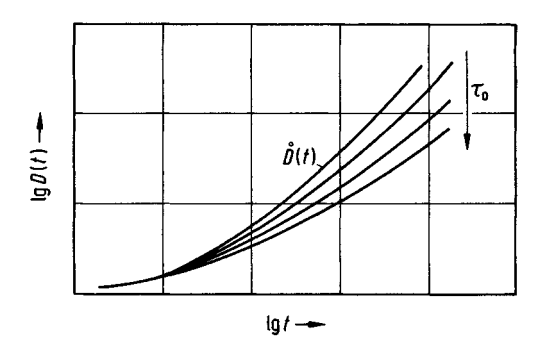


Figure 1.35 Initial state of tensile creep under nonlinear extension [21]

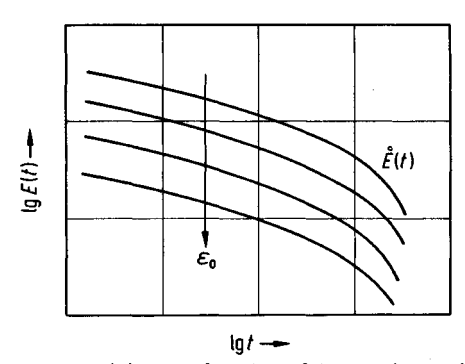


Figure 1.36 Tensile relaxation modulus as a function of time under nonlinear tensile extension [21]

1.4.3 Maxwell Model

The viscoelastic properties of a polymer can be used to calculate the deformation of a bubble in a film blowing process. In this case, the Maxwell model, which defines a viscoelastic body as an ideal spring and a dashpot in series (Figure 1.37) can be applied [18, 19].

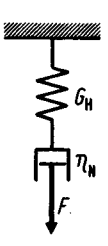


Figure 1.37 Maxwell fluid [1]

The total rate of deformation $\dot{\gamma}$ is the sum of the elastic component $\dot{\gamma}_{\rm H}$ and viscous component $\dot{\gamma}_{\rm N}$

$$\dot{\gamma} = \dot{\gamma}_{\rm H} + \dot{\gamma}_{\rm N} \tag{1.79}$$

leading to [22]

$$\eta_{\rm N} \ \dot{\gamma} = t_{\rm s} \ \dot{\tau} + \tau \tag{1.80}$$

where

$$t_{\rm s} = \frac{\eta_{\rm N}}{G_{\rm H}} \tag{1.81}$$

The time t_s is called the relaxation time, as the stress τ relaxes with the time.

 $\eta_{\rm H}$ = Newtonian viscosity

 $G_{\rm H}$ = elastic shear modulus of the spring (Hooke element)

At a given rate of deformation, the viscosity $\eta_{N,S}$ reaches the Newtonian value asymptotically (Figure 1.38). After the release of strain the stress delays according to

$$\tau = \tau_0 \exp(-t/t_s) \tag{1.82}$$

It can be seen from Equation 1.82 that the relaxation time is the period, in which the stress decreases to 1/e (37%) of its original value [23]. It also follows from Equation 1.82 that the modulus of relaxation G for $\gamma = \gamma_0$ is given by

$$G = G_0 \exp(-t/t_s) \tag{1.83}$$

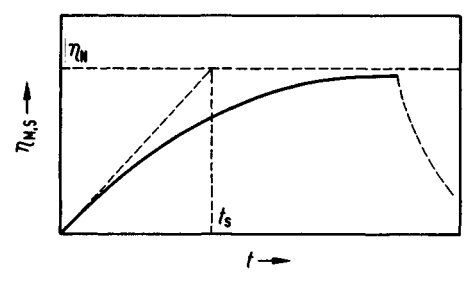


Figure 1.38 Tensile viscosity of Maxwell fluid [1]

The expression for the elongation of the bubble in a film blowing process can now be given as

$$\sigma + t_{\rm s} \frac{\partial \sigma}{\partial t} = \mu \frac{\mathrm{d}\nu}{\mathrm{d}x} \tag{1.84}$$

where

 σ = tensile stress,

 t_s = relaxation time,

 μ = tensile viscosity of the melt,

v =vertical velocity component of the bubble,

x = axial coordinate.

As the elongation of the bubble occurs biaxially, the deformation in the circumferential direction has to be calculated on similar lines. Assuming that the tensile viscosities and the relaxation times in both directions are equal, the influence of viscoelasticity on the bubble form can be predicted [18]. Wagner [18] estimates the relaxation time in the order of 5 to 11 s, depending on the operating conditions.

1.4.4 Practical Formulas for Die Swell and Extensional Flow

Elastic effects are responsible for die swell, which occurs when the melt exits through a die as shown in Figure 1.39 [20].

The following equation for the die swell is given by Cogswell [24]:

$$B_{\rm L}^2 = \frac{2}{3} \gamma_{\rm R} \left[\left(1 + \frac{1}{\gamma_{\rm R}^2} \right)^{\frac{3}{2}} - \frac{1}{\gamma_{\rm R}^3} \right]$$
 (1.85)

where

 $B_{\rm L}={
m die\ swell}\ {d\over d_0}$ (Figure 1.39) in a capillary with a length-to-diameter ratio greater than 16 and

 γ_R = recoverable shear strain

In Figure 1.40, the recoverable shear strain is presented as a function of die swell according to Equation 1.85 [24].

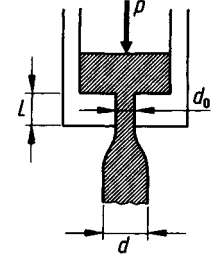


Figure 1.39 Die swell in extrusion

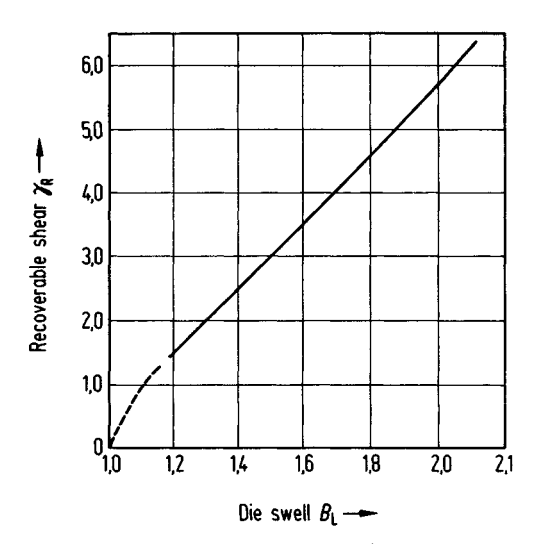


Figure 1.40 Dependence of recoverable shear on die swell [24]

Extensional Flow

The following relationships for extensional flow of melt after Cogswell [24] are important in practice:

Elongational stress σ_E :

$$\sigma_{\rm E} = \frac{3}{8}(n_{\rm R} + 1) \cdot p_{\rm c} \tag{1.86}$$

Tensile viscosity μ :

$$\mu = \frac{9}{32} \cdot \frac{(n_{\rm R} + 1)^2}{\eta_{\rm a}} \cdot \left(\frac{p_{\rm c}}{\dot{\gamma}_{\rm a}}\right)^2 \tag{1.87}$$

Reversible extension $\varepsilon_{\rm R}$

$$\varepsilon_{\rm R} = \ln B_0^2 \tag{1.88}$$

Rupture stress σ_{R}

$$\sigma_{\rm R} = \frac{3}{8} (3 n_{\rm R} + 1) \cdot p_{\rm c} \tag{1.89}$$

where

 $n_{\rm R}$ = reciprocal of power law index n in Equation 1.28

 p_c = entrance pressure loss according to Equation 1.20

 $\dot{\gamma}_{\rm a}$, $\eta_{\rm a}=$ apparent shear rate and apparent shear viscosity, respectively

 B_0 = die swell in melt flow through an orifice with zero length

References

- [1] Pahl, M., Baldhuhn, R., Linnemann, D.: Praktische Rheologie der Kunststoffschmelzen and Lösungen, VDI Kunststofftechnik, Düsseldorf (1982)
- [2] MUNSTEDT, H.: Kunststoffe 68, 92 (1978)
- [3] Kunststoff Physik im Gespräch, brochure, BASF, 1977
- [4] Eyring, H.: I. Chem. Phys. 4, 283 (1963)
- [5] Prandtl, L.: Phys. Blätter 5, 161 (1949)
- [6] OSTWALD, W.: Kolloid Z. 36, 99 (1925)
- [7] DE WAALE, A.: J. Oil and Color Chem. Assoc. 6, 33 (1923)
- [8] RAO, N. S.: Berechnen von Extrudierwerkzeugen, VDI Verlag, Düsseldorf (1978)
- [9] RAUWENDAAL, C.: Polymer Extrusion, Hanser Publishers, Munich (2001)
- [10] Rao, N. S.: Designing Machines and Dies for Polymer Processing with Computer Programs, Hanser Publishers, Munich (1981)
- [11] Carreau, P. J.: Dissertation, Univ. Wisconsin, Madison (1968)
- [12] HERTLEIN, T., FRITZ, H. G.: Kunststoffe 78, 606 (1988)
- [13] MICHAELI, W.: Extrusion Dies, Hanser Publishers, Munich (2003)
- [14] KLEIN, L, MARSHALL, D. I., FRIEHE, C. A.: J. Soc. Plastics Engrs. 21, 1299 (1965)
- [15] AVENAS, P., AGASSANT, J. F., SERGENT, J.PH.: La Mise en Forme des Matieres Plastiques, Technique & Documentation (Lavoisier), Paris (1982)
- [16] MUNSTEDT, H.: Berechnen von Extrudierwerkzeugen, VDI Verlag, Düsseldorf (1978)
- [17] Carley, J. F.: Antec 84, S. 439
- [18] WAGNER, M. H.: Dissertation, Univ. Stuttgart (1976)
- [19] Fischer, E.: Dissertation, Univ. Stuttgart (1983)
- [20] LAUN, H. M.: Rheol. Acta 18, 478 (1979)
- [21] LAUN, H. M.: Progr. Colloid & Polymer Sci. 75, 111 (1987)
- [22] BRYDSON, J. A.: Flow Properties of Polymer Melts, Iliffe Books, London (1970)
- [23] Bernhardt, E. C.: Processing of Thermoplastic Materials, Reinhold, New York (1963)
- [24] Cogswell, F. N.: Polymer Melt Rheology, John Wiley, New York (1981)

2 Thermodynamic Properties of Polymers

In addition to the rheological data, thermodynamic properties of polymers are necessary for designing machines and dies. It is often the case that the local values of these data are required as functions of temperature and pressure. Besides physical relationships, this chapter presents regression equations developed from experimental data for calculating thermodynamic properties, as these polynomials are often used in the practice, for example, in data acquisition for data banks [1].

2.1 Specific Volume

According to the Spencer Gilmore equation, which is similar to the van der Waal equation for real gases, the relationship between pressure p, specific volume ν , and temperature T of a polymer can be written as

$$(v - b^*)(p + p^*) = \frac{RT}{W}$$
 (2.1)

In this equation, b^* is the specific individual volume of the macromolecule, p^* is the cohesion pressure, W is the molecular weight of the monomer, and R is the universal gas constant [2].

Example

Following values are given for a LDPE:

$$W = 28.1 \text{ g/Mol};$$

 $b^* = 0.875 \text{ cm}^3/\text{g};$
 $p^* = 3240 \text{ atm}$

Calculate the specific volume ν at T=190 °C and p=1 bar.

Solution

Using Equation 2.1 and the conversion factors to obtain the volume ν in cm³/g, we obtain

$$v = \frac{10 \times 8.314 \times (273 + 190)}{28.1 \times 3240.99 \times 1.013} + 0.875 = 1.292 \text{ cm}^3/\text{g}$$

The density ρ is the reciprocal value of the specific volume so that

$$\rho = \frac{1}{\nu} \tag{2.2}$$

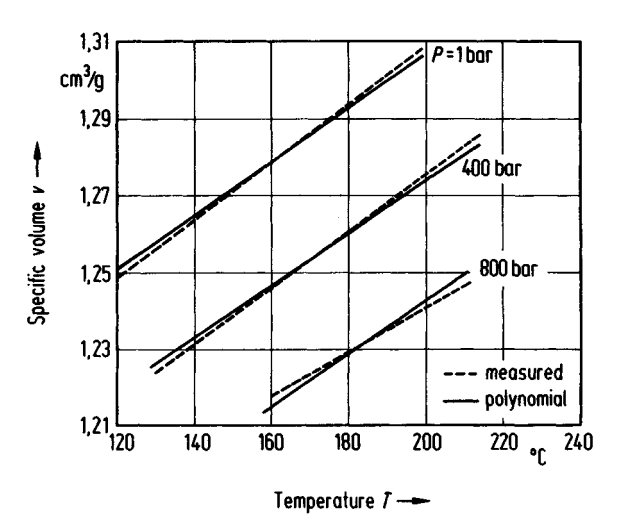


Figure 2.1 Specific volume as a function of temperature and pressure for LDPE [1]

The functional relationship between specific volume v, pressure p, and temperature T can also be expressed by a polynomial of the form [1,3]

$$v = A(0)_{y} + A(1)_{y} \cdot p + A(2)_{y} \cdot T + A(3)_{y} \cdot T \cdot p \tag{2.3}$$

if experimental data are available (Figure 2.1). The empirical coefficients $A(0)_v \dots A(3)_v$ can be determined by means of the computer program given in [1].

2.2 Specific Heat

The specific heat c_p is defined as

$$c_{\rm p} = \left(\frac{\partial h}{\partial T}\right)_{\rm p} \tag{2.4}$$

where

h = Enthalpy

T = Temperature

The specific heat c_p defines the amount of heat that is supplied to a system in a reversible process at a constant pressure to increase the temperature of the substance by dT.

The specific heat at constant volume c_v is given by

$$c_{v} = \left(\frac{\partial u}{\partial T}\right) \tag{2.5}$$

where

u = internal energy

T = temperature

In the case of c_v the supply of heat to the system occurs at constant volume.

 $c_{\rm p}$ and $c_{\rm v}$ are related to each other through the Spencer-Gilmore equation (Equation 2.1):

$$c_{\rm v} = c_{\rm p} - \frac{R}{W} \tag{2.6}$$

The numerical values of c_p and c_v differ by roughly 10%, so that for approximate calculations c_v can be considered equal to c_p [2].

Plots of c_p as a function of temperature are shown in Figure 2.2 for amorphous, semicrystalline, and crystalline polymers.

As shown in Figure 2.3, the measured values can be expressed by a polynomial of the type

$$c_{p}(T) = A(0) c_{p} + A(1) c_{p} \cdot T + A(2) c_{p} \cdot T^{2}$$
 (2.7)

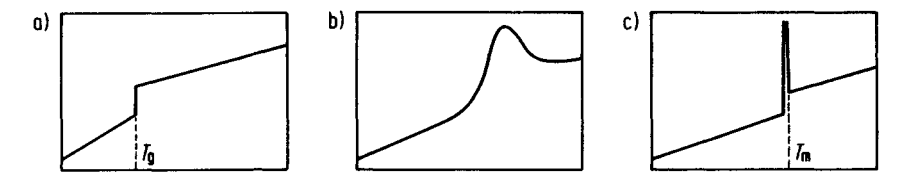


Figure 2.2 Specific heat as a function of temperature for amorphous (a), semi crystalline (b), and crystalline polymers (c) [4]

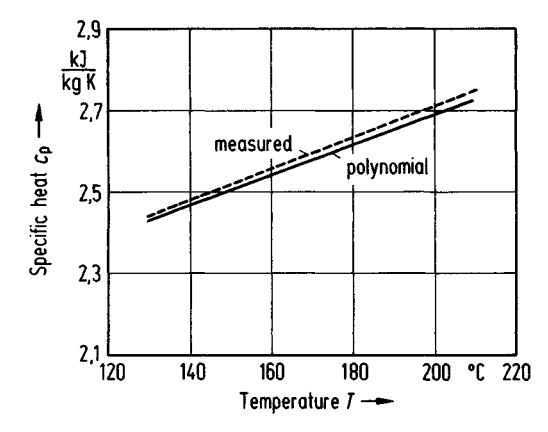


Figure 2.3 Comparison between measured values of $c_{\rm p}$ [6] and polynomial for LDPE [1]

The use of thermal properties $c_{\rm p}$ and ρ in design problems is illustrated in the examples given in Chapter 6.

The expansion coefficient α_v at constant pressure is given by [4]

$$\alpha_{\rm v} = \frac{1}{\nu} \left(\frac{\partial \nu}{\partial T} \right)_{\rm p} \tag{2.8}$$

The linear expansion coefficient α_{lin} is approximately

$$\alpha_{\rm lin} \approx \frac{1}{3} \alpha_{\rm v}$$
 (2.9)

The isothermal compression coefficient γ_K is defined as [4]

$$\gamma_{\rm K} = -\frac{1}{\nu} \left(\frac{\partial \nu}{\partial p} \right)_{\rm T} \tag{2.10}$$

 $a_{\rm v}$ and $\gamma_{\rm K}$ are related to each other by the expression [4]

$$c_{\rm p} = c_{\rm v} + \frac{T \cdot v \cdot \alpha_{\rm v}^2}{\gamma_{\rm K}} \tag{2.11}$$

2.3 Enthalpy

Equation 2.4 leads to

$$dh = c_{p} \cdot dT \tag{2.12}$$

As shown in Figure 2.4, the measured data on h = h(T) [6] for a polymer melt can be expressed by the polynomial

$$h(T) = A(0)_{h} + A(1)_{h} \cdot T + A(2)_{h} \cdot T^{2}$$
(2.13)

The specific enthalpy defined as the total energy supplied to the polymer divided by throughput of the polymer is a useful parameter for designing extrusion and injection molding equipment such as screws. It provides the theoretical amount of energy required to bring the solid polymer to the process temperature.

Values of this parameter for different polymers are given in Figure 2.5 [4].

If, for example, the throughput of an extruder is 100 kg/h of polyamide (PA) and the processing temperature is 260 °C, the theoretical power requirement would be 20 kW. This can be assumed to be a safe design value for the motor horse power, although theoretically it includes the power supply to the polymer by the heater bands of the extruder as well.

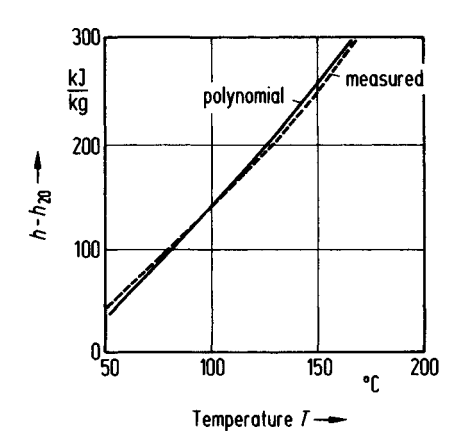


Figure 2.4 Comparison between measured values of h [6] and polynomial for PA-6 [1]

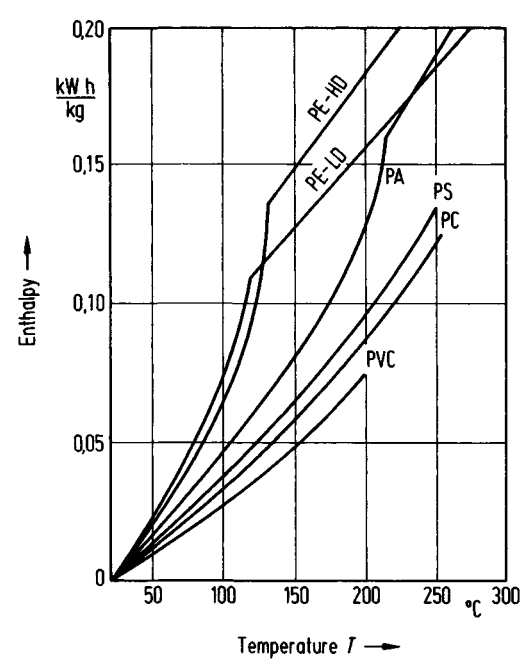


Figure 2.5 Specific enthalpy as a function of temperature [4]

2.4 Thermal Conductivity

The thermal conductivity λ is defined as

$$\lambda = \frac{Q \cdot l}{t \cdot A \cdot (T_1 - T_2)} \tag{2.14}$$

where

Q = heat flow through the surface of area A in a period of time t (T_1-T_2) = temperature difference over the length l

Analogous to the specific heat c_p and enthalpy h, the thermal conductivity λ can be expressed as [1]

$$\lambda(T) = A(0)_{\lambda} + A(1)_{\lambda} \cdot T + A(2)_{\lambda} \cdot T^{2}$$
(2.15)

as shown in Figure 2.6.

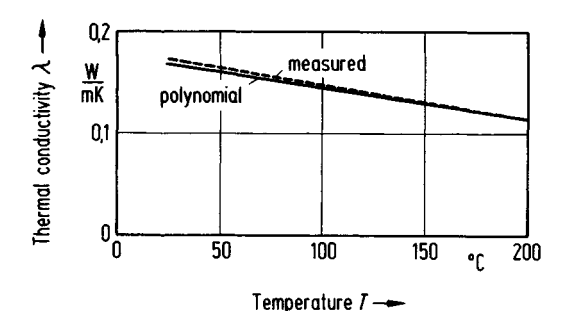


Figure 2.6 Comparison between measured values of λ [6] and polynomial for PP [1]

The thermal conductivity increases only slightly with pressure. A pressure increase from 1 bar to 250 bar leads to an increase of only less than 5% of its value at 1 bar.

Within a particular resin category such as LDPE, HDPE, the thermal properties are largely independent of the molecular structure. Exhaustive measured data of the quantities c_p , h, and λ and pressure-volume-temperature diagrams of polymers are given in the VDMA-Handbook [5].

Approximate values of thermal properties useful for plastics engineers are summarized in Table 2.1 [4].

 Table 2.1
 Approximate Values for the Thermal Properties of Selected Polymers [4]

Polymer	Thermal conductivity	Specific heat	Density	Glass transition temperature	Melting point range
	λ W/m · K	c _p kJ/kg K	ρ g/cm³	T₅ °C	T _m °C
PS	0.12	1.20	1.06	101	
PVC	0.21	1.10	1.40	80	_
PMMA	0.20	1.45	1.18	105	_
SAN	0.12	1.40	1.08	115	_
ABS	0.25	1.40	1.02	115	_
PC	0.19	1.40	1.20	150	
LDPE	0.24	2.30	0.92	-120/-90	ca. 110
LLDPE	0.24	2.30	0.92	-120/-90	ca. 125
HDPE	0.25	2.25	0.95	-120/-90	ca. 130
PP	0.15	2.10	0.91	-10	160-170
PA-6	0.25	2.15	1.13	50	215-225
PA-6.6	0.24	2.15	1.14	55	250-260
PET	0.29	1.55	1.35	70	250-260
PBT	0.21	1.25	1.35	45	ca. 220

References

- [1] RAO, N. S.: Designing Machines and Dies for Polymer Processing, Hanser Publishers, Munich (1981)
- [2] Kalivoda, P.: Lecture, Seminar: Optimieren von Kunststoffmaschinen und -werkzeugen mit EDV, Haus der Technik, Essen (1982)
- [3] MUNSTEDT, H.: Berechnen von Extrudierwerkzeugen, VDI-Verlag, Düsseldorf (1978)
- [4] RAUWENDAAL, C.: Polymer Extrusion, Hanser Publishers, Munich (2001)
- [5] Kenndaten für die Verarbeitung thermoplastischer Kunststoffe, Teil I, Thermodynamik, Hanser Publishers, Munich (1979)
- [6] Proceedings, 9. Kunststofftechnisches Kolloquium, IKV, Aachen (1978), p. 52

3 Formulas of Heat Transfer

Heat transfer and flow processes occur in the majority of polymer processing machinery and often determine the production rate. Designing and optimizing machine elements and processes therefore require knowledge of the fundamentals of these phenomena. The flow behavior of polymer melts has been dealt with in Chapter 2. In the present chapter, the principles of heat transfer relevant to polymer processing are treated and explained with examples.

3.1 Steady State Conduction

Fourier's law for one-dimensional conduction is given by

$$\dot{Q} = -\lambda A \frac{\mathrm{d}T}{\mathrm{d}x} \tag{3.1}$$

where

Q = heat flow thermal conductivity

A =area perpendicular to the direction of heat flow

T = temperature

x = distance (Figure 3.1)

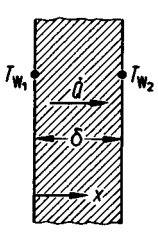


Figure 3.1 Plane wall [1]

3.1.1 Plane Wall

Temperature profile (Figure 3.1) [1]:

$$T(x) = \frac{(T_{W_2} - T_{W_1})}{\delta} \cdot x + T_{W_1}$$
(3.2)

Heat flow:

$$\dot{Q} = \frac{\lambda}{\delta} \cdot A \cdot (T_{W_1} - T_{W_2}) \tag{3.3}$$

Analogous to Ohm's law in electric circuit theory, Equation 3.3 can be written as [2]

$$\dot{Q} = \frac{\Delta T}{R} \tag{3.4}$$

in which

$$R = \frac{\delta}{\lambda \cdot A} \tag{3.5}$$

where

 ΔT = temperature difference

 δ = wall thickness

R = thermal resistance

Example

The temperatures of a plastic sheet (30 mm thick) with a thermal conductivity $\lambda = 0.335 \text{ W/(m K)}$ are $T_{W_1} = 100 \,^{\circ}\text{C}$ and $T_{W_2} = 40 \,^{\circ}\text{C}$ according to Figure 3.1. Calculate the heat flow per unit area of the sheet.

Solution

Substituting the given values in Equation 3.3 we obtain

$$\frac{\dot{Q}}{A} = \frac{0.335}{(30/1000)} \cdot (100 - 40) = 670 \text{ W/m}^2$$

3.1.2 Cylinder

Temperature distribution (Figure 3.2) [1]:

$$T(r) = T_{W_1} + \frac{T_{W_2} - T_{W_1}}{\ln\left(\frac{r_2}{r_1}\right)} \cdot \ln\left(\frac{r}{r_1}\right)$$
 (3.6)

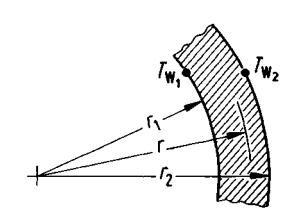


Figure 3.2 Cylindrical wall [1]

Heat flow:

$$\dot{Q} = \frac{\lambda}{\delta} \cdot A_{\rm m} \cdot (T_{W_1} - T_{W_2}) \tag{3.7}$$

with the log mean surface area $A_{\rm m}$ of the cylinder

$$A_{\rm m} = \frac{A_2 - A_1}{\ln\left(\frac{A_2}{A_1}\right)} \tag{3.8}$$

where $\delta = r_2 - r_1$.

3.1.3 Hollow Sphere

Temperature distribution [1]:

$$T(r) = \frac{1}{r} \frac{(T_{W_1} - T_{W_2}) r_1 r_2}{r_2 - r_1} - \frac{(T_{W_1} r_1 - T_{W_2} r_2)}{r_2 - r_1}$$
(3.9)

with the boundary conditions

$$T(r = r_1) = T_{W_1}$$
 and $T(r = r_2) = T_{W_2}$

Heat flow:

$$\dot{Q} = \frac{\lambda}{\delta} \cdot A_{\rm m} \cdot (T_{W_1} - T_{W_2}) \tag{3.10}$$

The geometrical mean area $A_{\rm m}$ of the sphere is

$$A_{\rm m} = \sqrt{A_1 A_2} \tag{3.11}$$

The wall thickness δ is

$$\delta = r_2 - r_1 \tag{3.12}$$

3.1.4 Sphere

Heat flow from a sphere in an infinite medium $(r_2 \rightarrow \infty)$ [1]

$$\dot{Q} = 4\pi r_1 \lambda (T_{W_1} - T_{\infty}) \tag{3.13}$$

where T_{∞} = temperature at a very large distance.

Figure 3.3 shows the temperature profiles of the one-dimensional bodies treated above [1].

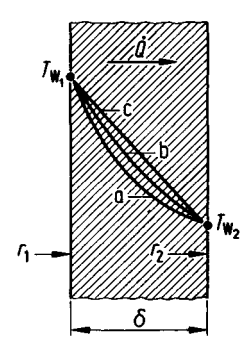


Figure 3.3 One-dimensional heat transfer [1] a: sphere, b: cylinder, c: plate

3.1.5 Heat Conduction in Composite Walls

Following the electrical analogy, heat conduction through a multiple layer wall can be treated as a current flowing through resistances connected in series. With this concept we obtain for the heat flow through the composite wall as shown in Figure 3.4

$$T_{W_1} - T_{W_2} = \dot{Q} \frac{\delta_1}{\lambda_1 A_1} \tag{3.14}$$

$$T_{W_2} - T_{W_3} = \dot{Q} \frac{\delta_2}{\lambda_2 A_2} \tag{3.15}$$

$$T_{W_3} - T_{W_4} = \dot{Q} \frac{\delta_3}{\lambda_3 A_3} \tag{3.16}$$

Adding Equation 3.14 to Equation 3.16 and setting $A_1 = A_2 = A_3 = A$ gives

$$T_{W_1} - T_{W_4} = \dot{Q} \left(\frac{\delta_1}{\lambda_1} + \frac{\delta_2}{\lambda_2} + \frac{\delta_3}{\lambda_3} A \right) = \Delta T$$
 (3.17)

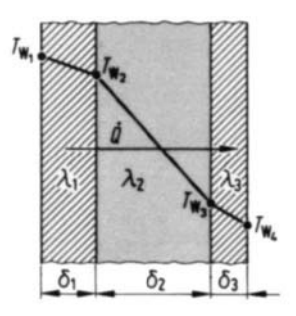


Figure 3.4 Heat transfer through a composite wall [1]

Thus

$$\dot{Q} = \frac{\Delta T}{\left(\frac{\delta_1}{\lambda_1 A} + \frac{\delta_2}{\lambda_2 A} + \frac{\delta_3}{\lambda_3 A}\right)}$$
(3.18)

Inserting the conduction resistances

$$R_1 = \frac{\delta_1}{\lambda_1 A_1} \tag{3.19}$$

$$R_2 = \frac{\delta_2}{\lambda_2 A_2} \tag{3.20}$$

$$R_3 = \frac{\delta_3}{\lambda_3 A_3} \tag{3.21}$$

into Equation 3.18 we get

$$\dot{Q} = \frac{\Delta T}{(R_1 + R_2 + R_3)} = \frac{\Delta T}{R} \tag{3.22}$$

Example 1

A two-layer wall consists of the following insulating materials (see Figure 3.4):

$$d_1 = 16 \text{ mm}, \quad l_1 = 0.048 \text{ W/(m K)}$$

 $d_2 = 140 \text{ mm}, \quad l_2 = 0.033 \text{ W/(m K)}$

The temperatures are $T_{W_1} = 30$ °C, $T_{W_2} = 2$ °C. Calculate the heat loss per unit area of the wall.

Solution

$$\Delta T = T_{W_1} - T_{W_2} = 30 - 2 = 28 \, ^{\circ}\text{C}$$

Area $A = 1 \text{ m}^2$

$$R_1 = \frac{\delta_1}{\lambda_1 A} = \frac{16/1000}{0.048 \cdot 1} = 0.33 \text{ K/W}$$

$$R_2 = \frac{\delta_2}{\lambda_2 A} = \frac{140/1000}{0.033 \cdot 1} = 4.24 \text{ K/W}$$

$$\dot{Q} = \frac{\Delta T}{(R_1 + R_2)} = \frac{28}{(4.24 + 0.33)} = 6.13 \text{ W}$$

The following example [2] illustrates the calculation of heat transfer through a tube as shown in Figure 3.5.

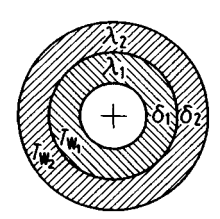


Figure 3.5 Heat flow in a multilayered cylinder

Example 2

A tube with an outside diameter of 60 mm is insulated with the following materials:

$$d_1 = 50 \text{ mm}, \quad l_1 = 0.055 \text{ W/(m K)}$$

 $d_2 = 40 \text{ mm}, \quad l_2 = 0.05 \text{ W/(m K)}$

The temperatures are $T_{\rm W_1}=150~\rm ^{\circ}C$ and $T_{\rm W_2}=30~\rm ^{\circ}C$. Calculate the heat loss per unit length of the tube.

Solution

Resistance R_1 :

$$R_1 = \frac{\delta_1}{\lambda_1 \ \overline{A}_1} = \frac{0.05}{0.055 \cdot 2 \pi \overline{\tau}_1 \cdot L} \text{ K/W}$$

average radius $\overline{r_i}$:

$$\overline{t_1} = \frac{(80 - 30)}{\ln\left(\frac{80}{30}\right)} = 50.97 \text{ mm}$$

$$R_1 = \frac{2.839}{I} \text{ K/W}$$

Resistance R_2 :

$$R_2 = \frac{\delta_2}{\lambda_2 \, \overline{A}_2} = \frac{0.04}{0.05 \cdot 2 \, \pi \, \overline{r}_2 \cdot L} \, \text{K/W}$$

average radius \overline{r}_2 :

$$\overline{r_2} = \frac{(120 - 80)}{\ln\left(\frac{120}{80}\right)} = 98.64 \text{ mm}$$

$$R_2 = \frac{1.291}{L} \text{ K/W}$$

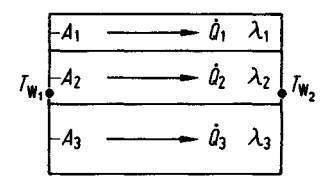


Figure 3.6 Heat transfer in composite walls in parallel [1]

Heat loss per unit length of the tube according to Equation 3.22:

$$\frac{\dot{Q}}{L} = \frac{150 - 30}{2.839 + 1.291} = 29.1 \text{ W/m}$$

In the case of multiple-layer walls, in which the heat flow is divided into parallel flows as shown in Figure 3.6, the total heat flow is the sum of the individual heat flows. Therefore we have

$$\dot{Q} = \sum_{i=1}^{z} Q_i \tag{3.23}$$

$$\dot{Q} = \sum_{i=1}^{z} (\lambda_i \ A_i) \frac{T_{W_1} - T_{W_2}}{\delta}$$
 (3.24)

3.1.6 Overall Heat Transfer through Composite Walls

If heat exchange takes place between a fluid and a wall as shown in Figure 3.7, in addition to the conduction resistance we also have convection resistance, which can be written as

$$R_{c_1} = \frac{1}{\alpha_1 A_1} \tag{3.25}$$

where α_I = heat transfer coefficient in the boundary layer near the walls adjacent to the fluids.

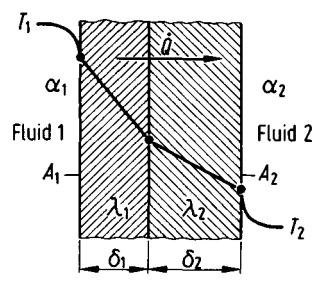


Figure 3.7 Conduction and convection through a composite wall [1]

The combination of convection and conduction in stationary walls is called overall heat transfer and can be expressed as

$$\dot{Q} = k A (T_1 - T_2) = \frac{1}{R_W} (T_1 - T_2)$$
 (3.26)

where k is denoted as the overall heat transfer coefficient with the corresponding overall resistance $R_{\rm W}$

$$R_{\rm W} = \frac{1}{k A} \tag{3.27}$$

Analogous to conduction for the composite wall in Figure 3.7, the overall resistance R_W can be given by

$$R_{W} = R_{c_1} + \sum_{i=1}^{z} R_i + R_{c_2}$$
 (3.28)

or

$$\frac{1}{k A} = \frac{1}{\alpha_1 A_1} + \sum_{i=1}^{z} \frac{\delta_i}{\lambda_i A_i} + \frac{1}{\alpha_2 A_2}$$
 (3.29)

A simplified form of Equation 3.29 is

$$k = \frac{1}{\frac{1}{\alpha_1} + \sum_{i=1}^{z} \frac{\delta_i}{\lambda_i} + \frac{1}{\alpha_2}}$$
(3.30)

Calculation of the convection heat transfer coefficient is shown in the Section 3.5.

3.2 Transient State Conduction

The differential equation for the transient one-dimensional conduction after Fourier is given by

$$\frac{\partial T}{\partial t} = a \frac{\partial^2 T}{\partial x^2} \tag{3.31}$$

where

T = temperature

t = time

x = distance

The thermal diffusivity a in this equation is defined as

$$a = \frac{\lambda}{\rho c_{\rm p}} \tag{3.32}$$

where

 λ = thermal conductivity

 $c_{\rm p}$ = specific heat at constant pressure

 \vec{p} = density

The numerical solution of Equation 3.31 is given in Section 4.3.4. For commonly occurring geometrical shapes, analytical expressions for transient conduction are given in the following sections.

3.2.1 Temperature Distribution in One-Dimensional Solids

The expression for the heating or cooling of an infinite plate [2] follows from Equation 3.31 (Figure 3.8):

$$\frac{T_{\rm W} - \overline{T}_{\rm b}}{T_{\rm W} - T_{\rm a}} = \frac{8}{\pi^2} \left(e^{-a_1 F_0} + \frac{1}{9} e^{-9a_1 F_0} + \frac{1}{25} e^{-25a_1 F_0} + \dots \right)$$
(3.33)

The Fourier number F_0 is defined by

$$F_0 = \frac{a \cdot t_k}{X^2} \tag{3.34}$$

where

 $T_{\rm W}$ = constant surface temperature of the plate

 T_a = initial temperature

 $\vec{T}_{\rm b}$ = average temperature of the plate at time $t_{\rm T}$

 t_k = heating or cooling time

 \ddot{X} = half thickness of the plate [$X = \frac{3}{2}$]

 $a_1 = (\pi/2)^2$

a =thermal diffusivity, Equation 3.32

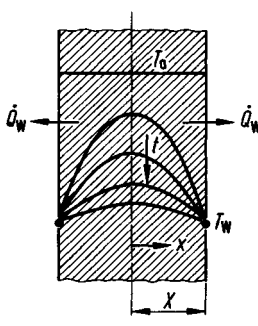


Figure 3.8 Non-steady-state conduction in an infinite plate

The equation for an infinite cylinder with the radius $r_{\rm m}$ is given by [2]

$$\frac{T_{\rm W} - \bar{T}_{\rm b}}{T_{\rm W} - T_{\rm a}} = 0.692 \, e^{-5.78 \, F_{\rm 0}} + 0.131 \, e^{-30.5 \, F_{\rm 0}} + 0.0534 \, e^{-74.9 \, F_{\rm 0}} + \dots \tag{3.35}$$

and for a sphere with the radius $r_{\rm m}$

$$\frac{T_{\rm W} - \bar{T}_{\rm b}}{T_{\rm W} - T_{\rm a}} = 0.608 \, e^{-9.87 \, F_{\rm 0}} + 0.152 \, e^{-39.5 \, F_{\rm 0}} + 0.0676 \, e^{-88.8 \, F_{\rm 0}} + \dots \tag{3.36}$$

where

$$F_0 = \frac{a \cdot t_{\rm k}}{r_{\rm m}^2} \tag{3.37}$$

In the range of $F_0 > 1$, only the first term of these equations is significant. Therefore, for the heating or cooling time we obtain [2]

Plate:

$$t_{k} = \frac{1}{a} \cdot \left(\frac{s}{\pi}\right)^{2} \ln \left[\left(\frac{8}{\pi^{2}}\right) \left(\frac{T_{W} - T_{a}}{T_{W} - \overline{T}_{b}}\right) \right]$$
(3.38)

Cylinder:

$$t_{k} = \frac{r_{\rm m}^{2}}{5.78 \, a} \ln \left[0.692 \left(\frac{T_{\rm W} - T_{\rm a}}{T_{\rm W} - \overline{T}_{\rm b}} \right) \right] \tag{3.39}$$

Sphere:

$$t_{k} = \frac{r_{\rm m}^{2}}{9.87 \, a} \ln \left[0.608 \left(\frac{T_{\rm W} - T_{\rm a}}{T_{\rm W} - \overline{T}_{\rm b}} \right) \right] \tag{3.40}$$

The solutions of Equation 3.32 to Equation 3.37 are presented in a semi-logarithmic plot in Figure 3.9, in which the temperature ratio $\Theta_{\overline{T}_b} = (T_W - \overline{T}_b)/(T_W - T_a)$ is shown as a function of the Fourier number F_0 .

Not considering small Fourier numbers, these plots are straight lines approximated by Equation 3.38 to Equation 3.40.

If the time t_k is based on the centre line temperature T_b instead of the average temperature \overline{T}_b , we get [3]

$$t_{k} = \frac{s^{2}}{\pi^{2} \cdot a} \ln \left[\frac{4}{\pi} \left(\frac{T_{W} - T_{a}}{T_{W} - T_{b}} \right) \right]$$
 (3.41)

Analogous to Figure 3.9, the ratio $\Theta_{\overline{T}_b}$ with the centre line temperature T_b at time t_k is plotted in Figure 3.10 over the Fourier number for bodies of different geometry [4].

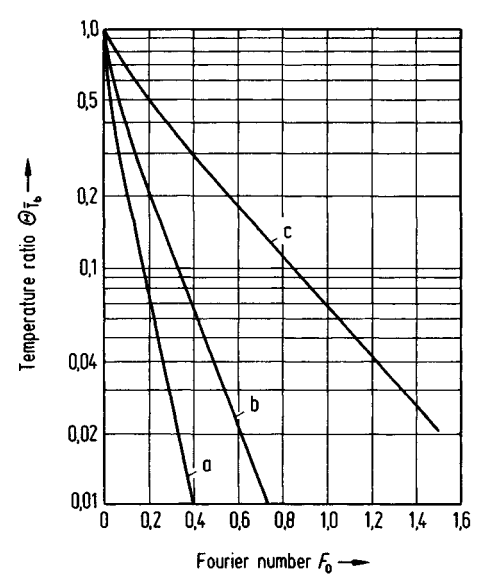


Figure 3.9 Average temperature of an infinite slab (c), a long cylinder (b) and a sphere (a) during non-steady heating of cooling [2]

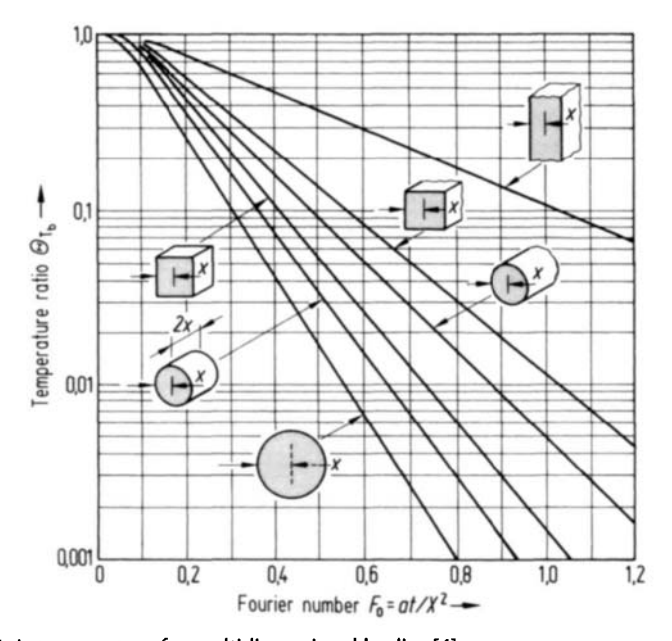


Figure 3.10 Axis temperature for multidimensional bodies [4]

The foregoing equations apply to cases, in which the thermal resistance between the body and the surroundings is negligibly small ($\alpha_0 \rightarrow \infty$), for example, in injection molding between the part and the coolant. This means that the Biot number should be very large, Bi $\rightarrow \infty$. The Biot number for a plate is

$$Bi_{\text{plate}} = \frac{\alpha_{\text{a}} \cdot X}{\lambda} \tag{3.42}$$

where

 α_a = heat transfer coefficient of the fluid λ = thermal conductivity of the plastic

As the heat transfer coefficient has a finite value in practice, the temperature ratio Θ_{T_h} based on the centre line temperature, is given in Figure 3.11 as a function of the Fourier number with the reciprocal of the Biot number as parameter [5].

Example 1 [6]

Cooling of a part in an injection mold for the following conditions:

Resin: **LDPE**

Thickness of the plate: = 12.7 mmS Temperature of the melt: $T_a = 243.3$ °C $T_{\rm W} = 21.1 \,{\rm ^{\circ}C}$ Mold temperature: Demolding temperature: $T_b = 76.7 \text{ °C}$ Thermal diffusivity: $a = 1.29 \cdot 10^{-3} \text{ cm}^2/\text{s}$

The cooling time t_k is to be calculated.

Solution

The temperature ratio Θ_{T_b} :

$$\Theta_{T_b} = \frac{T_b - T_W}{T_W - T_a} = \frac{76.7 - 21.1}{243.3 - 21.1} = 0.25$$

Fourier number F_0 from Figure 3.10 at $\Theta_{T_h} = 0.25$

$$F_0 = 0.65$$

cooling time t_k :

$$X = \frac{s}{2} = \frac{12.7}{2} = 6.35 \text{ mm}$$

$$F_0 = \frac{a \cdot t_k}{X^2} = \frac{1.29 \cdot 10^{-3} \cdot t_k}{0.635^2} = 0.65$$

$$t_{\rm k} = 203 {\rm s}$$

Example 2 [6]

Calculate the cooling time t_k in Example 1 if the mold is cooled by a coolant with a heat transfer coefficient of $\alpha_a = 2839 \text{ W/(m}^2 \cdot \text{K})$.

Solution

$$\alpha_a = 2839 \text{ W/(m}^2 \cdot \text{K)}$$

 $\lambda_{\text{plastic}} = 0.242 \text{ W/(m} \cdot \text{K)}$

The resulting Biot number is

Bi =
$$\frac{\alpha_a \cdot X}{\lambda} = \frac{2839 \cdot 6.35}{0.242 \cdot 1000} = 74.49$$
 $\frac{1}{Bi} = 0.01342$

As can be extrapolated from Figure 3.11, the Fourier number does not differ much from the one in the previous example for $\Theta_{T_b} = 0.25$ and 1/Bi = 0.01342. The resistance due to convection is therefore negligible and the cooling time remains almost the same. However, the convection resistance has to be taken into account in the case of a film with a thickness of 127 μ that is cooling in quiescent air, as shown in the following calculation:

The heat transfer coefficient for this case is approximately

$$a_a = 56.78 \text{ W/(m}^2 \cdot \text{K)}$$

The Biot number Bi

Bi =
$$\frac{56.78 \cdot 63.5}{10^6 \cdot 0.242} = 0.0149$$
 $\frac{1}{\text{Bi}} = 67.1$

 F_0 from Figure 3.11

$$F_0 = 95$$

The cooling time

$$t_{\rm k} = \frac{X^2 \cdot F_0}{a} = \frac{65.5^2 \cdot 10^3 \cdot 95}{10^8 \cdot 1.29} = 2.97 \, s$$

Example 3 [7]

Cooling of an extruded wire

A polyacetal wire of diameter 3.2 mm is extruded at 190 °C into a water bath at 20 °C. Calculate the length of the water bath to cool the wire from 190 °C to a centre line temperature of 140 °C. The following conditions are given:

$$\alpha_{\rm a} = 1700 \text{ W/(m}^2 \cdot \text{K)}$$
 $a_{\rm plastic} = 10^{-7} \text{ m}^2 / \text{s}$
 $\lambda_{\rm plastic} = 0.23 \text{ W/(m} \cdot \text{K)}$

haul-off rate of the wire $V_{\rm H} = 0.5$ m/s

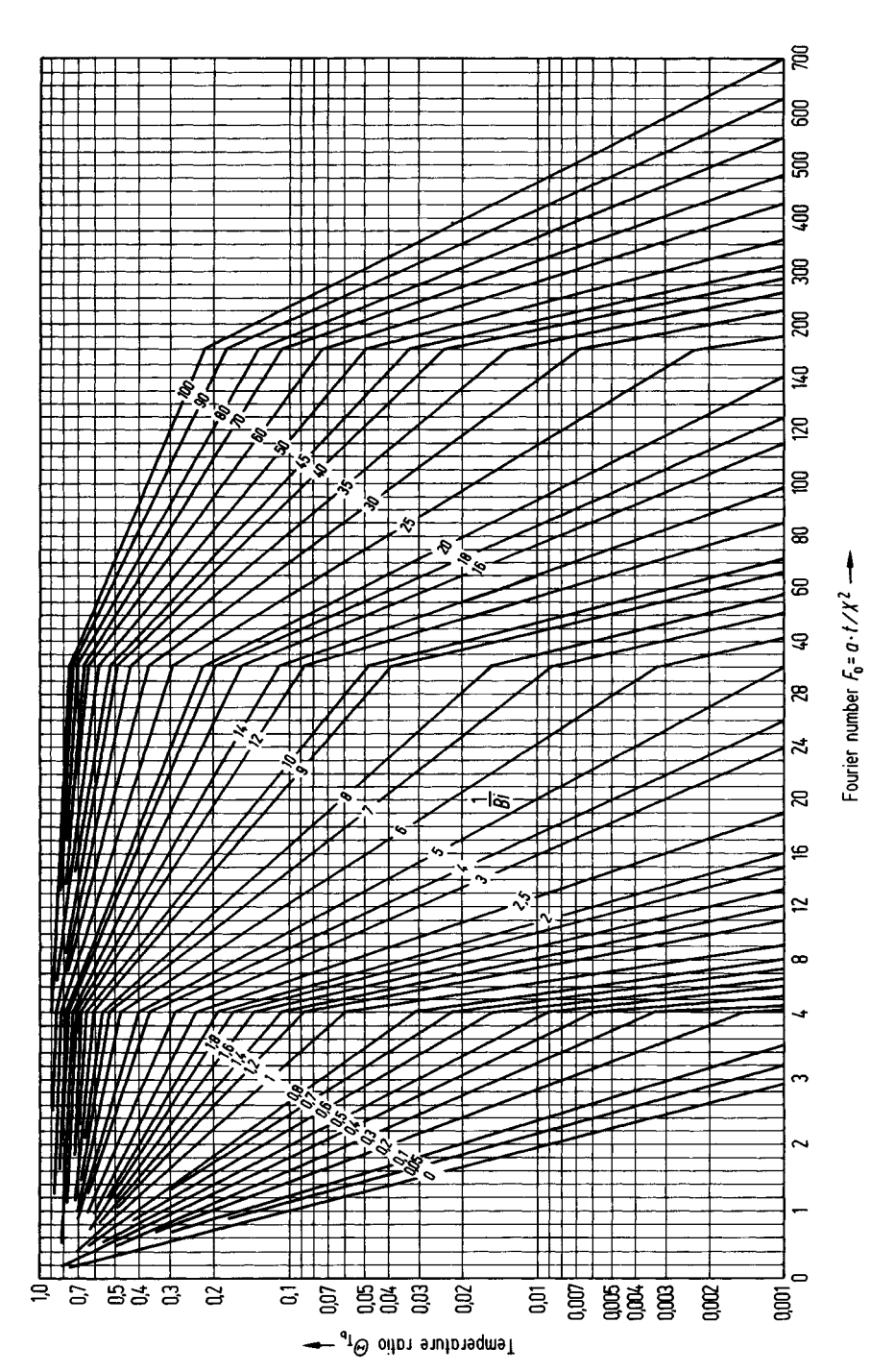


Figure 3.11 Midplane temperature for an infinite plate [5]

Solution

The Biot number Bi =
$$\frac{\alpha_a \cdot X}{\lambda}$$

where R = radius of the wire

Bi =
$$\frac{1700 \cdot 1.6}{1000 \cdot 0.23} = 11.13$$
 $\frac{1}{Bi} = 0.0846$

The temperature ratio Θ_{T_b}

$$\Theta_{T_b} = \frac{T_b - T_W}{T_W - T_a} = \frac{140 - 20}{190 - 20} = 0.706$$

The Fourier number F_0 for $\Theta_{T_b} = 0.706$ and $\frac{1}{\text{Bi}} = 0.0846$ from Figure 3.11 is approximately

$$F_0 \approx 0.16$$

The cooling time t_k follows from

$$\frac{a \cdot t_k}{R^2} = \frac{10^{-7} \cdot t_k}{(1.6 \cdot 10^{-3})^2} = \frac{t_k}{2.56 \cdot 10} = 0.16$$

$$t_k = 4.1 \text{ s}$$

The length of the water bath is

$$V_{\rm H} \cdot t_{\rm k} = 0.5 \cdot 4.1 = 2.05 \,\rm m$$

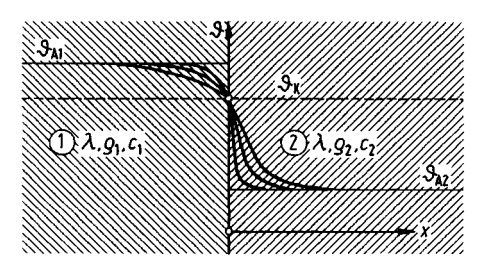
3.2.2 Thermal Contact Temperature

If two semi infinite bodies of different initial temperatures Θ_{A_1} and Θ_{A_2} are brought into contact as indicated in Figure 3.12, the resulting contact temperature Θ_K is given by [3]

$$\Theta_{K} = \frac{\Theta_{A_{1}} + \frac{(\sqrt{\lambda \rho c})_{2}}{(\sqrt{\lambda \rho c})_{1}} \Theta_{A_{2}}}{1 + \frac{(\sqrt{\lambda \rho c})_{2}}{(\sqrt{\lambda \rho c})_{1}}}$$
(3.43)

where

$$\begin{array}{ll} \lambda & = \text{thermal conductivity} \\ \rho & = \text{density} \\ c & = \text{specific heat} \\ \sqrt{\lambda \rho c} & = \text{coefficient of heat penetration} \end{array}$$



Temperature distribution in semi infinite solids in contact [3] Figure 3.12

Equation 3.43 also applies for the case of contact of short duration between thick bodies. It follows from this equation that the contact temperature depends on the ratio of the coefficients of heat penetration and lies nearer to the initial temperature of body that has a higher coefficient of penetration. The ratio of the temperature differences $(\Theta_{A_1} - \Theta_K)$ and $(\Theta_K - \Theta_{A_2})$ are inversely proportional to the coefficient of penetration:

$$\frac{\Theta_{A_1} - \Theta_K}{\Theta_K - \Theta_{A_2}} = \frac{(\sqrt{\lambda \rho c})_2}{(\sqrt{\lambda \rho c})_1}$$
(3.44)

Example

According to Equation 3.43 [8] the contact temperature $\Theta_{w_{max}}$ of the wall of an injection mold at the time of injection is

$$\Theta_{w_{\text{max}}} = \frac{b_{\text{W}} \Theta_{w_{\text{min}}} + b_{\text{p}} \Theta_{\text{M}}}{b_{\text{w}} + b_{\text{p}}}$$
(3.45)

where

$$b = \sqrt{\lambda \rho c}$$

 $\begin{array}{ll} b & = \sqrt{\lambda \, \rho \, c} \\ \Theta_{w_{\min}} & = \text{temperature before injection} \\ \Theta_{M} & = \text{melt temperature} \end{array}$

Indices w and p refer to mold and polymer, respectively.

As shown in Table 3.1 [8], the coefficients of heat penetration of metals are much higher than those of polymer melts. Hence the contact temperature lies in the vicinity of the mold wall temperature before injection.

The values given in the Table 3.1 refer to the following units of the properties:

thermal conductivity λ : W/(m · K) density ρ : kg/m³ specific heat c: $kJ/(kg \cdot K)$

Material	Coefficient of heat penetration b Ws ^{0.5} · m ⁻² · K ⁻¹	
Beryllium copper (BeCu 25)	17.2 · 10³	
Unalloyed steel (C45W3)	$13.8\cdot10^{3}$	
Chromium steel (X40Crl3)	$11.7\cdot 10^3$	
Polyethylene (HDPE)	$0.99\cdot10^3$	
Polystyrene (PS)	$0.57\cdot 10^{^3}$	

Table 3.1 Coefficients of Heat Penetration of Mold Material and Resin [8]

The approximate values for steel are

$$\lambda = 50 \text{ W/(m} \cdot \text{K})$$

 $\rho = 7850 \text{ kg/m}^3$
 $c = 0.485 \text{ kJ/(kg} \cdot \text{K})$

The coefficient of heat penetration b

$$b = \sqrt{\lambda \cdot \rho \cdot c} = \sqrt{50 \cdot 7.85 \cdot 10^3 \cdot 0.485 \cdot 10^3} = 13.8 \cdot 10^3 \text{ Ws}^{0.5} \cdot \text{m}^{-2} \cdot \text{K}^{-1}$$

3.3 Heat Conduction with Dissipation

The power created by the tangential forces in the control volume of the fluid flow is denoted as dissipation [9]. In shear flow the rate of energy dissipation per unit volume is equal to the product of shear force and shear rate [10]. The power due to dissipation [11] therefore is:

$$\dot{E}_{\rm d} = \tau \cdot \dot{\gamma} \tag{3.46}$$

From the power law we get

$$\dot{E}_{d} = \left(\frac{1}{K}\right)^{\frac{1}{n}} \cdot \dot{\gamma}^{\frac{1}{n+1}} \tag{3.47}$$

For a Newtonian fluid with n = 1 we obtain

$$\dot{E}_{\rm d} = \eta \cdot \dot{\gamma}^2 \tag{3.48}$$

The applicable differential equation for a melt flow between two plates, where the upper plate is moving with a velocity U_x (Figure 2.4) and the lower plate is stationary [11] is

$$\lambda \frac{\partial^2 T}{\partial y^2} + \eta \left(\frac{\partial u_x}{\partial y} \right)^2 = 0 \tag{3.49}$$

For drag flow the velocity gradient is given by

$$\frac{\partial u}{\partial y} = \frac{U_{x}}{H} \tag{3.50}$$

Equation 3.49 can now be written as

$$\lambda \frac{\partial^2 T}{\partial y^2} + \eta \left(\frac{U_x}{H}\right)^2 = 0 \tag{3.51}$$

If the temperature of the upper plate is T_1 and that of lower plate is T_0 , the temperature profile of the melt is obtained by integrating Equation 3.51. The resulting expression is

$$T = \frac{\eta U_{x} \cdot y}{2 \lambda H} \left(1 - \frac{y}{H} \right) + \frac{y}{H} (T_{1} - T_{0}) + T_{0}$$
 (3.52)

As shown in Section 4.2.3, this equation can be used to calculate the temperature of the melt film in an extruder.

3.4 Dimensionless Groups

Dimensionless groups can be used to describe complicated processes that are influenced by a large number of variables with the advantage that the entire process can be analyzed on a sound basis by means of a few dimensionless parameters. Their use in correlating experimental data and in scaling-up of equipment is well known.

Table 3.2 shows some of the dimensionless groups often used in plastics engineering.

Table 3.2 Dimensionless Groups

Symbol	Name	Definition	
Bi	Biot number	α, 1 / λ,	
Br	Brinkman number	$\eta w^2 / (\lambda \Delta T)$	
Deb	Deborah number	$t_{\rm D}$ / $t_{\rm p}$	
$\mathbf{F}_{_{0}}$	Fourier number	at/l^2	
Ğr	Grashof number	$g \boldsymbol{\beta} \cdot \Delta T l^3 / v^2$	
Gz	Graetz number	$l^2/(a \cdot t_v)$	
Le	Lewis number	a / δ	
Na	Nahme number	$oldsymbol{eta}_{\!\scriptscriptstyle { m T}} w^2 oldsymbol{\eta} / oldsymbol{\lambda}$	
Nu	Nusselt number	$\alpha l / \lambda$	
Pe	Peclet number	w l / a	
Pr	Prandtl number	v / a	
Re	Reynolds number	$\rho w l / \eta$	
Sh	Sherwood number	β1/δ	
Sc	Schmidt number	v/δ	
Sk	Stokes number	$P \cdot l / (\eta \cdot w)$	

Nomenclature:

	thermal diffusivity	(m^2/s)
g:	acceleration due to gravity	(m/s^2)
	characteristic length	(m)
p:	ressure	(N/m^2)
t:	time	(s)

Indices

D, P: memory and process of polymer respectively

 ΔT : Temperature difference (K)

w: Velocity of flow (m/s)

 α_a : Outside heat transfer coefficient [W/(m² · K)]

 β : Coefficient of volumetric expansion (K^{-1})

 β_{Γ} : Temperature coefficient in the power law of viscosity (K^{-1})

 β_s : Mass transfer coefficient (m/s) δ : Diffusion coefficient (m²/s)

 η : Viscosity (Ns/m²)

 λ : Thermal conductivity (Index *i* refers to the inside value) [W/(m K)]

 ν : Kinematic viscosity (m^2/s)

 $t_{\rm v}$: Residence time (s)

 ρ : Density (kg/m³)

3.4.1 Physical Meaning of Dimensionless Groups

Biot number: Ratio of thermal resistances in series: $(l/\lambda_i)/(1/\alpha_a)$

Application: heating or cooling of solids by heat transfer through conduction and

convection

Brinkmann number: ratio of heat dissipated (ηw^2) to heat conducted $(\lambda \Delta T)$

Application: polymer melt flow

Fourier number: ratio of a characteristic body dimension to an approximate temperature wave penetration depth for a given time [16]

Application: unsteady state heat conduction

Deborah number: ratio of the period of memory of the polymer to the duration of processing [13]. At Deb > 1 the process is determined by the elasticity of the material, whereas at Deb < 1 the viscous behavior of the polymer influences the process remarkably.

Grashof number: ratio of the buoyant force $\hat{g} \hat{\beta} \cdot \Delta T l^3$ to frictional force (ν)

Application: heat transfer by free convection

Graetz number: ratio of the time to reach thermal equilibrium perpendicular to the flow direction (l^2/a) to the residence time (t_v)

Application: heat transfer to fluids in motion

Lewis number: ratio of thermal diffusivity (a) to the diffusion coefficient (δ) Application: phenomena with simultaneous heat and mass transfer.

Nusselt number: ratio of the total heat transferred $(\alpha \cdot l)$ to the heat by conduction (λ) Application: convective heat transfer.

Peclet number: ratio of heat transfer by convection $(\rho c_p \cdot w \cdot l)$ to the heat by conduction (λ)

Application: heat transfer by forced convection.

Nahme or Griffith number: ratio of viscous dissipation $(\beta_T w^2 \eta)$ to the heat by conduction (λ) perpendicular to the direction of flow

Application: heat transfer in melt flow

Prandtl number: ratio of the kinematic viscosity (ν) to thermal diffusivity (a) Application: convective heat transfer

Reynolds number: ratio of the inertial force $(\rho w l)$ to viscous force (η)

Application: The Reynolds number serves as a criterium to judge the type of flow. In pipe flow, when Re is less than 2300 the flow is laminar. The flow is turbulent at Re greater than about 4000. Between 2100 and 4000 the flow may be laminar or turbulent depending on conditions at the entrance of the tube and on the distance from the entrance [2]

Application: fluid flow and heat transfer.

Sherwood number: ratio of the resistance to diffusion (l/δ) to the resistance to mass transfer $(1/\beta_s)$

Application: mass transfer problems

Schmidt number: ratio of kinematic viscosity (ν) to the diffusion coefficient (δ) Application: heat and mass transfer problems

Stokes number: ratio of pressure forces $(p \cdot l)$ to viscous forces $(\eta \cdot w)$

Application: pressure flow of viscous media like polymer melts.

The use of dimensionless numbers in calculating non Newtonian flow problems is illustrated in Section 4.3.3 with an example.

3.5 Heat Transfer by Convection

Heat transfer by convection, particularly by forced convection, plays an important role in many polymer processing operations such as in cooling a blown film or a part in an injection mold, to mention only two examples. A number of expressions can be found in the literature on heat transfer [3] for calculating the heat transfer coefficient α (see Section 3.1.6). The general relationship for forced convection has the form

$$Nu = f(Re, Pr) (3.53)$$

The equation for the turbulent flow in a tube is given by [16]

$$Nu = 0.027 \text{ Re}^{0.8} \cdot \text{Pr} \tag{3.54}$$

where

n = 0.4 for heating n = 0.3 for cooling

The following equation applies to laminar flow in a tube with a constant wall temperature [3]

$$Nu_{lam} = \sqrt[3]{3.66^3 + 1.61^3 \text{ Re} \cdot \text{Pr} \cdot d_i / l}$$
 (3.55)

where

 d_i = inside tube diameter

l = tube length

The expression for the laminar flow heat transfer to flat plate is [3]

$$Nu_{lam} = 0.664 \sqrt{Re} \sqrt[3]{Pr}$$
 (3.56)

Equation 3.56 is valid for Pr = 0.6 to 2000 and $Re < 10^5$.

The equation for turbulent flow heat transfer to flat plate is given as [3]

$$Nu_{turb} = \frac{0.037 \text{ Re}^{0.8} \cdot Pr}{1 + 2.448 \text{ Re}^{-0.1} (Pr^{2/3} - 1)}$$
(3.57)

Equation 3.57 applies for the conditions:

$$Pr = 0.6 \text{ to } 2000 \text{ and } 5 \cdot 10^5 < Re < 10^7.$$

The properties of the fluids in the equations above are to be found at a mean fluid temperature.

Example

A flat film is moving in a coating equipment at a velocity of 130 m/min on rolls that are 200 mm apart. Calculate the heat transfer coefficient α if the surrounding medium is air at a temperature of 50 °C.

Solution

The properties of air at 50 °C are:

Kinematic viscosity $\nu = 17.86 \cdot 10^{-6} \text{ m}^2/\text{s}$ Thermal conductivity $\lambda = 28.22 \cdot 10^{-3} \text{ W}/(\text{m} \cdot \text{K})$

Prandtl number Pr = 0.69

The Reynolds number Re_1 , based on the length L = 200 mm is

$$Re_L = 130 \cdot \frac{1}{60} \cdot 0.2/17.86 \cdot 10^{-6} = 24262$$

Substituting $Re_L = 24262$ and Pr = 0.69 into Equation 3.56 gives

$$Nu_{lam} = 0.664 \cdot 24262^{0.5} \cdot 0.69^{1/3} = 91.53$$

As the fluid is in motion on both sides of the film, the Nusselt number is calculated according to [3]

$$Nu = \sqrt{Nu_{lam}^2 + Nu_{turb}^2}$$

For turbulent flow Nu_{turb} follows from Equation 3.57:

$$Nu_{turb} = \frac{0.037 \cdot 24262^{0.8} \cdot 0.69}{1 + 2.448 \cdot 24262^{-0.1} (0.69^{2/3} - 1)} = 102$$

The resulting Nusselt number Nu is

$$Nu = \sqrt{91.53^2 + 102^2} = 137$$

Heat transfer coefficient α results from

$$\alpha = \frac{\text{Nu} \cdot \lambda}{l} = \frac{137 \cdot 28.22 \cdot 10^{-3}}{0.2} = 19.33 \text{ W/(m}^2 \cdot \text{K)}$$

3.6 Heat Transfer by Radiation

Heating by radiation is used in thermoforming processes to heat sheets or films, so that the shaping process can take place. Because at temperatures above 300 °C a substantial part of the thermal radiation consists of wavelengths in the infrared range, heat transfer by radiation is also termed as infrared radiation [14]. According to the Stefan-Boltzmann law the rate of energy radiated by a black body per unit area \dot{e}_s is proportional to the absolute temperature T to the fourth power (Figure 3.13) [1]:

$$\dot{e}_{\rm s} = \sigma T^4 \tag{3.58}$$

The Stefan-Boltzmann constant has the value

$$\sigma = 5.77 \cdot 10^{-12} \,\mathrm{W/(cm^2 \cdot K^4)}$$

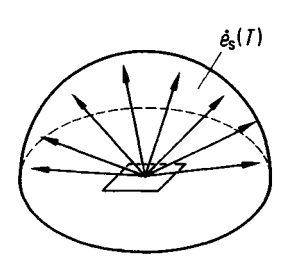


Figure 3.13
Black body radiation [1]

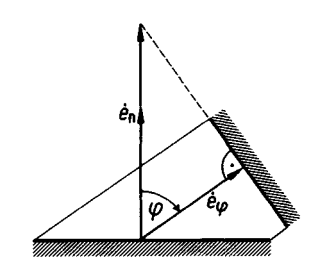


Figure 3.14 Lambert's law [1]

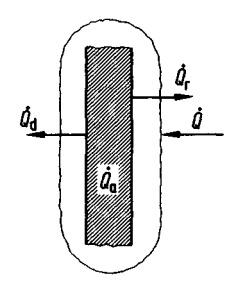


Figure 3.15
Properties of radiation

Equation 3.58 can also be written as

$$\dot{e}_s = c_s \left(\frac{T}{100}\right)^4 \tag{3.59}$$

where $c_s = 5.77 \text{ W/(m}^2 \cdot \text{K}^4)$

The dependence of the black body radiation on the direction (Figure 3.14) [1] is given by the cosine law of Lambert

$$\dot{e}_{\rm s} = \dot{e}_{\rm n} \cos \phi \tag{3.60}$$

The radiation properties of technical surfaces are defined as (Figure 3.15) [1]:

Reflectivity
$$\rho \equiv \frac{\dot{Q}_{\rm r}}{\dot{Q}}$$
 (3.61)

Absorptivity
$$\alpha \equiv \frac{\dot{Q}_a}{\dot{Q}}$$
 (3.62)

Transmissivity
$$\delta = \frac{\dot{Q}_d}{\dot{Q}}$$
 (3.63)

The sum of these fractions must be unity, or

$$\rho + \alpha + \delta = 1$$

The transmissivity δ of opaque solids is zero so that

$$\rho + \alpha = 1$$

The reflectivity of gases ρ is zero and for those gases which emit and absorb radiation

$$\alpha + \delta = 1$$

Real bodies emit only a fraction of the radiant energy that is emitted by a black body at the same temperature. This ratio is defined as the emissivity ε of the body,

$$\varepsilon = \frac{\dot{e}}{\dot{e}_{\rm s}} \tag{3.64}$$

At thermal equilibrium according to Kirchhoff's identity

$$\varepsilon = \alpha$$
 (3.65)

Radiation heat transfer between nonblack surfaces.

The net rate of radiant heat exchange between two infinite parallel plates is given by [15]

$$\dot{Q}_{12} = A \, \varepsilon_{12} \, c_s \left[\left(\frac{T_1}{100} \right)^4 - \left(\frac{T_2}{100} \right)^4 \right] \tag{3.66}$$

where

A = area

 ε_{12} = emissivity factor and is defined by

$$\varepsilon_{12} = \frac{1}{\frac{1}{\varepsilon_1} + \frac{1}{\varepsilon_{12}} - 1} \tag{3.67}$$

Indices 1 and 2 refer to the two plates.

When T_2 is much smaller than T_1 , the heat flow is approximately

$$\dot{Q}_{12} = \varepsilon_1 c_s A \left(\frac{T_1}{100}\right)^4 \tag{3.68}$$

When the heat transfer takes place by radiation and convection, the total heat transfer coefficient can be written as [15]

$$\alpha_{\text{total}} = \alpha_{\text{convection}} + \alpha_{\text{radiation}}$$

where

$$\alpha_{\text{radiation}} = \frac{\dot{Q}_{12}}{A(T_1 - T_2)}$$

Example

A plastic sheet moving at a speed of 6 m/min is heated by two high-temperature heating elements. Calculate the power required for heating the sheet from 20 °C to 140 °C:

net enthalpy of the plastic for a temperature difference of 120 °C: $\Delta h = 70 \text{ kJ/kg}$

Width of the sheet w = 600 mmThickness $s = 250 \mu$ Density of the resin $\rho = 900 \text{ kg/m}^3$ Area of the heating element $A = 0.0093 \text{ m}^2$ Emissivity of the heater $\epsilon = 0.9$

Solution

Heating power $N_{\rm H}$:

Mass flow rate of the plastic \dot{m} :

$$\dot{m} = U \cdot w \cdot s \cdot \rho = \frac{6 \cdot 0.6 \cdot 250 \cdot 900}{10^6} = 0.81 \text{ kg/min}$$

$$N_{\text{H}} = \dot{m} \Delta h = \frac{0.81 \cdot 70 \cdot 1000}{60} = 945 \text{ W}$$

As the area of the heating element is small compared to that of the sheet the equation applies [14]

$$\dot{e} = \varepsilon \, c_s \cdot \left(\frac{T}{100}\right)^4 \, \text{W/m}^2$$

total area of the heating element $A_g = 2 \cdot A$ so that we have

$$\dot{e} A_{\rm g} = N_{\rm H}$$

$$0.9 \cdot 5.77 \cdot 2 \cdot 0.0093 \cdot \left(\frac{T}{100}\right)^4 = 945$$

$$\frac{T}{100} = 9.95$$

$$T = 995 \text{ K}$$

3.7 Dielectric Heating

The dielectric heat loss that occurs in materials of low electrical conductivity when placed in an electric field alternating at high frequency is used in bonding operations, for example, to heat-seal plastic sheets or films.

The power dissipated in the polymer is given by [14]

$$N_{\rm H} = 2\pi f \cdot C \cdot E^2 \cdot \cot \phi \tag{3.69}$$

where

 $N_{\rm H}$ = power (W) f = frequency of the alternating field (s⁻¹) C = capacitance of the polymer (farads) E = applied voltage (Volt) ϕ = phase angle The rate of heat generation in a plastic film can be obtained from Equation 3.69 and given as [15]

$$N_{\rm H} = 55.7 \left(\frac{E^2 \cdot f \cdot \varepsilon_{\rm r}''}{4 b^2} \right) \tag{3.70}$$

where

 $N_{\rm H}$ = rate of heat generation (W/m³) $\varepsilon_{\rm r}''$ = dielectric loss factor b = half thickness of the film (μ)

Example

Given:

$$E = 500 \text{ V}$$

$$f = 10 \text{ MHz}$$

$$\varepsilon''_{r} = 0.24$$

$$b = 50 \text{ u}$$

Calculate the rate of heat generation and the time required to heat the polymer from 20 °C to 150 °C.

Substituting the given values in Equation 3.70 gives

$$N_{\rm H} = \frac{55.7 \cdot 500^2 \cdot 10 \cdot 10^6 \cdot 0.24}{4 \cdot 50^2} = 3.34 \cdot 10^9 \text{ W/m}^3$$

The maximum heating rate ΔT per second is calculated from

$$\Delta T = \frac{N_{\rm H}}{c_{\rm p} \cdot \rho} \tag{3.71}$$

For

$$N_{\rm H} = 3.39 \cdot 109 \text{ W/m}^2$$

 $c_{\rm p} = 2.2 \text{ kJ/(kg} \cdot \text{K)}$
 $p = 800 \text{ kg/m}^3$
 $\Delta T = \frac{3.39 \cdot 10^6}{800 \cdot 2.2} = 1926 \text{ K/s}$

Finally the heating time is

$$t = \frac{150 - 20}{1926} = 0.067 \,\mathrm{s}$$

3.8 Fick's Law of Diffusion

Analogous to Fourier's law of heat conduction (Equation 3.1) and the equation for shear stress in shear flow, the diffusion rate in mass transfer is given by Fick's law. This can be written as [16]

$$\frac{\dot{m}_{\rm A}}{A} = -D_{\rm AB} \frac{\partial c_{\rm A}}{\partial x} \tag{3.72}$$

where

 $\dot{m}_{\rm A}$ = mass flux per unit time

A = Area

 D_{AB} = diffusion coefficient of the constituent A in constituent B

 c_A = mass concentration of component A per unit volume

x = distance.

The governing expression for the transient rate of diffusion is [2]

$$\frac{\partial c_{\rm A}}{\partial t} = D_{\rm AB} \frac{\partial^2 c_{\rm A}}{\partial x^2} \tag{3.73}$$

where

t = time

x = distance

The desorption of volatile or gaseous components from a molten polymer in an extruder can be calculated from [17] using Equation 3.73

$$R_{\rm i} = A_c C_0 \sqrt{\frac{4 \cdot D}{\pi \cdot t}} \tag{3.74}$$

where

 R_1 = rate of desorption (g/s)

 $A_{\rm c}$ = area of desorption (cm²)

 C_0 = initial concentration of the volatile component (g/cm³) in the polymer

 $D = \text{diffusion coefficient } (\text{cm}^2/\text{s})$

t = time of exposure (s) of the polymer to the surrounding atmosphere

3.8.1 Permeability

Plastics are permeable by gases, vapors and liquids to a certain extent. The diffusional characteristics of polymers can be described in terms of a quantity known as permeability.

The mass of the fluid permeating through the polymer at equilibrium conditions is given by [7]

$$m = \frac{P \cdot t \cdot A \cdot (p_1 - p_2)}{5} \tag{3.75}$$

where

m =mass of the fluid permeating (g)

 $p = \text{permeability } [g/(\mathbf{m} \cdot \mathbf{s} \cdot \mathbf{Pa})]$

t = time of diffusion (s)

A = area of the film or membrane (m²)

 p_1, p_2 = partial pressures on the side 1 and 2 of the film (Pa)

s = thickness of the film (mm)

In addition to its dependence on temperature, the permeability is influenced by the difference in partial pressures of the fluid and thickness of the film. Other factors influencing permeability are the structure of the polymer film, such as crystallinity, and the type of fluid.

3.8.2 Absorption and Desorption

The process by which the fluid is absorbed or desorbed by a plastic material is time-dependent, governed by its solubility and by the diffusion coefficient [7]. The period until equilibrium value is reached can be very long. Its magnitude can be estimated by the half-life of the process given by [7]

$$t_{0.5} = \frac{0.04919 \cdot s^2}{D} \tag{3.76}$$

where

 $t_{0.5}$ = half life of the process

s = thickness of the polymer assumed to be penetrated by one side

D = diffusion coefficient

The value of $t_{0.5}$ for moisture in polymethyl methacrylate (PMMA) for

$$D = 0.3 \cdot 10^{-12} \text{ m}^2/\text{s}$$
 and $s = 3 \text{ mm}$

is 17.1 days when the sheet is wetted from one side only [7]. However, the equilibrium absorption takes much longer, as the absorption rate decreases with saturation.

References

- [1] Bender, E.: Lecture notes, Wärme and Stoffübergang, Univ. Kaiserslautern (1982)
- [2] McCabe, W. L., Smith, J. C., Harriott, P.: Unit Operations of Chemical Engineering. McGraw Hill, New York (1985)
- [3] MARTIN, H.: in VDI Wärmeatlas, VDI Verlag, Düsseldorf (1984)
- [4] Welty, J. R., Wicks, C. E., Wilson, R. E.: Fundamentals of Momentum, Heat and Mass Transfer, John Wiley, New York (1983)
- [5] Kreith, F., Black, W. Z.: Basic Heat Transfer, Harper & Row, New York (1980)
- [6] THORNE, J. L.: Plastics Process Engineering, Marcel Dekker, New York (1979)
- [7] OGORKIEWICZ, R. M.: Thermoplastics Properties and Design, John Wiley, New York (1974)
- [8] WÜBKEN, G.: Berechnen von Spritzgießwerkzeugen, VDI Verlag, Düsseldorf (1974)
- [9] Gersten, K.: Einführung in die Strömungsmechanik, Vieweg, Braunschweig (1981)
- [10] WINTER, H. H.: Extruder als Plastifiziereinheit, VDI Verlag, Düsseldorf (1977)
- [11] RAUWENDAAL, C.: Polymer Extrusion, Hanser Publishers, Munich (2001)
- [12] Kremer, H.: Grundlagen der Feuerungstechnik, Engler-Bunte-Institut, Univ. Karlsruhe (1964)
- [13] Cogswell, F. N.: Polymer Melt Rheology, George Godwin, London (1981)
- [14] Bernhardt, E. C.: Processing of Thermoplastic Materials, Reinhold, New York (1959)
- [15] McKelvey, J. M.: Polymer Processing, John Wiley, New York (1962)
- [16] HOLMAN, J. P.: Heat Transfer, McGraw Hill, New York (1980)
- [17] SECOR, R. M.: Polym. Eng. Sci. 26 (1986) p. 647

4 Designing Plastics Parts

The deformational behavior of polymeric materials depends mainly on the type and magnitude of loading, time of application of the load, and temperature. The deformation is related to these factors in a complex manner, so that the mathematical treatment of deformation requires a great computational effort [1]. However, in recent times computational procedures for designing plastic parts have been developed using stress-strain data, which were carefully measured by employing computer-aided testing of polymers [2].

4.1 Strength of Polymers

The basic equation for calculating the design stress of a part under load is given by [1]

$$\sigma_{\nu_{\text{max}}} \le \sigma_{\text{zul}} = \frac{K}{S \cdot A}$$
 (4.1)

where

K = material strength as a mechanical property

 $\sigma_{v_{\text{max}}}$ = maximum stress occurring in the part

 $\sigma_{\text{zul}}^{\text{max}}$ = allowable stress S = factor of safety

A = material reduction factor

The relation between allowable stress and the polymer-dependent reduction factors can be written as [1]

$$\sigma_{\text{zul}} = \frac{K}{S} \cdot \frac{1}{A_{\theta}} \cdot \frac{1}{A_{\text{st}}} \cdot \frac{1}{A_{\text{dyn}}} \cdot \frac{1}{A_{\text{A}}} \cdot \frac{1}{A_{\text{W}}} \dots$$
(4.2)

The factor A_{Θ} considers the influence of temperature on the strength of the material and can be calculated from [1]

$$A_{\theta} = \frac{1}{1 - [k(\Theta - 20)]} \tag{4.3}$$

where Θ = temperature. The limits of applicability of Equation 4.3 are $20 \le \Theta \le 100$ °C.

The value k based on the reference temperature of 20 °C is given for the following materials as [1]

PA66 = 0.0112 PA6 = 0.0125 PBT = 0.0095 GR-PA and GR-PBT = 0.0071 POM = 0.0082 ABS = 0.0117

The other reduction factors in Equation 4.2 consider the following effects:

The factor A_{st} represents the effect of the time of static loading and can have following values depending on time [1]:

time	hours	weeks	months	years
$A_{\scriptscriptstyle st}$	1.3	1.6	1.7	2

The factor $A_{\rm dyn}$ takes the effect of dynamic loading into account and lies in the range of 1.3 to 1.6.

The factor A_A , considers the influence of aging and has to be determined experimentally.

The reduction of strength caused by the absorption of moisture by the plastic can be estimated from the factor A_W . For unreinforced polyamides A_W is roughly [1]

$$A_{\rm w} = \frac{1}{1 - 0.22 \, f} \tag{4.4}$$

with f ranging from 0 < f < 3 where f = weight percentage of moisture. The value of A_w is 3.4 when f is greater than 3.

4.2 Part Failure

Usually stresses resulting from loading of the part are multiaxial. Because measured material properties do not exist for combined stresses, the multiaxial state has to be reduced to an uniaxial state by applying the principle of equivalence. According to Huber, von Mises and Henky [1] the governing equation for the equivalent stress is

$$\sigma_{\nu_{\text{HMH}}} = \frac{1}{\sqrt{2}} \left[(\sigma_1 - \sigma_2)^2 + (\sigma_3 - \sigma_1)^2 + (\sigma_2 - \sigma_3)^2 \right]^{0.5}$$
 (4.5)

where σ_1 , σ_2 and σ_3 are normal stresses. The equivalent strain $\overline{\varepsilon}$ is defined by [3]

$$\overline{\varepsilon} = \frac{\sqrt{2}}{3} [(\varepsilon_1 - \varepsilon_2)^2 + (\varepsilon_2 - \varepsilon_3)^2 + (\varepsilon_3 - \varepsilon_1)^2]^{0.5}$$
(4.6)

Materials, whose compressive stress is higher than the tensile stress, can be better described by the conical or parabolic criterion [1]. The equivalent stress $\sigma_{\nu_{\rm kon}}$, according to the conical criterion, is given as [1]

$$\sigma_{v_{\text{kon}}} = \frac{1}{2m} \left[(m-1)(\sigma_1 + \sigma_2 + \sigma_3) \pm \frac{1+m}{\sqrt{2}} \cdot \{(\sigma_1 - \sigma_2)^2 + (\sigma_3 - \sigma_1)^2 + (\sigma_2 - \sigma_3)^2\}^{0.5} \right] (4.7)$$

The parabolic failure criterion is defined by

$$\sigma_{\nu_{\text{parab}}} = \frac{m-1}{2 m} (\sigma_1 + \sigma_2 + \sigma_3)$$

$$\pm \left\{ \frac{(m-1)^2}{4 m^2} (\sigma_1 + \sigma_2 + \sigma_3)^2 + \frac{1}{2 m} \left[(\sigma_1 - \sigma_2)^2 + (\sigma_3 - \sigma_1)^2 + (\sigma_2 - \sigma_3)^2 \right] \right\}$$
(4.8)

where m is the ratio of compressive stress to tensile stress.

Example

Figure 4.1 [1] shows a press fit assembly consisting of a metal shaft and a hub made of POM. The joint strength can be determined as follows:

For the numerical values $r_a/r_i = 1.6$ and $p = 22 \text{ N/mm}^2$ the equivalent stress is to be calculated.

The tangential stress σ_t is given by

$$\sigma_{\rm t} = p \cdot \frac{\left[(r_{\rm a} / r_{\rm i})^2 + 1 \right]}{(r_{\rm a} / r_{\rm i})^2 - 1}$$

Substituing the values above

$$\sigma_{\rm t} = 22 \cdot \frac{(1.6^2 + 1)}{1.6^2 - 1} = 50.2 \tag{4.9}$$

The radial compressive stress σ_r is

$$\sigma_{\rm r} = -p = -22 \text{ N/mm}^2$$

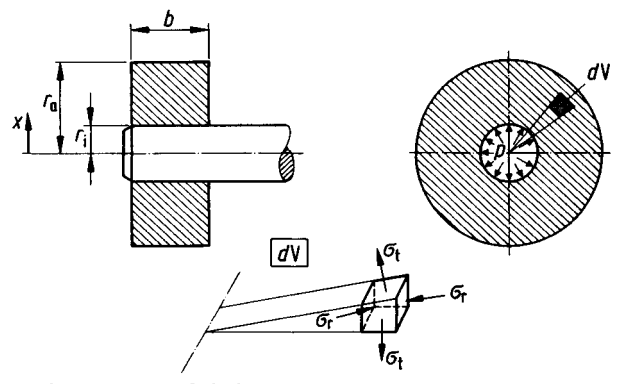


Figure 4.1 Stress analysis in a press fit hub

Substituting $\sigma_t = 50.2 \text{ N/mm}^2$, $\sigma_2 = -22 \text{ N/mm}^2$ and $\sigma_3 = 0$ in Equation 4.5 gives

$$\sigma_{v_{\text{HMH}}} = \frac{2}{\sqrt{2}} \left[(50.2 + 22)^2 + 50.2^2 + 22^2 \right] = 64.1 \text{ N/mm}^2$$

The equivalent stress $\sigma_{\nu_{\rm kon}}$, according to Equation 4.7 for the conical failure criterion, is obtained from

$$\sigma_{v_{\text{kon}}} = \frac{1}{2.8} \left[0.4 (50.2 - 22) + \frac{2.4}{1.414} \sqrt{(50.2 + 22)^2 + 50.2^2 + 22^2} \right] = 58.98 \text{ N/mm}^2$$

with m = 1.4 for POM.

The yield point of POM is around 58 N/mm². Thus, the assumed joint strength is too high. In the case of deformation of the part by shear, the shear stress is given by [1]

$$\tau = 0.5 \ \sigma \tag{4.10}$$

4.3 Time-Dependent Deformational Behavior

4.3.1 Short-Term Stress-Strain Behavior

As mentioned in Section 1.4, polymers are viscoelastic materials and their deformational behavior is nonlinear. A typical stress-strain curve of POM under short-term loading is shown in Figure 4.2. Curves of this type can be expressed by a fifth degree polynomial of the form [4]

$$\sigma = PK_0 + PK_1 \cdot |\varepsilon| + PK_2 \cdot |\varepsilon|^2 + PK_3 \cdot |\varepsilon|^3 + PK_4 \cdot |\varepsilon|^4 + PK_5 \cdot |\varepsilon|^5 \quad (4.11)$$

where $PK_0 \dots PK_5$ are polynomial coefficients dependent on the resin at a given temperature.

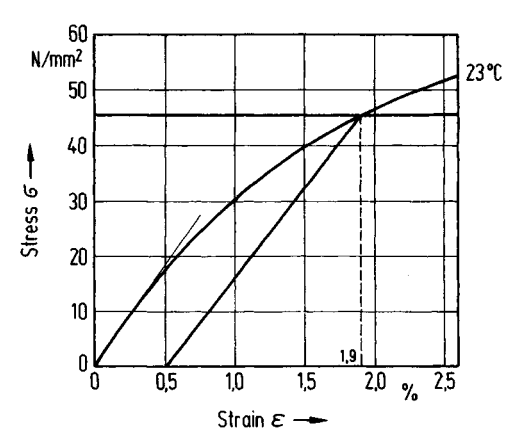


Figure 4.2 Stress-strain diagram for POM

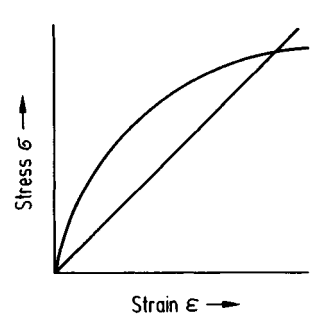


Figure 4.3 Secant modulus [4]

The secant modulus (Figure 4.3) is given by

$$E_{\varepsilon} = \frac{\sigma}{\varepsilon} \tag{4.12}$$

Setting $PK_0 = 0$ it follows from Equation 4.11

$$E_{\varepsilon} = PK_1 + PK_2 \cdot |\varepsilon| + PK_3 |\varepsilon|^2 + PK_4 \cdot |\varepsilon|^3 + PK_5 \cdot |\varepsilon|^4$$
(4.13)

4.3.2 Long-Term Stress-Strain Behavior

The dimensioning of load bearing plastic components requires knowledge of stress-strain data obtained under long-term loading at different temperatures. Retardation experiments provide data on time-dependent strain in the form of creep plots, see Figure 4.4a. In Figure 4.4b the stress is given as a function of time for different values of strain. Isochronous stress-strain-time curves are illustrated in Figure 4.4c.

The critical strain method according to Menges [10] provides a useful criterion for designing plastic parts. The experiments of Menges and Taprogge [10] show that safe design is possible when the critical strain is taken as the allowable deformation. The corresponding tensile stress can be obtained from the isochronous stress-strain diagram.

The expression for calculating the time-dependent strain according to FINDLEY [8] is given as

$$\mathcal{E}(t) = A \sinh B \, \sigma + C \cdot t^n \sinh D \, \sigma \tag{4.14}$$

The power function of FINDLEY [2] is written as

$$\mathcal{E}(t) = \frac{\sigma(t)}{E_0} + m(\sigma) \cdot t^{n(\sigma)} \tag{4.15}$$

The function for the coefficient m is a fifth degree polynomial and that of n is a straight line. With the Findley power function the long-term behavior of plastics up to 10^5 hours can be described on the basis of measurements covering shorter periods of approx. 10^3 hours [2].

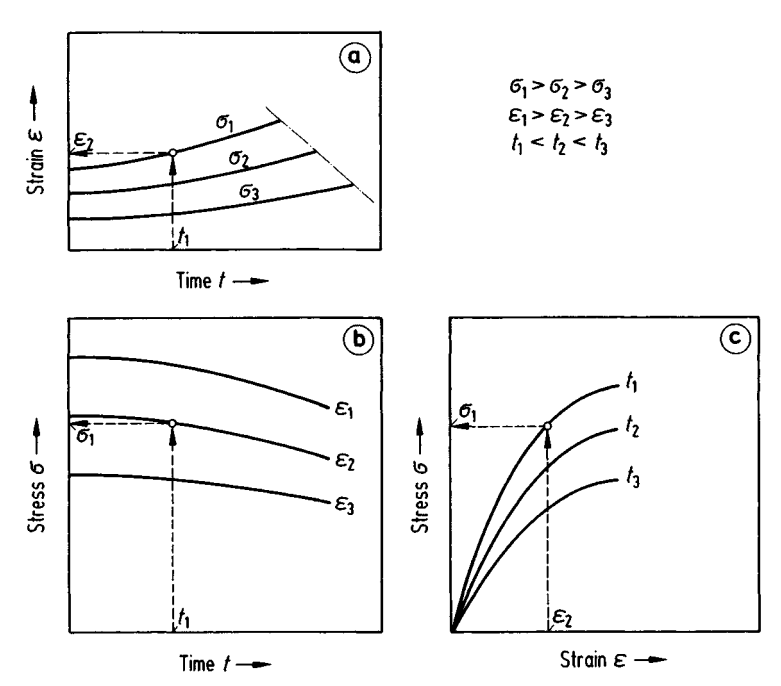


Figure 4.4 Long-term stress-strain behavior [7]

Example [9]

The minimum depth of the simple beam made of SAN shown in Figure 4.5 is to be determined for the following conditions:

The beam should support a mid-span load of 11.13 N for 5 years without fracture and without causing a deflection exceeding 2.54 mm.

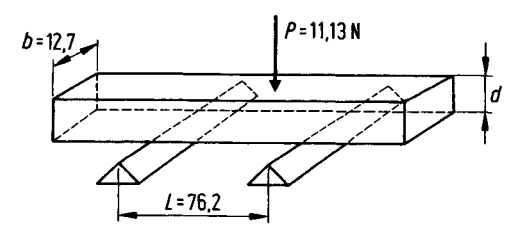


Figure 4.5 Beam under midspan load [9]

Solution

The maximum stress is given by

$$\sigma_{\text{max}} = \frac{1.5 \cdot P \cdot L}{b \cdot d^2} \tag{4.16}$$

where

$$P = load(N)$$

L, b, d = dimensions in (mm) as shown in Figure 4.5

The creep modulus E_c is calculated from

$$E_{c} = \frac{p \cdot L^{3}}{4 \cdot f \cdot b \cdot d^{3}} \tag{4.17}$$

where f is deflection in mm. The maximum stress from Figure 4.6 after a period of 5 years (= 43800 h) is

$$\sigma_{\rm max}$$
 23.44 N/mm²

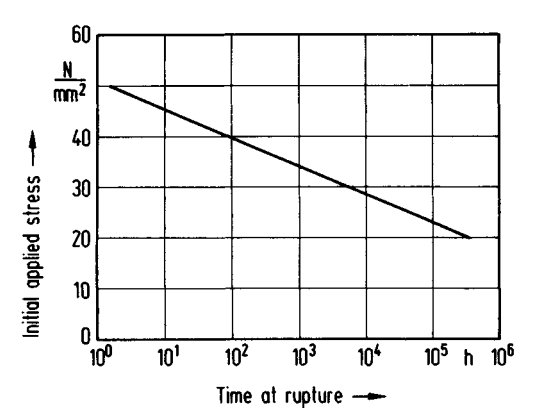


Figure 4.6 Creep curve for SAN [9]

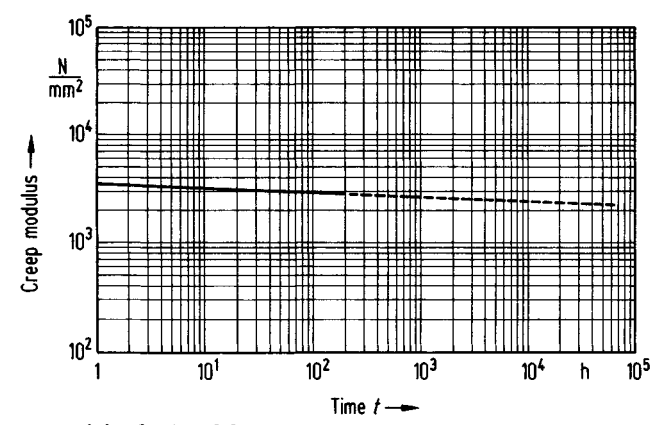


Figure 4.7 Creep modulus for SAN [9]

Working stress σ_{w} with an assumed safety factor S = 0.5:

$$\sigma_{\rm w} = 23.44 \cdot 0.5 = 11.72 \text{ N/mm}^2$$

Creep modulus E_c at $\sigma < \sigma_w$ and a period of 5 years from Figure 4.7

$$E_c = 2413 \text{ N/mm}^2$$

Creep modulus E_c with a safety factor S = 0.75:

$$E_c = 2413 \cdot 0.75 = 1809.75 \text{ N/mm}^2$$

The depth of the beam results from Equation 4.16

$$d = \left(\frac{1.5 \cdot P \cdot L}{b \cdot \sigma_{\text{max}}}\right)^{0.5} = \left(\frac{1.5 \cdot 11.13 \cdot 76.2}{12.7 \cdot 11.72}\right)^{0.5} = 2.92 \text{ mm}$$

The deflection is calculated from Equation 4.17

$$f = \frac{P \cdot L^3}{4 \cdot E_c \cdot b \cdot d^3} = \frac{11.13 \cdot 76.2^3}{4 \cdot 1809.75 \cdot 12.7 \cdot 2.92^3} = 2.15 \text{ mm}$$

f is smaller than 2.54 mm.

References

- [1] Erhard, G.: Berechnen von Kunststoff-Formteilen VDI-Verlag, Düsseldorf (1986)
- [2] Hahn, H.: Berechnen von Kunststoff-Formteilen, VDI-Verlag, Düsseldorf (1986)
- [3] OGORKIEWICZ, R. M.: Thermoplastics Properties and Design, John Wiley, New York (1973)
- [4] AUMER, B.: Berechnen von Kunststoff-Formteilen, VDI-Verlag, Düsseldorf (1986)
- [5] Rao, N.: Designing Machines and Dies for Polymer Processing, Hanser Publishers, Munich (1981)
- [6] Werkstoffblätter, BASF Kunststoffe, BASF, Ludwigshafen
- [7] BERGMANN, W.: Werkstofftechnik Teil 1, Hanser Publishers, Munich (1984)
- [8] FINDLEY, W. N.: ASTM Symposium on Plastics (1944) p. 18
- [9] Design Guide, Modern Plastics Encyclopedia (1978–1979)
- [10] Menges, G., Taprogge, R.: Kunststoff-Konstruktionen. VDI-Verlag Düsseldorf (1974)

5 Formulas for Designing Extrusion and Injection Molding Equipment

5.1 Extrusion Dies

The design of extrusion dies is based on the principles of rheology, thermodynamics, and heat transfer, which have been dealt with in Chapters 2 to 4. The strength of the material is the determining factor in the mechanical design of dies. The major quantities to be calculated are pressure, shear rate, and residence time as functions of the flow path of the melt in the die. The pressure drop is required to predict the performance of the screw. Information on shear rates in the die is important to determine whether the melt flows within the range of permissible shear rates. Overheating of the melt can be avoided when the residence time of the melt in the die is known, which also provides an indication of the uniformity of the melt flow.

5.1.1 Calculation of Pressure Drop

The relation between volume flow rate and pressure drop of the melt in a die can be expressed in the general form as [2]

$$\dot{Q} = K G^n \Delta p^n \tag{5.1}$$

where

 \dot{Q} = volume flow rate

G = die constant

 Δp = pressure difference

K = factor of proportionality in Equation 1.26

n =power law exponent Equation 1.30

It follows from Equation 5.1

$$\Delta p = \frac{\dot{Q}^{\frac{1}{n}}}{\frac{1}{K^{\frac{1}{n}}G}} \tag{5.2}$$

5.1.1.1 Effect of Die Geometry on Pressure Drop

The die constant G depends on the geometry of the die. The most common geometries are circle, slit and annulus cross-sections. G for these shapes is given by the following relationships [2].

$$G_{\text{circle}} = \left(\frac{\pi}{4}\right)^{\frac{1}{n}} \cdot \frac{R^{\frac{3}{n}+1}}{2L} \tag{5.3}$$

where

R = Radius

L =Length of flow channel

$$G_{\text{slit}} = \left(\frac{W}{6}\right)^{\frac{1}{n}} \cdot \frac{H^{\frac{2}{n}+1}}{2L}$$
 (5.4)

for
$$\frac{W}{H} \ge 20$$

where H is the height of the slit and W is the width.

For $\frac{W}{H}$ < 20 , $G_{\rm slit}$ has to be multiplied by the correction factor $F_{\rm p}$ given in Figure 5.1

The factor F_p can be expressed as

$$F_{\rm p} = 1.008 - 0.7474 \cdot \left(\frac{H}{W}\right) + 0.1638 \left(\frac{H}{W}\right)^2$$
 (5.5)

The die constant $G_{annulus}$ is calculated from

$$H = R_0 - R_i \tag{5.6}$$

and

$$W = \pi \left(R_0 + R_i \right) \tag{5.7}$$

where R_0 is the outer radius and R_i is the inner radius. G_{annulus} then follows from Equation 5.4

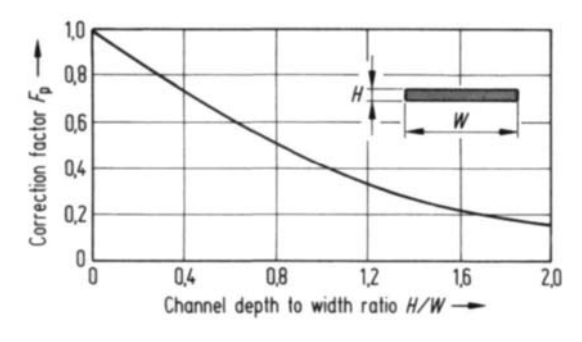


Figure 5.1 Correction factor F_p as a function of H/W [12]

$$G_{\text{annulus}} = \left(\frac{\pi}{6}\right)^{\frac{1}{n}} \frac{(R_0 + R_1)^{\frac{1}{n}} \cdot (R_0 - R_1)^{\frac{2}{n} + 1}}{2L}$$
 (5.8)

for values of the ratio $\pi (R_0 + R_i) / (R_0 - R_i) \ge 37$

For smaller values of this ratio, G_{annulus} has to be multiplied by the factor F_{p} given in Figure 5.1. The height H and width W are obtained in this case from Equation 5.6 and Equation 5.7.

5.1.1.2 Shear Rate in Die Channels

The shear rate for the channels treated above can be computed from [3]

$$\dot{\gamma}_{\rm a_{circle}} = \frac{4 \,\dot{Q}}{\pi \,R^3} \tag{5.9}$$

$$\dot{\gamma}_{a_{\text{slit}}} = \frac{6 \cdot \dot{Q}}{W \cdot H^2} \tag{5.10}$$

$$\dot{\gamma}_{\text{a}_{\text{annulus}}} = \frac{6 \cdot \dot{Q}}{\pi (R_0 + R_i) (R_0 - R_i)^2}$$
(5.11)

The shear rate for an equilateral triangle is given by [4]

$$\dot{\gamma}_{\text{a}_{\text{triangle}}} = \frac{10}{3} \cdot \frac{\dot{Q}}{d^3} \tag{5.12}$$

where d is the half length of a side of the triangle.

The relation for a quadratic cross-section is [4]

$$\dot{\gamma}_{\rm a_{square}} = \frac{3}{0.42} \cdot \frac{\dot{Q}}{a^3} \tag{5.13}$$

where a is the length of a side of the square.

In the case of channels with varying cross-sections along the die length, for example, convergent or divergent channels, the channel is divided into a number of sufficiently small increments and the average dimensions of each increment are used in the equations given above [3].

5.1.1.3 General Relation for Pressure Drop in Any Given Channel Geometry

By means of the substitute radius defined by SCHENKEL [5] the pressure drop in crosssections other than the ones treated in the preceding sections can be calculated. The substitute radius is expressed by [5]

$$R_{\rm rh} = \left[\frac{2^{n+1}}{\pi} \cdot A^{n+2} \right]^{\frac{1}{n+3}}$$
 (5.14)

where

 $R_{\rm rh}$ = substitute radius

A = cross-sectional area

B = circumference

5.1.1.4 Examples

The geometrical forms of the dies used in the following examples are illustrated in Figure 5.2.

Example 1

It is required to calculate the pressure drop Δp of a LDPE melt at 200 °C flowing through a round channel, 100 mm long and 25 mm diameter, at a mass flow rate of $\dot{m} = 10$ g/s.

The constants of viscosity in the Equation 1.36 for the given LDPE are

$$A_0 = 4.2968$$

$$A_1 = -3.4709 \cdot 10^{-1}$$

$$A_2 = -1.1008 \cdot 10^{-1}$$

$$A_3 = 1.4812 \cdot 10^{-2}$$

$$A_4 = -1.1150 \cdot 10^{-3}$$

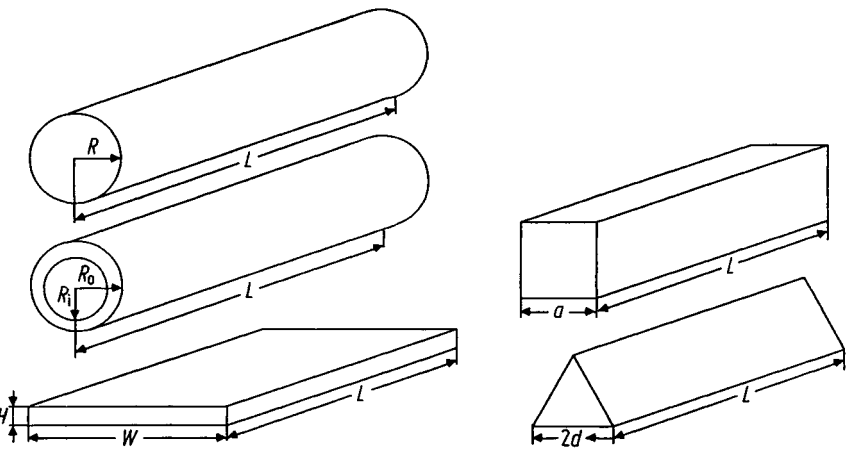


Figure 5.2 Flow channel shapes in extrusion dies

$$b_1 = 1.29 \cdot 10^5$$

 $b_2 = 4.86 \cdot 10^3 \text{ K}$

melt density $\rho_{\rm m} = 0.7 \, {\rm g/cm^3}$

Solution

Volume flow rate
$$\dot{Q} = \frac{\dot{m}}{\rho_m} = \frac{10}{0.7} = 14.29 \text{ cm}^3/\text{s} = 1.429 \cdot 10^{-5} \text{ m}^3/\text{s}$$

Shear rate $\dot{\gamma}_a$ from Equation 5.9:

$$\dot{\gamma} = \frac{4 \cdot \dot{Q}}{\pi \cdot R^3} = \frac{4 \cdot 1.429 \cdot 10^{-5}}{\pi \cdot (0.0125)^3} = 9.316 \,\mathrm{s}^{-1}$$

Shift factor a_T from Equation 1.34:

$$a_{\rm T} = b_1 \cdot \exp(b_2/T) = 1.29 \cdot 10^5 \exp[4860/(200 + 273)] = 0.374$$

By Equation 1.37, the power law exponent n is

$$\frac{1}{n} = 1 + A_1 + 2 A_2 \left[\lg(a_T \cdot \dot{\gamma}_a) + 3 \cdot A_3 \left[\lg(a_T \cdot \dot{\gamma}_a) \right]^2 + 4 A_4 \left[\lg(a_T \cdot \dot{\gamma}_a) \right]^3$$

Substituting the constants $A_1 \dots A_4$ results in

$$n = 1.832$$

Viscosity η_a from Equation 1.36

$$\begin{split} \lg \eta_{\rm a} &= \lg a_3 + A_0 + A_1 \lg (a_{\rm T} \cdot \dot{\gamma}_{\rm a}) + A_2 \left[\lg (a_{\rm T} \cdot \dot{\gamma}_{\rm a}) \right]^2 \\ &+ A_3 \left[\lg (a_{\rm T} \cdot \dot{\gamma}_{\rm a}) \right]^3 + A_4 \left[\lg (a_{\rm T} \cdot \dot{\gamma}_{\rm a}) \right]^4 \end{split}$$

With $a_T = 0.374$, $\dot{\gamma}_a = 9.316$ and the constants $A_0 \dots A_4$ we get

$$\lg \eta = 3.6514$$

$$\eta_a = 4481 \text{ Pa} \cdot \text{s}$$

Shear stress τ from Equation 1.22

$$\tau = \eta_a \cdot \dot{\gamma}_a = 4481 \cdot 9.316 = 41745 \text{ N/m}^2$$

Factor of proportionality *K* from Equation 1.26:

$$K = \frac{\dot{\gamma}_a}{\tau^n} = 3.194 \cdot 10^{-8}$$

Die constant G_{circle} from Equation 5.3:

$$G_{\text{circle}} = \left(\frac{\pi}{4}\right)^{\frac{1}{n}} \cdot \frac{R^{\frac{3}{n}+1}}{2L} = \left(\frac{\pi}{4}\right)^{\frac{1}{1.832}} \frac{(0.0125)^{\frac{3}{1.832}+1}}{2 \cdot 0.1} = 4.19 \cdot 10^{-5}$$

Pressure drop from Equation 5.2:

$$\Delta p = \frac{\dot{Q}^{\frac{1}{n}}}{\frac{1}{K^{\frac{1}{n}} \cdot G_{\text{circle}}}} = \frac{(1.429 \cdot 10^{-5})^{\frac{1}{1.832}}}{(3.194 \cdot 10^{-8})^{\frac{1}{1.832}} \cdot 4.19 \cdot 10^{-5}} = 668447 \text{ Pa} = 6.68 \text{ bar}$$

Example 2

Melt flow through a slit of width W = 75 mm, height H = 1 mm, and length L = 100 mm.

The resin is LDPE with the same viscosity constants as in Example 1. The mass flow rate and the melt temperature have the same values, $\dot{m} = 10$ g/s and T = 200 °C. The pressure drop Δp is to be calculated.

Solution

Volume flow rate
$$\dot{Q} = \frac{\dot{m}}{\rho_{\rm m}} = \frac{0.01}{700} = 1.429 \cdot 10^{-5} \text{ m}^3/\text{s}$$

Shear rate from Equation 5.10:

$$\dot{\gamma}_{a} = \frac{6 \cdot \dot{Q}}{W H^{2}} = \frac{6 \cdot 1.429 \cdot 10^{-5}}{0.075 \cdot 0.001^{2}} = 1143.2 \text{ s}^{-1}$$

Shift factor a_T from Equation 1.34:

$$a_{\rm T} = 0.374$$

power law exponent n from Equation 1.37:

$$n = 3.334$$

Viscosity η_a from Equation 1.36:

$$\eta_a = 257.6 \text{ Pa} \cdot \text{s}$$

Shear stress τ from Equation 1.22:

$$\tau = 294524.9 \text{ N/m}^2$$

Proportionality factor K from Equation 1.26:

$$K = 6.669 \cdot 10^{-16}$$

Correction factor F_p

$$\frac{W}{H} = 75$$

As the ratio W/H is greater than 20, the die constant which can be calculated from Equation 5.4 need not be corrected.

$$G_{\rm slit} = 2.1295 \cdot 10^{-5}$$

and finally the pressure drop Δp from Equation 5.2

$$\Delta p = 588.8 \text{ bar}$$

Example 3

Melt flow through a slit with width W = 25 mm, height H = 5 mm, and length L = 100 mm.

The resin is LDPE with the same viscosity constants as in Example 1. The mass flow rate $\dot{m} = 10$ g/s and the melt temperature T = 200 °C. The pressure drop Δp is to be calculated.

Solution

Volume flow rate
$$\dot{Q} = \frac{\dot{m}}{\rho_{\rm m}} = \frac{0.01}{700} = 1.429 \cdot 10^{-5} \text{ m}^3/\text{s}$$

Shear rate $\dot{\gamma}_a$ from Equation 5.10:

$$\dot{\gamma}_{a} = 137.2 \, \mathrm{s}^{-1}$$

Shift factor a_T from Equation 1.34:

$$a_{\rm T} = 0.374$$

Power law exponent n from Equation 1.37:

$$n = 2.604$$

Viscosity η_a from Equation 1.36:

$$\eta_a = 1044.7 \text{ Pa} \cdot \text{s}$$

Shear stress τ from Equation 1.22:

$$\tau = 143318.9 \text{ N/m}^2$$

Proportionality factor K from Equation 1.26:

$$K = 5.132 \cdot 10^{-12}$$

Correction factor F_p :

As the ratio W/H = 5, which is less than 20, the die constant $G_{\rm slit}$ has to be corrected. $F_{\rm p}$ from Equation 5.5:

$$F_{\rm p} = 1.008 - 0.7474 \cdot 0.2 + 0.1638 \cdot 0.2^2 = 0.865$$

$$G_{\rm slit} = 5.208 \cdot 10^{-5}$$

$$G_{\text{slit corrected}} = 5.208 \cdot 10^{-5} \cdot F_{\text{p}} = 4.505 \cdot 10^{-5}$$

Pressure drop Δp from Equation 5.2:

$$\Delta p = 66.24 \text{ bar}$$

Example 4

Melt flow through an annulus with an outside radius $R_0 = 40$ mm, an inside radius $R_i = 39$ mm, and of length L = 100 mm.

The resin is LDPE with the same viscosity constants as in Example 1. The process parameters, mass flow rate, and melt temperature remain the same.

Solution

Volume flow rate
$$\dot{Q} = \frac{\dot{m}}{\rho_{\rm m}} = \frac{0.01}{700} = 1.429 \cdot 10^{-5} \text{ m}^3/\text{s}$$

Shear rate $\dot{\gamma}_a$ from Equation 5.11:

$$\dot{\gamma}_{a} = \frac{6 \,\dot{Q}}{\pi \left(R_{0} + R_{i}\right) \left(R_{0} - R_{i}\right)^{2}} = \frac{6 \cdot 1.429 \cdot 10^{-5}}{\pi \left(0.04 + 0.039\right) 0.001^{2}} = 345.47 \,\mathrm{s}^{-1}$$

Shift factor a_T from Equation 1.34:

$$a_{\rm T} = 0.374$$

Power law exponent n from Equation 1.37:

$$n = 2.907$$

Viscosity η_a from Equation 1.36:

$$\eta_a = 579.43 \text{ Pa} \cdot \text{s}$$

Shear stress τ from Equation 1.22:

$$\tau = 200173.6 \text{ N/m}^2$$

Factor of proportionality K from Equation 1.26:

$$K = 1.3410 \cdot 10^{-13}$$

Correction factor F_p

As the ratio $\frac{\pi (R_0 + R_i)}{R_0 - R_i} = 248.19$ is greater than 37, no correction is necessary.

 G_{annulus} from Equation 5.8:

$$G_{\text{annulus}} = \left(\frac{\pi}{6}\right)^{\frac{1}{n}} \cdot \left(R_o + R_i\right)^{\frac{1}{n}} \cdot \frac{\left(R_0 - R_i\right)^{\frac{2}{n}+1}}{2L}$$

$$= \frac{\left(\frac{\pi}{6}\right)^{\frac{1}{2.907}} \cdot \left(0.04 + 0.039\right)^{\frac{1}{2.907}} \cdot 0.001^{\frac{2}{2.907}+1}}{2 \cdot 0.1}$$

$$= 1.443 \cdot 10^{-5}$$

Pressure drop Δp from Equation 5.2

$$\Delta p = 400.26 \text{ bar}$$

Example 5

Melt flow through a quadratic cross section with the length of a side a = 2.62 mm. The channel length L = 50 mm. The resin is LDPE with the following constants for the power law relation in Equation 1.32:

$$\eta_{a} = K_{OR} \exp(-\beta \cdot T) \cdot \dot{\gamma}^{n_{R}-1}$$

$$K_{OR} = 135990$$

$$\beta = 0.00863$$

$$n_{R} = 0.3286$$

Following conditions are given:

mass flow rate m = 0.01 g/smelt temperature T = 200 °Cmelt density $\rho_{\text{m}} = 0.7 \text{ g/cm}^3$

The pressure drop Δp is to be calculated.

Solution

Three methods of calculation will be presented to find the pressure drop in this example.

Method a

With this method, the melt viscosity is calculated according to the power law. Other than that, the method of calculation is the same as in the foregoing examples.

Volume flow rate
$$\dot{Q} = \frac{\dot{m}}{\rho_{\rm m}} = \frac{0.01}{0.7} = 0.014286 \,\text{cm}^3/\text{s}$$

Shear rate
$$\dot{\gamma}_a = \frac{6 \dot{Q}}{W H^2}$$

For a square with W = H the shear rate $\dot{\gamma}_a$ is

$$\dot{\gamma}_{a} = \frac{6 \,\dot{Q}}{H^{3}} = \frac{6 \cdot 0.014286}{0.262^{3}} = 4.766 \,\mathrm{s}^{-1}$$

Power law exponent n:

$$n = \frac{1}{n_{\rm P}} = \frac{1}{0.3286} = 3.043$$

Viscosity η_a from Equation 1.32:

$$\eta_{a} = K_{R} \exp(-\beta \cdot T) \cdot \dot{\gamma}^{n_{R}-1}$$

$$= 135990 \cdot \exp(-0.00863 \cdot 200) \cdot 4.766^{0.3286-1}$$

$$= 24205.54 \cdot 4.706^{0.3286-1}$$

$$= 8484 \text{ Pa} \cdot \text{s}$$

Shear stress τ from Equation 1.22:

$$\tau = 40434.88 \text{ N/m}^2$$

Proportionality factor K from Equation 1.26:

$$K = 4.568 \cdot 10^{-14}$$

Correction factor F_p

As $\frac{W}{H} = 1$ is less than 20, the correction factor is obtained from Equation 5.5

$$F_{\rm p} = 1.008 - 0.7474 \cdot 1 + 0.1638 \cdot 1^2 = 0.4244$$

Die constant G_{slit} from Equation 5.4:

$$G_{\text{slit}} = 4.22 \cdot 10^{-5}$$

 $G_{\text{slit corrected}} = 0.4244 \cdot 4.22 \cdot 10^{-5} = 1.791 \cdot 10^{-5}$

Pressure drop Δp from Equation 5.2:

$$\Delta p = 35.7 \text{ bar}$$

Method b

The shear rate $\dot{\gamma}_a$ is calculated from Equation 5.13

$$\dot{\gamma}_{\rm a} = \frac{3}{0.42} \cdot \frac{\dot{Q}}{a^3} = \frac{3000 \cdot 0.014286}{0.42 \cdot 2.62^3} = 5.674 \,\rm s^{-1}$$

Viscosity η_a from Equation 1.32:

$$\eta_{\rm a} = 24205.54 \cdot 5.674^{0.3286-1} = 7546.64 \; {\rm Pa \cdot s}$$

Shear stress τ from Equation 1.22:

$$\tau = 42819.6 \text{ N/m}^2$$

Power law exponent n from Equation 1.28:

$$n = \frac{1}{n_{\rm R}} = 3.043$$

Proportionality factor K from Equation 1.26:

$$K = 4.568 \cdot 10^{-14}$$

The pressure drop Δp is found from

$$\Delta p_{\text{square}} = \frac{2}{\frac{1}{K^n}} \cdot \left(\frac{3}{0.42}\right)^{\frac{1}{n}} \cdot \frac{\dot{Q}^{\frac{1}{n}}}{\frac{3}{n+1}} \cdot 2L$$
 (5.15)

with the die constant G_{square}

$$G_{\text{square}} = \frac{1}{2} \left(\frac{0.42}{3} \right)^{\frac{1}{n}} \cdot \frac{a^{\frac{3}{n}+1}}{2L}$$
 (5.16)

$$G_{\text{square}} = \frac{1}{2} \left(\frac{0.42}{3} \right)^{\frac{1}{3.043}} \cdot \left(\frac{2.62}{1000} \right)^{\frac{3}{3.043} + 1} \cdot \frac{1}{0.05} = 1.956 \cdot 10^{-5}$$

In Equation 5.15

$$K^{\frac{1}{n}} = (4.568 \cdot 10^{-14})^{\frac{1}{3.043}} = 4.134 \cdot 10^{-5}$$

$$\dot{O}^{\frac{1}{n}} = (0.014286 \cdot 10^{-6})^{\frac{1}{3.043}} = 2.643 \cdot 10^{-3}$$

Finally Δp_{square} from Equation 5.2:

$$\Delta p_{\text{square}} = \frac{\dot{Q}^{\frac{1}{n}}}{\frac{1}{K^{\frac{1}{n}} \cdot G}} = \frac{2.643 \cdot 10^{-3}}{4.134 \cdot 10^{-5} \cdot 1.956 \cdot 10^{-5}} = 32.686 \text{ bar}$$

The above relationship for shear rate developed by RAMSTEINER [4] leads to almost the same result as obtained by Method a.

Method c

In this method, a substitute radius is calculated from Equation 5.14; the pressure drop is then calculated using the same procedure as in the case of a round channel (Example 1):

Substitute radius $R_{\rm rh}$:

$$R_{\rm rh} = \left[\frac{(2^{n+1})}{\pi} \cdot A^{n+2} \right]^{\frac{1}{n+3}}$$

$$A = a^2 = 2.62^2 = 6.864 \text{ mm}^2$$

B = 4 a = 4.2.62 = 10.48 mm

n = 3.043

$$R_{\rm rh} = 1.363 \; \rm mm$$

Shear rate $\dot{\gamma}_a$ from Equation 5.13:

$$\dot{\gamma}_{\rm a} = \frac{4 \cdot 0.014286}{\pi \cdot 0.1363} = 7.183 \,\rm s^{-1}$$

Viscosity η_a from Equation 1.32:

$$\eta_{\rm a} = 24205.54 \cdot 7.183^{0.3216-1} = 6441.56 \, \text{Pa} \cdot \text{s}$$

Shear stress τ from Equation 1.22:

$$\tau = 46269.73 \text{ N/m}^2$$

Factor of proportionality from Equation 1.26:

$$K = 4.568 \cdot 10^{-14}$$

 G_{circle} from Equation 5.3:

$$G_{\text{cirlce}} = \frac{\left(\frac{\pi}{4}\right)^{\frac{1}{3.043}} \cdot \left(\frac{1.363}{1000}\right)^{\frac{3}{3.043}+1}}{2 \cdot 0.05} = 1.885 \cdot 10^{-5}$$

Pressure drop from Equation 5.2:

$$\Delta p_{\text{square}} = \frac{2.643 \cdot 10^{-3}}{4.134 \cdot 10^{-5} \cdot 1.885 \cdot 10^{-5}} = 33.92 \,\text{bar}$$

This result shows that the relationship, Equation 5.14 [5], is sufficiently accurate for practical purposes. This equation is particularly useful for dimensioning channels, whose geometry differs from the common shape, that is, circle, slit or annulus. The procedure of calculation for an equilateral triangle is shown in the following example:

Example 6

Melt flow through an equilateral triangular channel of length L = 50 mm. The side of the triangle 2 d = 4.06 mm. Other conditions remain the same as in Example 5.

Solution

Substitute radius $R_{\rm rh}$ from Equation 5.14 with

$$A = \sqrt{3} d^2 = 7.1376 \text{ mm}^2$$

$$B = 3 \cdot 2 d = 12.18 \text{ mm}$$

$$n = 3.043$$

$$R_{\rm rh} = 1.274 \; \rm mm$$

Shear rate $\dot{\gamma}_a$ from Equation 5.9:

$$\dot{\gamma}_{\rm a} = \frac{4 \cdot 0.014286}{\pi \cdot 0.1274^3} = 8.8 \, {\rm s}^{-1}$$

Viscosity η_a from Equation 1.32:

$$\eta_a = 24205.54 \cdot 8.8^{0.3286-1} = 5620.68 \text{ Pa} \cdot \text{s}$$

Shear stress τ from Equation 1.22:

$$\tau = 49462 \text{ N/m}^2$$

Factor of proportionality from Equation 1.26:

$$K = 4.568 \cdot 10^{-14}$$

 G_{circle} from Equation 5.3:

$$G_{\text{cirlce}} = \frac{\left(\frac{\pi}{4}\right)^{\frac{1}{3.043}} \cdot \left(\frac{1.274}{1000}\right)^{\frac{3}{3.043}+1}}{2 \cdot 0.05} = 1.648 \cdot 10^{-5}$$

Pressure drop Δp from Equation 5.2:

$$\Delta p = \frac{\dot{Q}^{\frac{1}{n}}}{\frac{1}{K^{\frac{1}{n}} \cdot G_{\text{circle}}}} = \frac{2.643 \cdot 10^{-3}}{4.134 \cdot 10^{-5} \cdot 1.648 \cdot 10^{-5}} = 38.79 \text{ bar}$$

Using the relation developed by RAMSTEINER [4] on the basis of rheological measurement on triangular channels, Example 6 is calculated as follows for the purpose of comparing both methods:

Shear rate from Equation 5.12:

$$\dot{\gamma}_{a} = \frac{10}{3} \cdot \frac{\dot{Q}}{d^{3}} = \frac{10}{3} \cdot \frac{0.014286}{2.03^{3}} = 5.692 \text{ s}^{-1}$$

Viscosity η_a from Equation 1.32:

$$\eta_{\rm a} = 24205.54 \cdot 5.692^{0.3286-1} = 7530.61 \text{ Pa} \cdot \text{s}$$

Shear stress τ from Equation 1.22:

$$\tau = 42864.2 \text{ N/m}^2$$

Factor of proportionality from Equation 1.26:

$$K = 4.568 \cdot 10^{-14}$$

Die constant G_{triangle} :

$$G_{\text{triangle}} = \frac{1}{\sqrt{3}} \cdot \left(\frac{3}{10}\right)^{\frac{1}{n}} \cdot \frac{d^{\frac{3}{n}+1}}{2L}$$
 (5.17)

$$G_{\text{triangle}} = \frac{1}{\sqrt{3}} \cdot \left(\frac{3}{10}\right)^{\frac{1}{3.043}} \cdot \frac{\left(\frac{2.03}{1000}\right)^{\frac{3}{3.043}+1}}{2 \cdot 0.05} = 1.75 \cdot 10^{-5}$$

Pressure drop Δp from Equation 5.2:

$$\Delta p = \frac{\dot{Q}^{\frac{1}{n}}}{\frac{1}{K^{\frac{1}{n}} \cdot G_{\text{triangle}}}} = \frac{2.643 \cdot 10^{-3}}{4.134 \cdot 10^{-5} \cdot 1.75 \cdot 10^{-5}} = 36.5 \text{ bar}$$

This result differs little from the one obtained by using the concept of substitute radius. Therefore this concept of SCHENKEL [5] is suitable for use in practice.

5.1.1.5 **Temperature Rise and Residence Time**

The adiabatic temperature increase of the melt can be calculated from

$$\Delta T = \frac{\Delta p}{10 \cdot \rho_{\rm m} \cdot c_{\rm pm}}$$
 (K) (5.18)

where

 ΔT = temperature rise (K)

= pressure difference (bar)

= melt density (g/cm^3) = specific heat of the melt kJ/(kg · K)

The residence time \overline{t} of the melt in the die of length L can be expressed as

$$\overline{t} = \frac{L}{\overline{u}} \tag{5.19}$$

 \overline{u} = average velocity of the melt

Equation 5.19 for a tube can be written as

$$\overline{t} = \frac{4 \cdot L}{\dot{\gamma}_a \cdot R} \tag{5.20}$$

R =tube radius

 $\dot{\gamma}_a$ = shear rate according to Equation 5.9

The relation of a slit is

$$\overline{t} = \frac{6 \cdot L}{\dot{\gamma}_a \cdot H} \tag{5.21}$$

H = height of slit

 $\dot{\gamma}_a$ = shear rate according to Equation 5.10

5.1.1.6 Adapting Die Design to Avoid Melt Fracture

Melt fracture can be defined as an instability of the melt flow leading to surface or volume distortions of the extrudate. Surface distortions [34] are usually created from instabilities near the die exit, while volume distortions [34] originate from the vortex formation at the die entrance. Melt fracture caused by these phenomena limits the production of articles manufactured by extrusion processes. The use of processing additives to increase the output has been dealt with in a number of publications given in [35]. However, processing aids are not desirable in applications such as pelletizing and blow molding. Therefore, the effect of die geometry on the onset of melt fracture was examined.

The onset of melt fracture with increasing die pressure is shown for LDPE and HDPE in Figure 5.3 [38]. As can be seen, the distortions appear differently depending on the resin. The volume flow rate is plotted in Figure 5.4 [39] first as a function of wall shear stress and then as a function of pressure drop in the capillary for LDPE and HDPE. The sudden increase in slope is evident for LDPE only when the flow rate is plotted against pressure, whereas in the case of HDPE it is the opposite. In addition, for HDPE the occurrence of melt fracture depends on the ratio of length L to diameter D of the capillary. The effect of temperature on the onset of melt fracture is shown in Figure 5.5 [36]. With increasing temperature the onset of instability shifts to higher shear rates. This behavior is used in practice to increase the output. However, exceeding the optimum processing temperature can lead to a decrease in the quality of the product in many processing operations. From these considerations it can be seen that designing a die by taking the resin behavior into account is the easiest method to obtain quality products at high throughputs.

Design procedure

Using the formulas given in this book and in reference [33], the following design procedure has been developed to suit the die dimensions to the melt flow properties of the resin to be processed with the die.

STEP 1: Calculation of the shear rate in the die channel

STEP 2: Expressing the measured viscosity plots by a rheological model

STEP 3: Calculation of the power law exponent

STEP 4: Calculation of the shear viscosity at the shear rate in Step 1

STEP 5: Calculation of the wall shear stress

STEP 6: Calculation of the factor of proportionality

STEP 7: Calculation of die constant

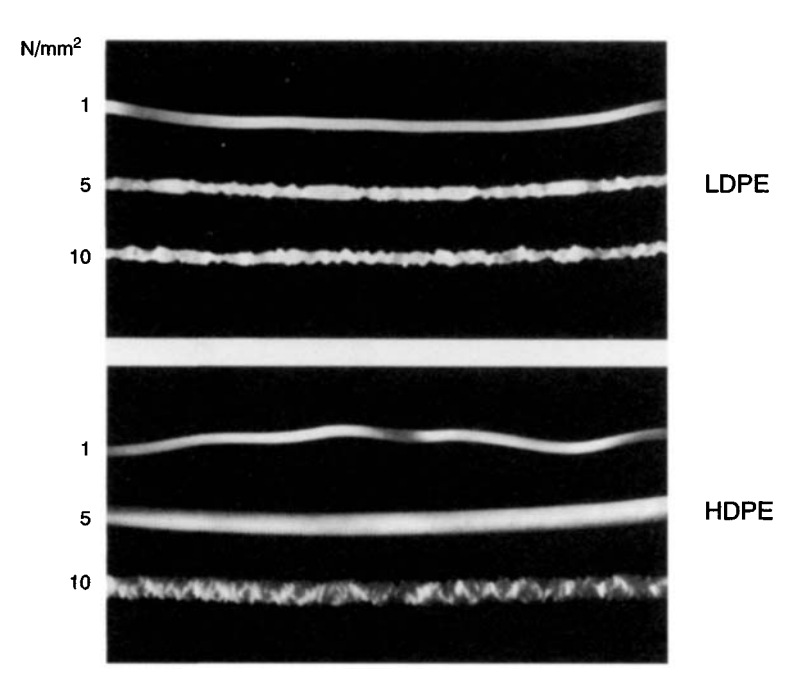


Figure 5.3 Irregularties of the extrudate observed at increasing extrusion pressure with LDPE and HDPE [38]

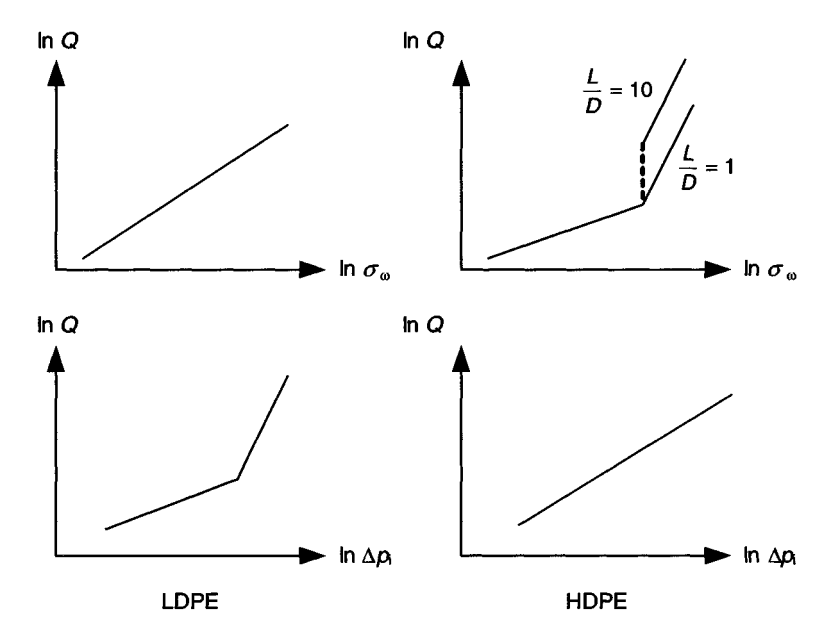


Figure 5.4 Volume rate vs. wall shear stress and vs. pressure drop in capillary for LDPE and HDPE [39]

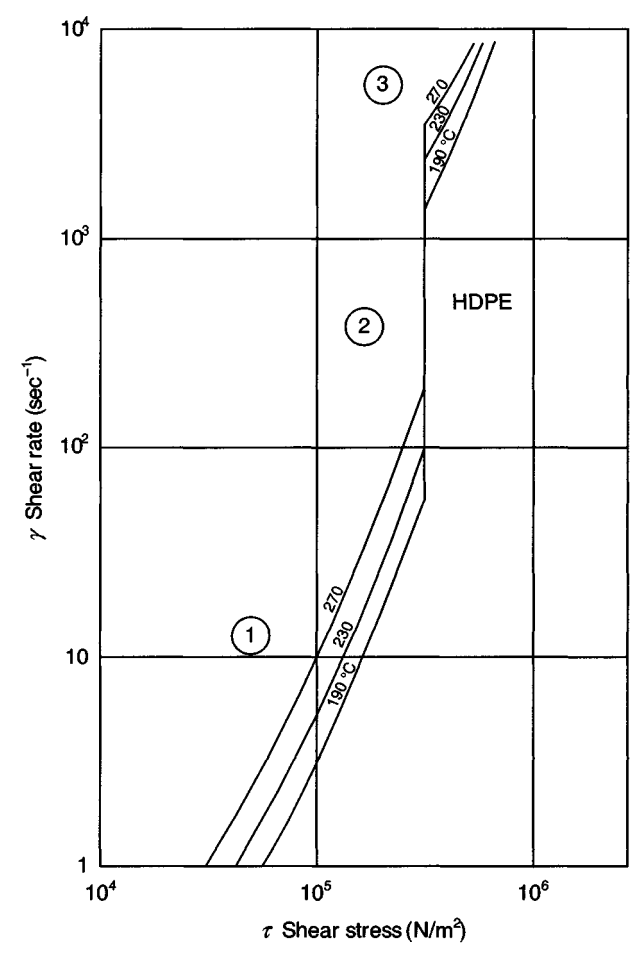


Figure 5.5 Effect of temperature on the melt fracture (region 2) for HDPE

STEP 8: Calculation of pressure drop in the die channel and

STEP 9: Calculation of the residence time of the melt in the channel

Applications

Based on the design procedure outlined above, computer programs have been developed for designing dies for various processes. The principles of the design methods are illustrated below for each process by means of the results of the simulation performed on the dies concerned. The designing principle consists basically of calculating the shear rate, pressure drop, and residence time of the melt during its flow in the die and keeping these values below the limits at which melt fracture can occur. This is achieved by changing the die dimensions in the respective zones of the die, in which the calculated values may exceed the limits set by the resin rheology.

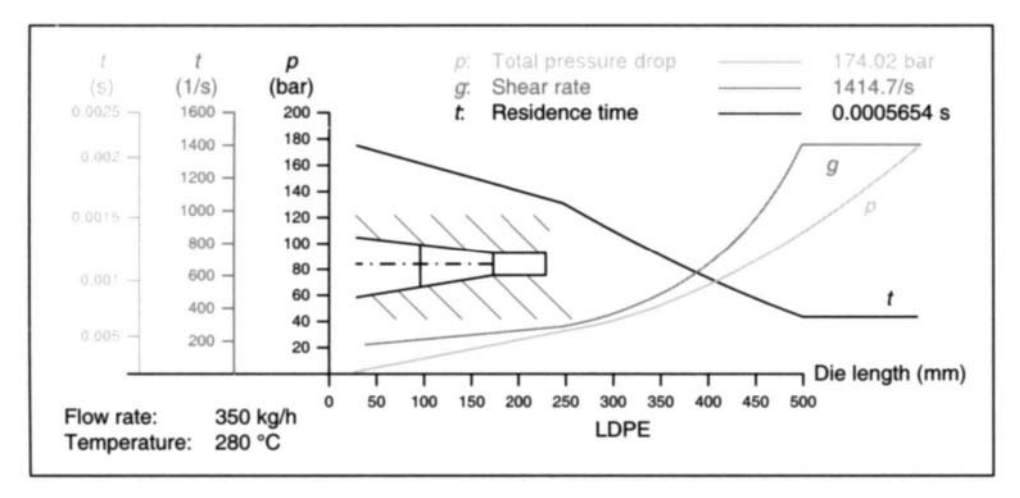


Figure 5.6 Simulation results for a pelletizer die

a) Pelletizer Dies

The aim here is to design a die for a given throughput or to calculate the maximum throughput possible without melt fracture for a given die. These targets can be achieved by performing simulations on dies of different tube diameters, flow rates, and melt temperatures. Figure 5.6 shows the results of one such simulation.

b) Blow Molding Dies

Figure 5.7 shows a blow molding parison and the surface distortion that occurs at a specific shear rate depending on the resin. In order to obtain a smooth product surface, the die contour has been changed in such a way that the shear rate lies in an appropriate range (Figure 5.8). In addition, the redesigned die creates lower extrusion pressures, as can be seen from Figure 5.8 [36].

c) Blown Film Dies

Following the procedure outlined above and using the relationships for the different shapes of the die channels concerned, a blown film spider die was simulated (Figure 5.9). On the basis of these results it can be determined whether these values exceed the boundary conditions at which melt fracture occurs. By repeating the simulations, the die contour can be changed to such an extent that shear rate, shear stress, and pressure drop are within a range, in which melt fracture will not occur. Figure 5.10 and 5.11 show the shear rate and the residence time of the melt along the flow path [37].

The results of simulation of a spiral die are presented in Figure 5.12 as an example. As in the former case, the die gap and the geometry of the spiral channel can be optimized for the resin used on the basis of shear rate and pressure drop.



Figure 5.7 Surface distortion on a parison used in blow molding

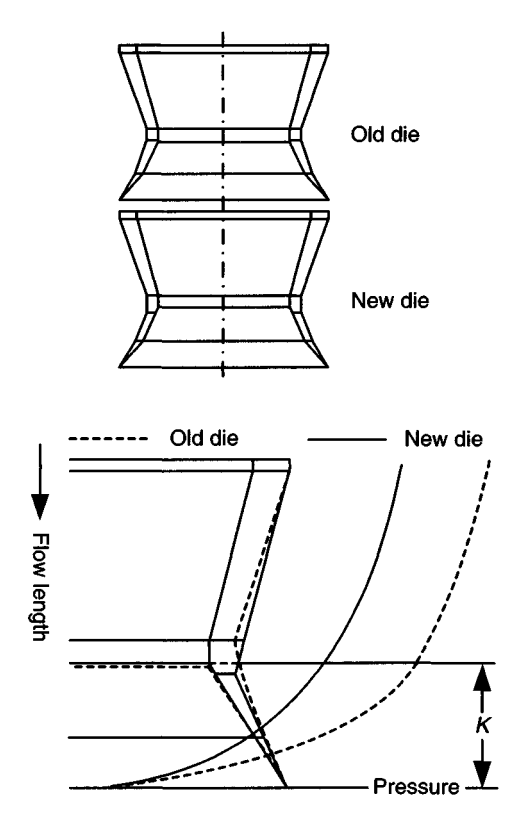


Figure 5.8 Die contour used for obtaining a smooth parison surface

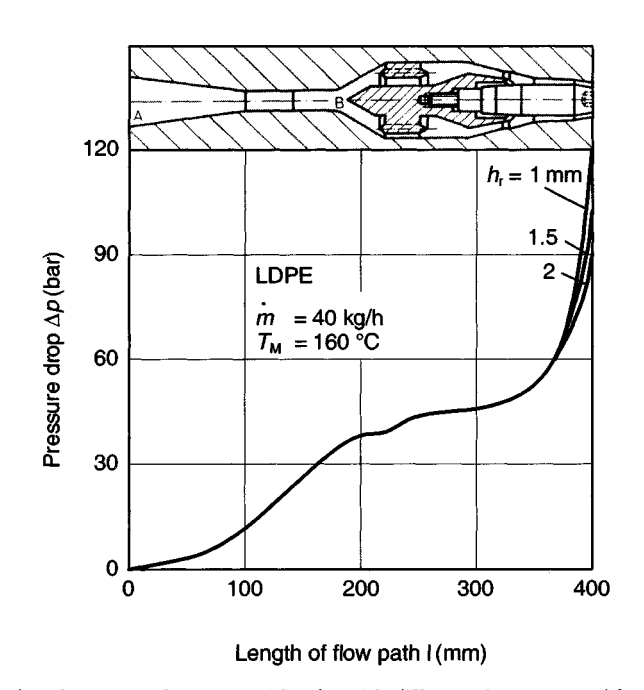


Figure 5.9 Calculated pressure drop in a spider die with different die gaps used for blown film

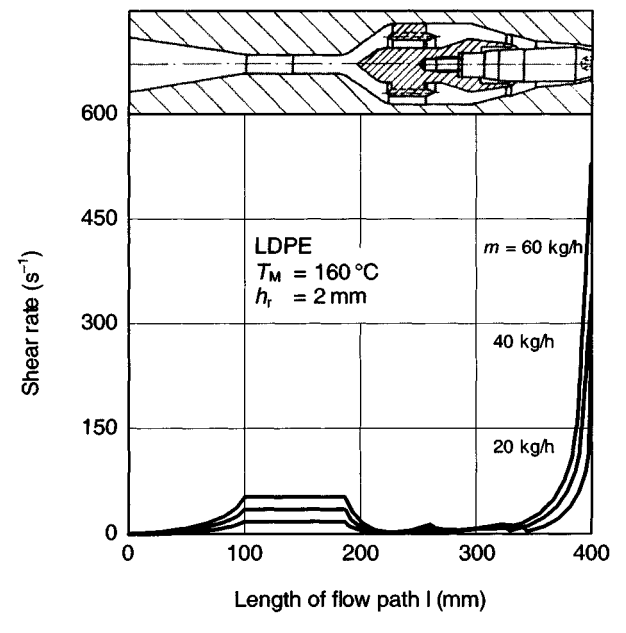


Figure 5.10 Shear rate along spider die

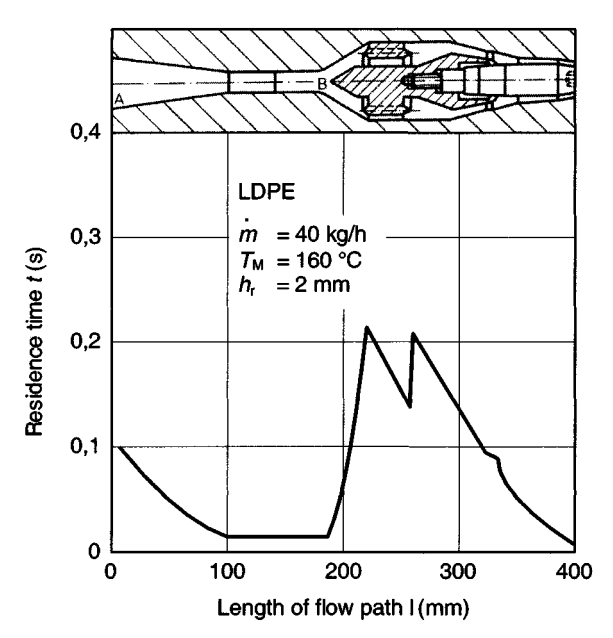


Figure 5.11 Residence time t of the melt as a function of the flow path I

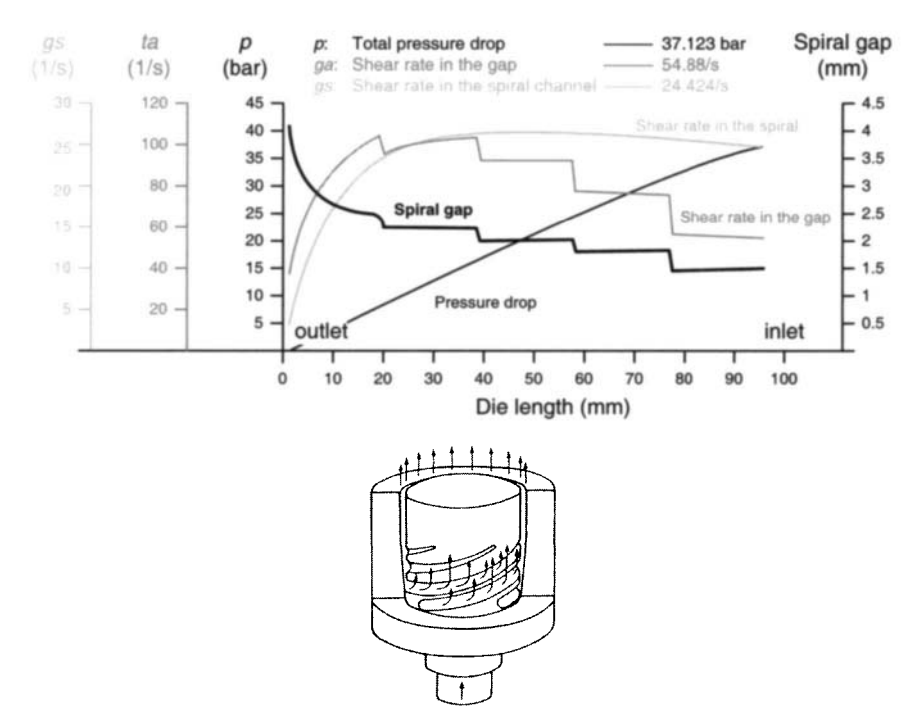


Figure 5.12 Results of simulation of a spiral die used for LLDPE blown film

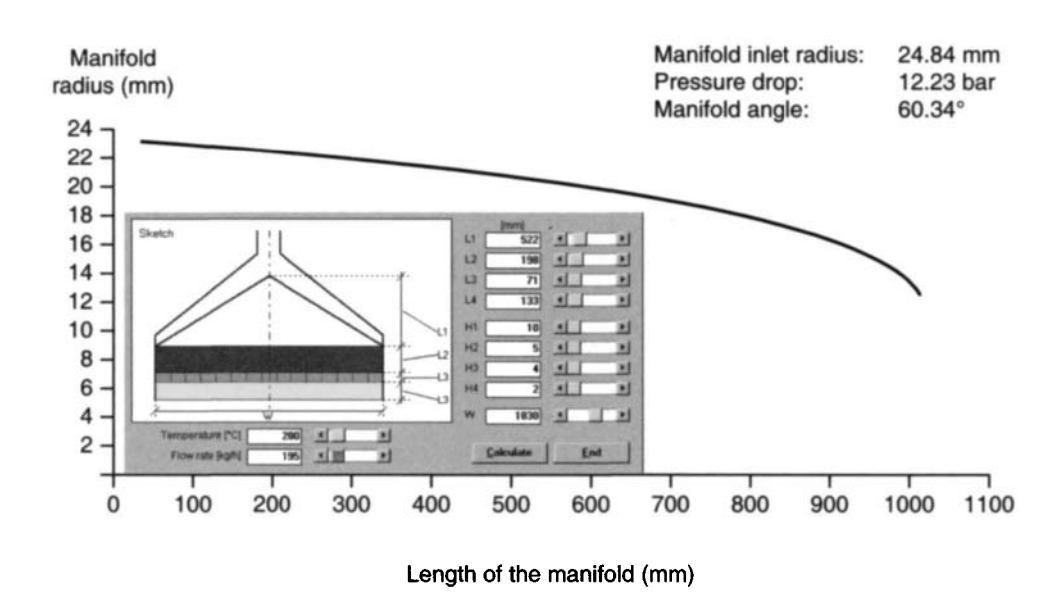


Figure 5.13 Manifold radius as a function of the distance along the length of the manifold

d) Extrusion Coating Dies

Taking the resin behavior and the process conditions into account, the flat dies used in extrusion coating can be designed following similar rules as outlined above. Figure 5.13 shows the manifold radius required to attain uniform melt flow out of the die exit as a function of the manifold length [37].

5.1.1.7 Designing Screen Packs for Extruders

Screen packs are used in polymer processing extruders to remove undesired particulate matter from the melt and are placed behind the breaker plate at the end of an extrusion screw (Figure 5.16). Another important reason to implement screen packs is their assistance in better back mixing of the melt in an extruder channel, which results from the higher resistance offered by the screen to the melt flow. Better back mixing in turn improves the melt homogenity. In addition, screen packs may also be used to attain higher melt temperatures to enable better plastication of the resin. Owing to the intimate relationship between melt pressure and extruder throughput it is important to be able to predict the pressure drop in the screen packs as accurately as possible.

Design Procedure

The volume flow rate \dot{q} through a hole for a square screen opening (Figure 5.14) is given by [42]

$$\dot{q} = (400 \cdot 6.45 \cdot \dot{M})/(3.6 \cdot \rho_{\rm m} \cdot m_{\rm n}^2 \cdot \pi \cdot D_{\rm s}^2)$$

0.053

0.030

Mesh size	Sieve opening mm	Nominal wire diameter mm	
42	0.354	0.247	
100	0.149	0.110	

0.074

0.044

Table 5.1 Dimensions of Square Screens [41]

200

325

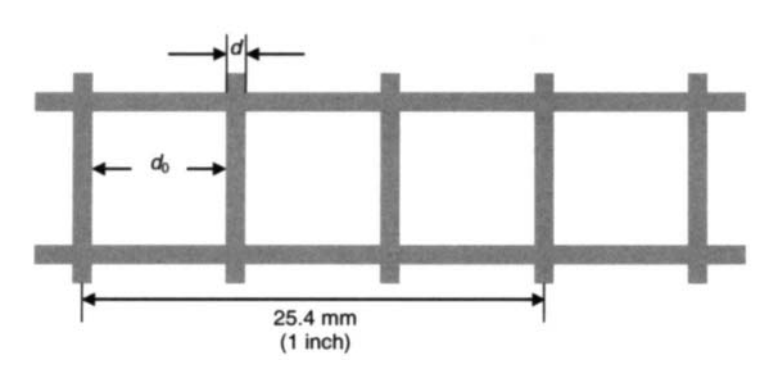


Figure 5.14 Mesh of a wire-gauze screen

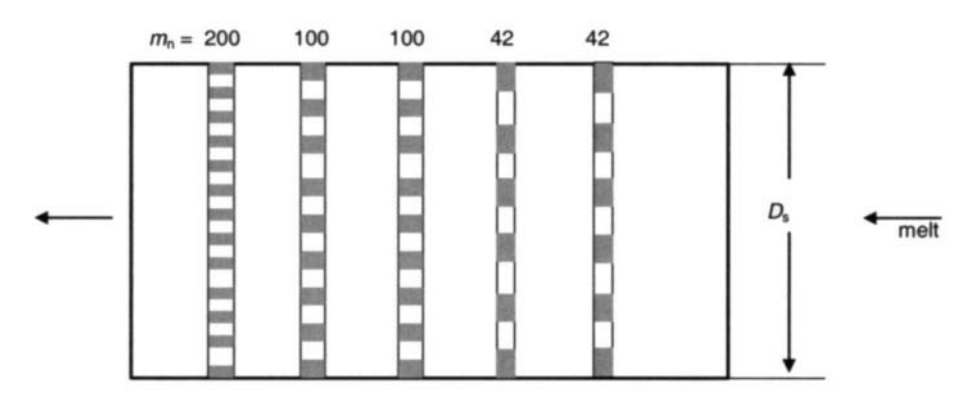


Figure 5.15 Screen pack with screens of varied mesh size

The shear rate of the melt flow for a square opening is calculated from

$$\dot{\gamma}_{\text{square}} = (3/0.42) \cdot \dot{q}/(0.001 \cdot d_0^3)$$

By means of these equations and the design procedure outlined in Section 4.1, following examples were calculated and the results are shown in Figure 5.17 to Figure 5.20.

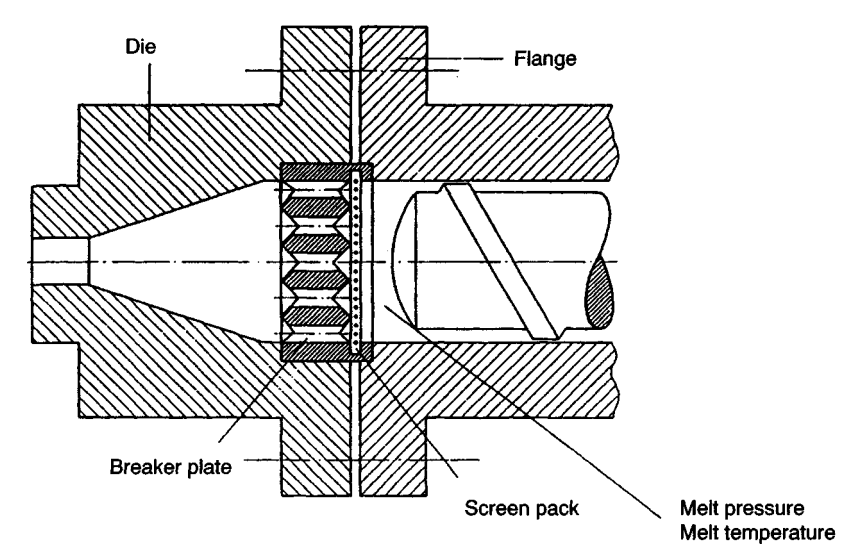


Figure 5.16 Position of screen pack in an extruder [43]

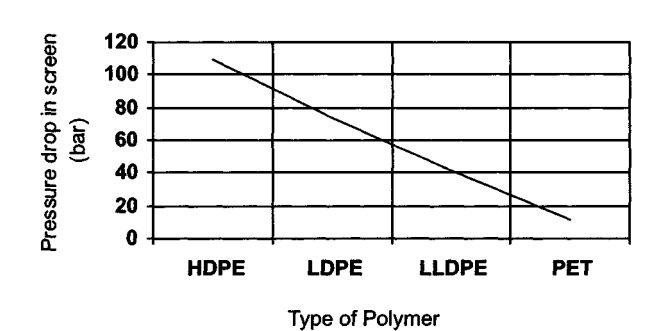


Figure 5.17 Effect of polymer type on pressure drop Δp in the screen pack

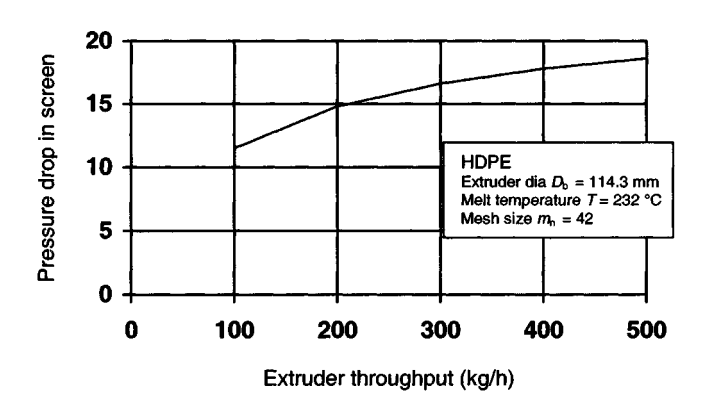


Figure 5.18 Extruder throughput

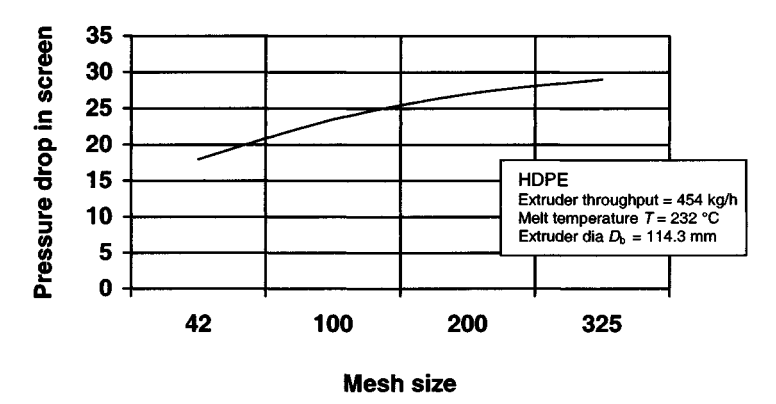


Figure 5.19 Effect of the mesh size on the pressure drop in the screen

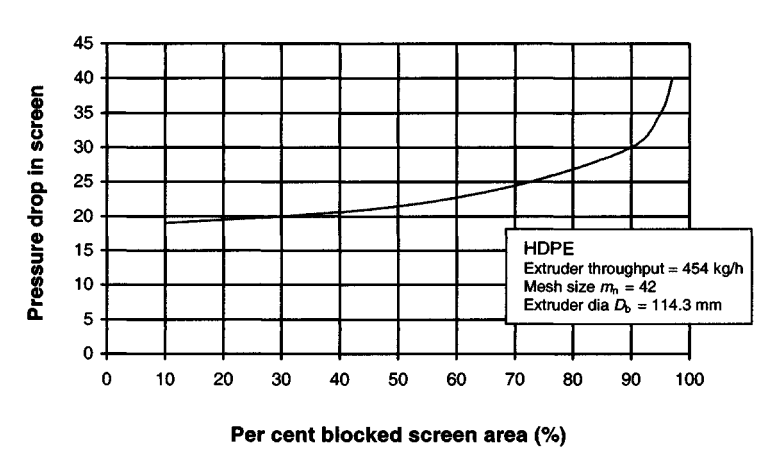


Figure 5.20 Effect of reduced screen area on the pressure drop in the screen

5.2 Extrusion Screws

In this chapter, formulas for the quantities often required when dimensioning extrusion screws are illustrated by specific examples.

5.2.1 Solids Conveying

Under the assumptions that:

- (a) the polymer moves through the screw channel as a plug,
- (b) there is no friction between the solid plastic and the screw, and
- (c) there is no pressure rise,

the maximum flow rate $(\dot{Q}_{\rm s})_{\rm max}$ (see Figure 5.21 and Figure 5.22) can be calculated from [6]

$$(\dot{Q}_{\rm s})_{\rm max} = \pi^2 \cdot H \cdot D_{\rm b} (D_{\rm b} - H) \cdot \sin\phi \cos\phi \cdot \frac{W}{W + w_{\rm FLT}} \cdot N \tag{5.22}$$

The actual flow rate \dot{Q}_s is given by [6]

$$\dot{Q}_{s} = \pi^{2} \cdot H \cdot D_{b} \left(D_{b} - H \right) \cdot \frac{\tan \Theta \cdot \tan \phi}{\tan \Theta + \tan \phi} \cdot \frac{W}{W + W_{ELT}} \cdot N \tag{5.23}$$

The conveying efficiency $\eta_{\rm F}$ can be expressed as

$$\eta_{\rm F} = \frac{\dot{Q}_{\rm s}}{(\dot{Q}_{\rm s})_{\rm max}} \tag{5.24}$$

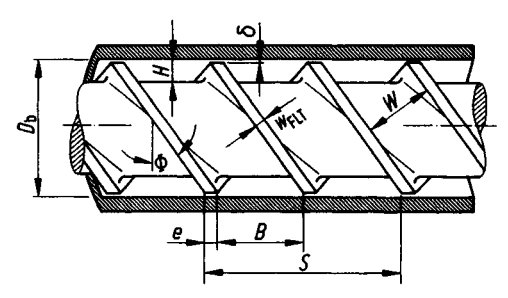


Figure 5.21 Screw zone of a single screw extruder [7]

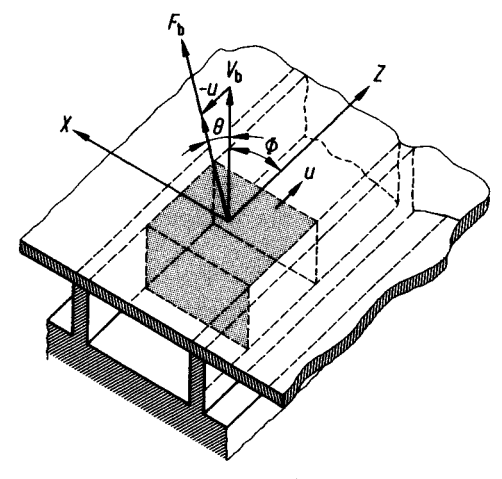


Figure 5.22 Movement of solids in a screw channel after TADMOR [6]

In practice, this efficiency is also defined as

$$\eta_{\rm F} = \frac{G_{\rm s}}{N \cdot V_{\rm s} \cdot \rho_{\rm os}} \tag{5.25}$$

where

 $G_s = \text{mass flow rate}$

 \vec{N} = screw speed

 $V_{\rm s}$ = volume of the screw channel

 ρ_{os} = bulk density

Example

The geometry of the feed zone of a screw, Figure 5.22, is given by the following data [6]

barrel diameter $D_b = 50.57 \text{ mm}$ screw lead s = 50.57 mmnumber of flights v = 1root diameter of the screw $D_s = 34.92 \text{ mm}$ flight width $w_{\text{FLT}} = 5.057 \text{ mm}$ depth of the feed zone H = 7.823 mm

The maximum specific flow rate and the actual flow rate are to be calculated.

Solution

Helix angle ϕ :

$$\phi = \tan^{-1} \left(\frac{s}{\pi D_b} \right) = \tan^{-1} \left(\frac{50.57}{\pi \cdot 50.57} \right) = 17.66$$
°

Width of the screw channel W:

$$W = \frac{s \cos \phi}{v} - w_{\text{FLT}}$$

= 50.57 \cdot \cos 17.66 - 5.057
= 50.57 \cdot 0.953 - 5.057 = 43.13 mm

Maximum specific flow rate from Equation 5.22:

$$\left(\frac{\dot{Q}_s}{N}\right)_{\text{max}} = \pi^2 \cdot 0.7823 \cdot 5.057 \cdot (5.057 - 0.7823) \cdot 0.3034 \cdot 0.953 \frac{4.313}{4.819}$$
$$= 43.19 \text{ cm}^3/\text{rpm}$$

Taking the bulk density $\rho_{os} = 0.475 \text{ g/cm}^3$ into account, the specific mass flow rate becomes

$$\left(\frac{\dot{G}}{N}\right)_{\text{max}} = 20.52 \text{ g/rpm}$$

The feed angle Θ is required to calculate the actual flow rate. With the assumptions already made and assuming equal friction coefficients on screw f_s and barrel f_b , the approximate feed angle may be calculated from [6]

$$\cos\Theta = K\sin\Theta + \sin\phi \left(K + \frac{D_s}{D_b}\cot\phi\right)$$
 (5.26)

where

$$K = \frac{\overline{D}(\sin\phi + f_s\cos\phi)}{D_b(\cos\phi - f_b\sin\phi)}$$
(5.27)

With $f_s = f_b = 0.25$ and the average diameter $\bar{D} = D_b - H = 5.057 - 0.7823 = 4.275$ cm

$$K = \frac{4.275 (0.3034 + 0.25 \cdot 0.953)}{5.057 (0.953 - 0.25 \cdot 0.3034)} = 0.522$$

With
$$K = 0.522$$
 and $\frac{D_s}{D_b} = \frac{3.492}{5.057} = 0.6906$ we obtain from Equation 5.26

$$\cos\Theta = K\sin\Theta + 0.816$$

$$\Theta \approx 15.8^{\circ}$$

Inserting $\Theta = 15.8^{\circ}$ into Equation 5.23

$$\frac{\dot{Q}_{\rm s}}{N} = \pi^2 \cdot H \cdot D_{\rm b} \left(D_{\rm b} - H \right) \cdot \frac{\tan \Theta \cdot \tan \phi}{\tan \Theta + \tan \phi} \cdot \frac{W}{W + w_{\rm BLT}}$$

gives

$$\frac{\dot{Q}_{s}}{N} = \pi^{2} \cdot 0.7823 \cdot 5.057 (5.057 - 0.7823) \cdot \frac{\tan 15.8 \cdot \tan 17.66}{\tan 15.8 + \tan 17.66} \cdot \frac{4.313}{4.819}$$
$$= 22.4 \text{ cm}^{3}/\text{rpm}$$

The actual specific mass flow rate using the bulk density $\rho_{os} = 0.475 \text{ g/cm}^3$ is therefore

$$\frac{\dot{G}}{N}$$
 = 10.62 g/rpm

The conveying/ efficiency η_F is

$$\eta_{\rm F} = \frac{10.62}{20.52} = 0.52$$

5.2.2 Melt Conveying

Starting from the parallel plate model and correcting it by means of appropriate correction factors [7], the throughput of melt in an extruder can be calculated. Although the following equation for the output applies to an isothermal quasi-Newtonian fluid, it was found to be useful for many practical applications [3].

For a given geometry of the melt zone (Figure 5.21), the output of a melt extruder or that of a melt pumping zone of a plasticating extruder can be determined as follows [3, 7]

Helix angle ϕ :

$$\phi = \tan^{-1} \left(\frac{s}{\pi D_{\rm b}} \right) \tag{5.28}$$

Volume flow rate of pressure flow \dot{Q}_p (m³/s):

$$\dot{Q}_{p} = \frac{-\pi \cdot D_{b} \cdot H^{3} \left(1 - \frac{v \cdot e}{s}\right) \cdot \sin^{2} \phi \cdot \Delta p \cdot 10^{-4}}{12 \cdot \eta_{a} \cdot L}$$
(5.29)

Mass flow rate $\dot{m}_{\rm p}$ (kg/h):

$$\dot{m}_{\rm p} = 3600 \cdot 1000 \cdot \dot{Q}_{\rm p} \cdot \rho_{\rm m} \tag{5.30}$$

Drag flow \dot{Q}_d (m³/s):

$$\dot{Q}_{\rm d} = \frac{\pi^2 \cdot D_{\rm b} \cdot N \cdot H^3 \left(1 - \frac{v \cdot e}{s}\right) \cdot \sin \phi \cdot \cos \phi \cdot 10^{-9}}{2 \cdot 60} \tag{5.31}$$

Mass flow rate \dot{m}_d (kg/h):

$$\dot{m}_{\rm d} = 3600 \cdot 1000 \cdot \dot{Q}_{\rm d} \cdot \rho_{\rm m} \tag{5.32}$$

The leakage flow through the screw clearance is found from the ratios

$$a_{\rm d} = -\frac{\dot{Q}_{\rm p}}{\dot{Q}_{\rm d}} \tag{5.33}$$

and

$$J = \frac{\delta}{H} \tag{5.34}$$

The extruder output \dot{m} is finally calculated from

$$\dot{m} = 6 \cdot 10^{-5} \cdot \pi^2 \cdot D_b^2 \cdot N \cdot H \left(1 - \frac{v \cdot e}{s} \right) \cdot \rho_m \cdot \sin \phi \cos \phi \cdot (1 - a - J) / 2 \quad (5.35)$$

The shear rate required for determining the viscosity η_a at the given melt temperature T is obtained from

$$\dot{\gamma}_{\rm a} = \frac{\pi \cdot D_{\rm b} \cdot N}{60 \cdot H} \tag{5.36}$$

Symbols and units used in the formulas above:

_		
$D_{\mathbf{b}}$:	Barrel diameter	mm
H:	Channel depth	mm
<i>e</i> :	Flight width	mm
s:	Screw lead	mm
δ:	Flight clearance	mm
L:	Length of melt zone	mm
<i>v</i> :	Number of flights	_
Δp :	Pressure difference across the melt zone	bar
$\dot{\gamma}_a$:	Shear rate	s^{-1}
$\dot{\gamma}_a$: \dot{Q}_p , \dot{Q}_d : \dot{m}_p , \dot{m}_d :	Volume flow rate of pressure flow and drag flow, respectively	m^3/s
$\dot{m}_{\rm p}^{\rm r}, \dot{m}_{\rm d}$:	Mass flow rate of pressure and drag flow, respectively	kg/s
m':	Extruder output	kg/h
$\eta_{ m a}$:	Melt viscosity	Pa·s
$a_{\rm d}$:	Ratio of pressure flow to drag flow	_
T:	Melt temperature	$^{\circ}\mathrm{C}$
N:	Screw speed	min ⁻¹

Example

For the following conditions the extruder output is to be determined:

Resin: LDPE with the same constants of viscosity as in Example 1 in Section 4.1.1.

Process parameters:

Screw speed $N = 80 \text{ min}^{-1} \text{ (rpm)}$

Melt temperature $T = 200 \,^{\circ}\text{C}$ Melt pressure $\Delta p = 300 \,\text{bar}$

Geometry of the metering zone:

 $D_{\rm b} = 60 \text{ mm}$; H = 3 mm; e = 6 mm; s = 60 mm; $\delta_{\rm FLT} = 0.1 \text{ mm}$; L = 600 mm; v = 1 mm; $v = 1 \text{$

Solution

$\dot{\gamma}_a$	$= 83.8 \text{ s}^{-1}$	Equation 5.36
a_{T}	= 0.374	Equation 1.34
η_a	$= 1406.34 \text{ Pa} \cdot \text{s}$	Equation 1.36
φ	= 17.66°	Equation 5.28
\dot{m}_{p}	= -3.146 kg/h	Equation 5.29 and Equation 5.30

 $\dot{m}_{\rm d} = 46.42 \text{ kg/h}$ Equation 5.31 and Equation 5.32 $\dot{m} = 41.8 \text{ kg/h}$ Equation 5.33, Equation 5.34 and Equation 5.35

Leakage flow $\dot{m}_1 = \dot{m}_d + \dot{m}_p - \dot{m} = 1.474 \text{ kg/h}$

5.2.2.1 Correction Factors

To correct the infinite parallel plate model for the flight edge effects, following factors are to be used along with the equations given above:

the shape factor for the drag flow F_d can be obtained from [8] with sufficient accuracy

$$F_{\rm d} = 1 - 0.571 \frac{H}{W} \tag{5.37}$$

and the factor for the pressure flow $F_{\rm p}$

$$F_{\rm p} = 1 - 0.625 \, \frac{H}{W} \tag{5.38}$$

The expressions for the corrected drag flow and pressure flow would be

$$\dot{Q}_{\rm dk} = F_{\rm d} \cdot \dot{Q}_{\rm d}$$

and

$$\dot{Q}_{\rm pk} = F_{\rm p} \cdot \dot{Q}_{\rm p}$$

The correction factor for the screw power, which is treated in the next section, can be determined from [9]

$$F_z = \exp(x) - x^3 + 2.2 x^2 - 1.05 x$$
 (5.39)

with

$$x = \frac{H}{W}$$

Equation 5.39 is valid in the range 0 < H/W < 2. For the range of commonly occurring H/W-ratios in extruder screws, the flight edge effect accounts for only less than 5% and can therefore be neglected [8]. The influence of screw curvature is also small so that $F_{\rm x}$ can be taken as 1.

Although the above mentioned factors are valid only for Newtonian fluids, their use for polymer melt flow is justified.

5.2.2.2 Screw Power

The screw power consists of the power dissipated as viscous heat in the channel and flight clearance and the power required to raise the pressure of the melt. Therefore, the total power $Z_{\rm N}$ for a melt filled zone [10] is

$$Z_{\rm N} = Z_{\rm c} + Z_{\rm FLT} + Z_{\Delta b} \tag{5.40}$$

where

 $Z_{\rm c}$ = power dissipated in the screw channel

 $Z_{\rm FLT}$ = power dissipated in the flight clearance

 $Z_{\Delta p}$ = power required to raise the pressure of the melt

The power dissipated in the screw channel Z_c is given by [10]

$$Z_{c} = \frac{v \cdot \pi^{2} \cdot D_{\text{FLT}}^{2} \cdot N^{2} \cdot W \cdot \eta_{c} \cdot \Delta L \left(F_{z} \cos^{2} \phi + 4 \sin^{2} \phi\right)}{36 \cdot 10^{14} \cdot \delta_{\text{FLT}} \cdot \sin \phi}$$
(5.41)

The power dissipated in the flight clearance can be calculated from [10]

$$Z_{\text{FLT}} = \frac{v \cdot \pi^2 \cdot D_{\text{FLT}}^2 \cdot N^2 \cdot w_{\text{FLT}} \cdot \eta_{\text{FLT}} \cdot \Delta L}{36 \cdot 10^{14} \cdot \delta_{\text{FLT}} \cdot \sin \phi}$$
 (5.42)

The power required to raise the pressure of the melt $Z_{\Delta p}$ can be written as

$$Z_{\Delta p} = 100 \cdot \dot{Q}_{p} \cdot \Delta p \tag{5.43}$$

The flight diameter D_{FLT} is obtained from

$$D_{\rm FLT} = D_{\rm b} - 2 \cdot \delta_{\rm FLT} \tag{5.44}$$

and the channel width W

$$W = -\frac{s}{v}\cos\phi - w_{\text{FLT}} \tag{5.45}$$

The symbols and units used in the equations above are given in the following example:

Example

For the following conditions the screw power is to be determined:

Resin: LDPE with the constants of viscosity as in Example 1 of Section 5.1.1.4

Operating conditions:

screw speed N = 80 rpmmelt temperature $T = 200 \,^{\circ}\text{C}$ die pressure $\Delta p = 300 \text{ bar}$

Geometry of the melt zone or metering zone:

D = 60 mm; H = 3 mm; e = 6 mm; s = 60 mm; $\delta_{FLT} = 0.1 \text{ mm}$; $\Delta L = 600 \text{ mm}$; v = 1

Solution

Power Z_c in the screw channel:

 $D_{\text{FLT}} = 59.8 \text{ mm from Equation } 5.44$

Shear rate in the screw channel $\dot{\gamma}_c$:

$$\dot{\gamma}_{\rm c} = 83.8 \, \rm s^{-1} \,$$
 from Equation 5.36

$$a_{\rm T} = 0.374$$
 from Equation 1.34

Viscosity of the melt in the screw channel η_{c}

$$\eta_{\rm c}$$
 = 1406.34 Pa·s from Equation 1.36

Channel width W:

$$W = 51.46$$
 mm from Equation 5.45

Number of flights v:

$$v = 1$$

Length of the melt zone ΔL :

$$\Delta L = 600 \text{ mm}$$

Faktor F_x :

$$F_{\rm x} = 1$$
 for $\frac{H}{W} = \frac{3}{51.46} = 0.058$ from Equation 5.39

Helix angle ϕ :

$$\phi = 17.66^{\circ}$$
; $\sin \phi = 0.303$ from Equation 5.28

Power in the screw channel Z_c from Equation 5.41:

$$Z_{c} = 1 \cdot \pi^{2} \cdot 59.8^{2} \cdot 80^{2} \cdot 51.46 \cdot 1406.34 \cdot 600 \cdot \frac{(1 \cdot \cos^{2} 17.66^{\circ} + 4 \sin^{2} 17.66^{\circ})}{36 \cdot 10^{14} \cdot 3 \cdot \sin 17.66^{\circ}}$$

= 3.84 kW

Power in the flight clearance Z_{FLT} :

Flight width w_{FLT} (Figure 5.22):

$$w_{\text{FLT}} = e \cos \phi = 6 \cdot \cos 17.66^{\circ} = 5.7 \text{ mm}$$

Shear rate in the flight clearance $\dot{\gamma}_{FLT}$:

$$\dot{\gamma}_{\text{FLT}} = \frac{\pi \cdot D_{\text{b}} \cdot N}{60 \cdot \delta_{\text{FLT}}} = \frac{\pi \cdot 60 \cdot 80}{60 \cdot 0.1} = 2513.3 \,\text{s}^{-1}$$

Shift factor a_T :

$$a_{\rm T} = 0.374$$
 at $T = 200$ °C from Equation 1.34

Viscosity in the flight clearance η_{FLT} :

$$\eta_{\rm FLT}$$
 = 219.7 Pa·s from Equation 1.36

Length of the melt zone ΔL :

$$\Delta L = 600 \text{ mm}$$

 $Z_{\rm FIT}$ from Equation 5.42:

$$Z_{\text{FLT}} = \frac{1 \cdot \pi^2 \cdot 59.8^2 \cdot 80^2 \cdot 600 \cdot 5.7 \cdot 219.7}{36 \cdot 10^{14} \cdot 0.1 \cdot 0.303} = 1.56 \text{ kW}$$

Power to raise the melt pressure $Z_{\Lambda n}$

Pressure flow \dot{Q}_{p} :

 $\dot{Q}_{\rm p}$ from the Example in Section 4.2.2

$$\dot{Q}_{\rm p} = 1.249 \cdot 10^{-6} \text{ m}^3/\text{s}$$

Die pressure Δp :

$$\Delta p = 300 \text{ bar}$$

 $Z_{\Delta p}$ from Equation 5.43:

$$Z_{\Delta p} = 100 \cdot 1.249 \cdot 10^{-6} \cdot 300 = 0.0375 \text{ kW}$$

Hence the power $Z_{\Delta p}$ is negligible in comparison with the sum $Z_c + Z_{FLT}$.

5.2.2.3 Heat Transfer between the Melt and the Barrel

To estimate the power required to heat the barrel or to calculate the heat lost from the melt, the heat transfer coefficient of the melt at the barrel wall is needed. This can be estimated from [11]

$$\alpha_{\rm sz} = \lambda_{\rm m} \left(\frac{N}{60 \cdot \pi \cdot a} \right)^{0.5} \left[1 - \frac{(T_{\rm f} - T_{\rm m}) \{ 1 - \exp(\beta) \}}{(T_{\rm b} - T_{\rm m})} \right]$$
 (5.46)

where the thermal diffusivity a

$$a = \frac{\lambda_{\rm m}}{10^6 \cdot c_{\rm m} \cdot \rho_{\rm m}} \tag{5.47}$$

and the parameter β

$$\beta = -\frac{10^{-6} \cdot \delta_{\text{FLT}}^2 \cdot N}{240 \cdot a} \tag{5.48}$$

Indices:

m: melt

f: melt film b: barrel

Example with symbols and units

Thermal conductivity $\lambda_{\rm m} = 0.174 \, \text{W/(m} \cdot \text{K)}$ Specific heat $c_{\rm pm} = 2 \, \text{kJ/(kg} \cdot \text{K)}$ Melt density $\rho_{\rm m} = 0.7 \, \text{g/cm}^3$

Thermal diffusivity a from Equation 5.47:

$$a = 1.243 \cdot 10^{-7} \text{ m}^2/\text{s}$$

Flight clearance $\delta_{\text{FLT}} = 0.1 \text{ mm}$ Screw speed N = 80 rpm

Parameter β from Equation 5.48:

$$\beta = 0.027$$

For $T_f = 137.74$ °C, $T_m = 110$ °C and $T_b = 150$ °C

 $\alpha_{\rm sz}$ from Equation 5.46:

$$\alpha_{sz} = 0.174 \left(\frac{80 \cdot 10^7}{60 \cdot \pi \cdot 1.243} \right)^{0.5} \left[1 - \frac{(137.7 - 110) \{1 - \exp(-0.027)\}}{150 - 110} \right]$$

$$= 315.5 \text{ W/(m}^2 \cdot K)$$

5.2.2.4 Melt Temperature

The exact calculation of melt or stock temperature can be done only on an iterative basis as shown in the computer program given in [9]. The following relationships and the numerical example illustrate the basis of calculating the stock temperature. The result obtained can only be an estimate of the real value, as it lacks the accuracy obtained by more exact iterative procedures.

Temperature rise ΔT :

$$\Delta T = (T_{\text{out}} - T_{\text{M}}) = \frac{3600 (Z_{\text{c}} + Z_{\text{FLT}} + N_{\text{H}})}{\dot{m} \cdot c_{\text{pm}}}$$
(5.49)

Heat through the barrel or heat lost from the melt:

$$N_{\rm H} = \frac{\alpha_{\rm sz} \cdot \pi \cdot D_{\rm FLT} \cdot \Delta L \left(T_{\rm b} - T_{\rm EIN} \right)}{10^6 \cdot \cos \phi} \tag{5.50}$$

Example for calculating N_H with symbols and units

$$\alpha_{\rm s} = 315.5 \text{ W/(m}^2 \cdot \text{K)}; D_{\rm FLT} = 59 \text{ mm}; \Delta L = 600 \text{ mm}; T_{\rm b} = 150 \text{ °C}; c_{\rm pm} = 2 \text{ kJ/(kg} \cdot \text{K)}$$

Stock temperature at the inlet of the screw increment considered:

$$T_{\rm in} = 200 \,{\rm ^{o}C}$$

 $N_{\rm H}$ from Equation 5.50:

$$N_{\rm H} = \frac{315.5 \cdot \pi \cdot 59.8 \cdot 600 \cdot 50}{10^6 \cdot \cos 17.66^\circ} = -1.86 \,\text{kW}$$
 (heat loss from the melt)

 ΔT with the values Z_c = 3.84 kW, $Z_{\rm FLT}$ = 1.56 kW and \dot{m} = 41.8 kg/h from the earlier example from Equation 5.50

$$\Delta T = \frac{3600 \cdot 3.54}{41.8 \cdot 2} = 152.4 \,^{\circ}\text{C}$$

Stock temperature at the outlet of the screw increment considered T_{out} :

$$T_{\rm out} = T_{\rm M} + 152.4 \,{\rm ^{\circ}C}$$

Melting point of the polymer $T_{\rm M} = 110$ °C

Hence,
$$T_{\text{out}} = 110 + 152.4 = 262.4$$
 °C

Average stock temperature \overline{T} :

$$\overline{T} = \frac{T_{\text{in}} + T_{\text{out}}}{2} = \frac{200 + 262.4}{2} = 231.2 \,^{\circ}\text{C}$$

As already mentioned, this result can only be an estimate because the effect of the change of temperature on the viscosity can be calculated only through an iterative procedure as shown in [9].

5.2.2.5 Melt Pressure

For a screw zone of constant depth the melt or stock pressure can generally be obtained from the pressure flow by means of Equation 5.29. However, the following empirical equation [10] has been found to give good results in practice:

$$|\Delta p| = \frac{F_1 \cdot 2 \cdot \eta_{\rm p} \cdot \Delta l}{\sin \phi \ (H_{\rm out} + \delta_{\rm FLT})} \cdot \left[\frac{|\dot{Q}_p| (2 \, \eta_{\rm R} + 1) \cdot (H_{\rm R} + H_{\rm R}^2) \cdot 10^9}{W \, (H_{\rm out} + \delta_{\rm f})^2 \cdot n_{\rm R} \cdot \nu} \right]^{n_{\rm R}} \cdot 10^{-5} \quad (5.51)$$

where

$$\eta_{\rm p} = \frac{\eta_{\alpha}}{\dot{\gamma}^{n_{\rm R}-1}} \tag{5.52}$$

The sign of Δp corresponds to that of the pressure flow \dot{Q}_{p} .

 $F_1 = 0.286$ $\eta_a = 1400 \text{ Pa} \cdot \text{s}$ $\dot{\gamma} = 84 \text{ s}^{-1}$

 $\Delta l = 600 \text{ mm}$

 $H_{\text{out}} = 3 \text{ mm}$

 $\delta_{\rm FLT} = 0.1 \, \rm mm$

= 0.5

 $\hat{W} = 51.46 \text{ mm}$

= 1

 $= 17.66^{\circ}$

 $\dot{Q}_{\rm p} = 1.249 \cdot 10.6 \,\mathrm{m}^3/\mathrm{s}$

 $H_{\rm R}$ = 1 (constant depth)

φ

Example with symbols and units

a) Screw zone of constant channel depth (metering zone)

Empirical factor

Melt viscosity in screw channel

Shear rate in channel

Length of screw zone (or of an increment)

Helix angle

Channel depth at the outlet of the zone or increment

Flight clearance

Pressure flow

Reciprocal of the power law exponent n

Ratio of channel depths at the outlet (H_{out})

and inlet (H_{in}) of the zone or increment H_{R}

Width of the channel

Thickness of the melt film

Number of flights

 $\eta_{\rm p}$ from Equation 5.52:

$$\eta_{\rm p} = \frac{1400}{84^{0.5-1}} = 12831$$

 Δp from Equation 5.51:

$$\Delta p = \left\{ \frac{0.286 \cdot 2 \cdot 600 \cdot 12831}{\sin 17.66^{\circ} (3+0.1)} \right\} \cdot \left[1.249 \cdot 10^{-6} (2 \cdot 0.5+1) \cdot \frac{(1+1) \cdot 10^{9}}{51.46 \cdot 3^{2} \cdot 0.5 \cdot 1} \right]^{0.5} \cdot 10^{-5}$$

$$= 218 \text{ bar}$$

b) Screw zone of varying depth (transition zone)

$$H_{\rm in} = 9 \text{ mm}$$
; $H_{\rm out} = 3 \text{ mm}$; $\Delta l = 240 \text{ mm}$; $\eta = 1800 \text{ Pa} \cdot \text{s}$; $\dot{\gamma} = 42 \text{ s}^{-1}$

 $\eta_{\rm p}$ from Equation 5.52:

$$\eta_{\rm p} = \frac{1800}{42^{0.5-1}} = 11665$$

 Δp from Equation 5.51:

$$\Delta p = \left\{ \frac{0.286 \cdot 2 \cdot 240 \cdot 11665}{\sin 17.66^{\circ} (3+0.1)} \right\} \cdot \left[1.249 \cdot 10^{-6} \cdot \left\{ \left(\frac{3}{9} \right) + \left(\frac{3}{9} \right)^{2} \right\} \cdot \frac{10^{9}}{51.46 \cdot 3^{2} \cdot 0.5} \right]^{0.5} \cdot 10^{-5}$$

$$= 37.2 \text{ bar}$$

A more exact calculation of the melt pressure profile in an extruder should consider the effect of the ratio of pressure flow to drag flow, the so called drossel quotient, as shown in [10].

5.2.3 Melting of Solids

Physical models describing the melting of solids in extruder channels were developed by many workers, notably the work of Tadmor [6]. Rauwendaal summarizes the theories underlying these models in his book [8]. Detailed computer programs for calculating melting profiles based on these models have been given by Rao in his books [3, 9].

The purpose of the following section is to illustrate the calculation of the main parameters of these models through numerical examples. The important steps for obtaining a melting profile are treated in another section for a quasi Newtonian fluid.

5.2.3.1 Thickness of Melt Film

According to the Tadmor model [6] the maximum, thickness of the melt film (Figure 5.23) is given by

$$\delta_{\text{max}} = \left(\frac{\left[2 \, \lambda_{\text{m}} (T_{\text{b}} - T_{\text{m}}) + \eta_{\text{f}} \, V_{\text{j}}^{2} \cdot 10^{-4}\right] \,\text{W}}{10^{3} \cdot V_{\text{bx}} \cdot \rho_{\text{m}} \left[c_{\text{ps}} \left(T_{\text{m}} - T_{\text{s}}\right) + i_{\text{m}}\right]}\right)^{0.5}$$
(5.53)

Example with symbols and units

Thermal conductivity of the melt Barrel temperature Melting point of the polymer Viscosity in the melt film Shear rate in the film Velocity of the barrel surface Velocity components Velocity of the solid bed Output of the extruder Average film thickness Temperature of the melt in the film Average film temperature Depth of the feed zone Width of the screw channel Melt density Density of the solid polymer Specific heat of the solid polymer Temperature of the solid polymer Heat of fusion of the polymer Maximum film thickness

 $= 150 \, {}^{\circ}\text{C}$ $= 110 \, {}^{\circ}\text{C}$ Pa · s $\eta_{\scriptscriptstyle \mathrm{f}}$ Ϋf cm/s $V_{\rm bx}$, $V_{\rm bz}$ cm/s (Figure 5.24) cm/s = 16.67 g/smm °C $^{\circ}C$ $= 9 \, \mathrm{mm}$ W $= 51.46 \, \text{mm}$ $= 0.7 \text{ g/cm}^3$ $\rho_{\rm m}$ $= 0.92 \text{ g/cm}^3$ $= 2.2 \text{ kJ/(kg} \cdot \text{K)}$ $= 20 \, ^{\circ}\text{C}$ =125.5 kJ/kgcm

= 0.174 W/(m K)

Indices:

m: melt s: solid

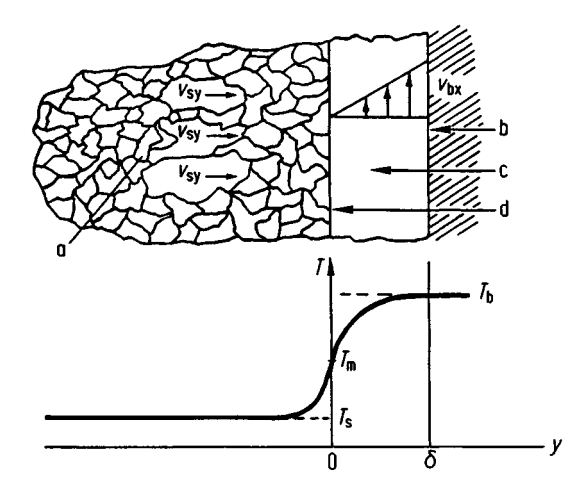


Figure 5.23 Temperature profile in the melt film after TADMOR [6] a: solid bed, b: barrel surface, c: melt film, d: solid melt interface

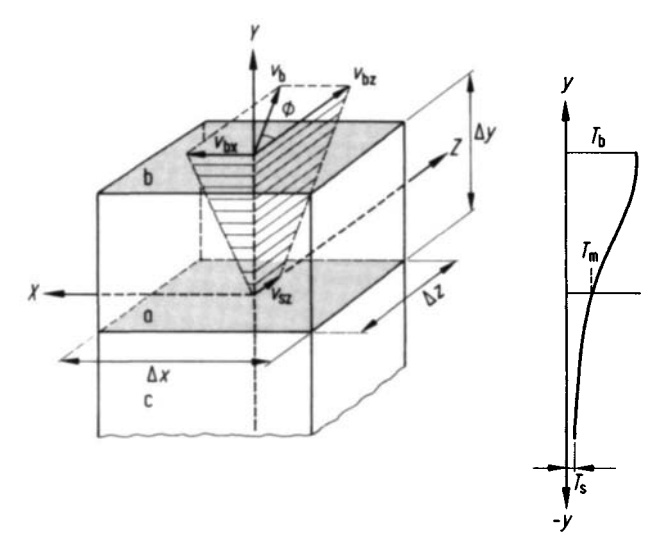


Figure 5.24 Velocity and temperature profiles in the melt and solid bed after TADMOR [6] a: solid melt interface, b: cylinder, c: solid bed

Following conditions are given:

The resin is LDPE with the same constants of viscosity as in Example 1 of Section 4.1.1.4. The barrel diameter $D_{\rm b}$ is 60 mm and the screw speed is 80 rpm.

$$V_{\rm b} = \frac{\pi \cdot D_{\rm b} \cdot N}{10 \cdot 60} = \frac{\pi \cdot 60 \cdot 80}{10 \cdot 60} = 25.13 \,\text{cm/s}$$

$$V_{\text{bx}} = V_{\text{b}} \sin \phi = 25.1 \cdot \sin 17.66^{\circ} = 7.62 \text{ cm/s}$$

$$V_{\text{bz}} = V_{\text{b}} \cos \phi = 25.1 \cdot \cos 17.66^{\circ} = 23.95 \text{ cm/s}$$

$$V_{\text{sz}} = \frac{10 \cdot G}{W \cdot H_1 \cdot \rho_s} = \frac{100 \cdot 16.67}{51.46 \cdot 9 \cdot 0.92} = 3.91 \text{ cm/s}$$

Relative velocity V_i (Figure 5.24):

$$V_{j} = (V_{b}^{2} + V_{sz}^{2} - 2 V_{b} \cdot V_{sz} \cdot \cos \phi)^{0.5}$$

$$= (25.13^{2} + 3.91^{2} - 2 \cdot 25.31 \cdot 3.91 \cdot \cos 17.66^{\circ})^{0.5}$$

$$= 21.44 \text{ cm/s}$$

Temperature \bar{T}_a :

$$\bar{T}_{a} = \frac{T_{b} + T_{m}}{2} = \frac{150 + 110}{2} = 130 \,^{\circ}\text{C}$$

$$\dot{\gamma}_{a} = \frac{V_{j}}{\mathcal{E}}$$

Starting from an assumed film thickness of 0.1 mm and using the temperature resulting when heat generation is neglected, the viscosity in the film is estimated first. By changing the film thickness and repeating this calculation, the final viscosity is obtained [3].

This iteration leads to

$$\dot{\gamma}_{\rm f} = \frac{V_{\rm j}}{\overline{\delta}} = \frac{2 \cdot 21.44 \cdot 10}{0.299} = 1434 \,\text{s}^{-1}$$
 $\eta_{\rm c} = 351.84 \,\text{Pa} \cdot \text{s}$

 $\delta_{
m max}$ from Equation 5.53

$$\delta_{\text{max}} = \left\{ \left[2 \cdot 0.174 (150 - 110) + 351.84 \cdot 21.44^{2} \cdot 10^{-4} \right] \cdot \frac{51.46}{10^{3} \cdot 7.62 \cdot 0.7 \left[2.2 (110 - 20) + 125.5 \right]} \right\}^{0.5}$$

$$= 0.0299 \text{ cm, or } 0.299 \text{ mm}$$

Temperature in Melt Film

Taking the viscous heat generation into account, the temperature in melt film can be obtained from [6]

$$\overline{T}_{f} = \overline{T}_{a} + \frac{10^{-4} \cdot \eta_{f} \cdot V_{j}^{2}}{12 \cdot \lambda_{m}}$$

$$\overline{T}_{f} - \overline{T}_{a} = \frac{10^{-4} \cdot 351.84 \cdot 21.44^{2}}{12 \cdot 0.174} = 7.75 \,^{\circ}\text{C}$$

$$\overline{T}_{f} = \left(\frac{150 + 110}{2}\right) + 7.75 = 137.5 \,^{\circ}\text{C}$$
(5.54)

As seen from the equations above, the desired quantities have to be calculated on an iterative basis. This is done by the computer program given in [3].

5.2.3.2 Melting Rate

The melting rate is described by TADMOR [6] by the parameter ϕ_p , which is expressed as

$$\phi_{p} = \left\{ \frac{V_{\text{bx}} \cdot \rho_{\text{m}} \cdot \left[\lambda_{\text{m}} \left(T_{\text{b}} - T_{\text{m}} \right) + 0.5 \, \eta_{\text{f}} \cdot V_{\text{j}}^{2} \cdot 10^{-4} \right]}{100 \cdot 2 \left[c_{\text{ps}} \left(T_{\text{m}} - T_{\text{s}} \right) + i_{\text{m}} \right]} \right\}^{0.5}$$
(5.55)

The numerator represents the heat supplied to the polymer by conduction through the barrel and dissipation, whereas the denominator shows the enthalpy required to melt the solid polymer. The melting rate increases with increasing $\phi_{\rm p}$.

By inserting the values given above into Equation 5.55 we obtain

$$\phi_{\rm p} = \left\{ \frac{7.62 \cdot 0.7 \left[0.174 \left(150 - 110 \right) + 0.5 \cdot 351.84 \cdot 21.44^2 \cdot 10^{-4} \right]}{100 \cdot 2 \left[2.2 \left(110 - 20 \right) + 125.5 \right]} \right\}^{0.5}$$

$$= 0.035 \frac{\rm g}{\rm cm}^{1.5} \, \rm s$$

5.2.3.3 Dimensionless Melting Parameter

The dimensionless melting parameter ψ is defined as [6]

$$\psi = \frac{\phi_{\rm p} \cdot H_1 \cdot W^{0.5}}{10^{1.5} \cdot G} \tag{5.56}$$

with

$$\phi_{\rm n} = 0.035 \text{ g/(cm}^{1.5} \cdot \text{s})$$
 $H_1 = 9 \text{ mm}$
 $W = 51.46 \text{ mm}$
 $G = 16.67 \text{ g/s}$

we get

$$\psi = 0.004$$

The dimensionless parameter is the ratio between the amount of melted polymer per unit down channel distance to the extruder output per unit channel feed depth.

5.2.3.4 Melting Profile

The melting profile provides the amount of unmelted polymer as a function of screw length (Figure 5.25) and is the basis for calculating the stock temperature and pressure. It thus shows whether the polymer at the end of the screw is fully melted. The plasticating and mixing capacity of a screw can be improved by mixing devices. Knowledge of the melting profile enables to find the suitable positioning of mixing and shearing devices in the screw [21].

The following equation applies to a screw zone of constant depth [6]

$$\frac{X_{\text{out}}}{W} = \frac{X_{\text{in}}}{W} \left(1 - \frac{\psi \cdot \Delta z}{2 \cdot H_1} \right)^2 \tag{5.57}$$

and for a tapered channel [6]

$$\frac{X_{\text{out}}}{W} = \frac{X_{\text{in}}}{W} \left[\frac{\psi}{A} - \left(\frac{\psi}{A} - 1 \right) \sqrt{\frac{H_{\text{in}}}{H_{\text{out}}}} \right]^2$$
 (5.58)

where

$$A = \frac{H_1 - H_2}{Z} \tag{5.59}$$

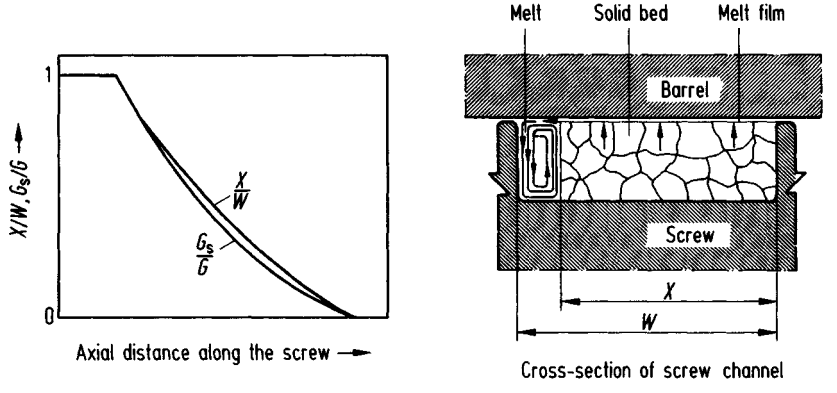


Figure 5.25 Solid bed or melting profiles X/W and G_s/G [21] G: total mass flow rate, G_s : mass flow rate of solids

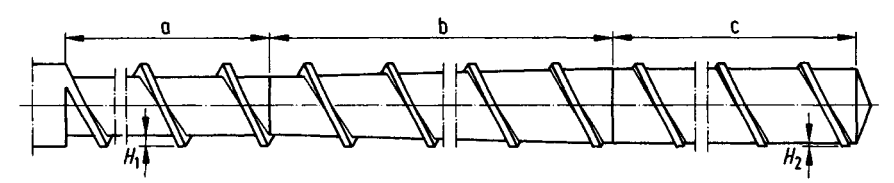


Figure 5.26 Three-zone screw [8]

The parameter ψ is obtained from Equation 5.56.

Symbols and units:

$X_{\rm out}$, $X_{\rm in}$	mm	Width of the solid bed at the outlet and inlet of a screw increment respectively
W	mm	Channel width
Ψ		Melting parameter
Δz	mm	Downchannel distance of the increment
$H_{\rm in}, H_{\rm out}$	mm	Channel depth at the inlet and outlet of an increment
H_1, H_2	mm	Channel depth of a parallel zone (feed zone) and depth
		at the end of a transition zone (Figure 5.26)
\boldsymbol{A}		Relative decrease of channel depth, Equation 5.59
Z	mm	Downchannel length of a screw zone

Example

a) Constant channel depth

For

 $H_1 = 9$ mm; $X_{\rm in}/W = 1$; $\Delta z = 99$ mm and $\psi = 0.004$ from Section 4.2.3.3, $X_{\rm out}/W$ can be calculated from Equation 5.57:

$$\frac{X_{\text{out}}}{W} = 1 \left(1 - \frac{0.004 \cdot 99}{2 \cdot 9} \right)^2 = 0.96$$

This means that at a distance of $\Delta z = 99$ mm, 4% of the solids were melted.

b) Varying channel depth

For the values

$$H_1 = 9 \text{ mm}$$
 $H_2 = 3 \text{ mm}$
 $Z = 1584 \text{ mm}$
 $X_{in}/W = 0.96$
 $H_{in} = 9 \text{ mm}$
 $H_{out} = 8.625$

 ψ can be obtained from Equation 5.56:

$$\psi = \frac{\phi_p \cdot H_1 \cdot W^{0.5}}{10^{1.5} \cdot \left(\frac{X_{\text{in}}}{W}\right) \cdot G} = \frac{0.035 \cdot 9 \cdot 51.46^{0.5}}{10^{1.5} \cdot 0.96 \cdot 16.67} = 0.00447$$

The relative decrease of the channel depth A is calculated from Equation 5.59:

$$A = \frac{H_1 - H_2}{Z} = \frac{9 - 3}{1584} = 0.00379$$

and X_{out}/W from Equation 5.58

$$\frac{X_{\text{out}}}{W} = 0.96 \left[\frac{0.0047}{0.00379} - \left(\frac{0.0047}{0.00379} - 1 \right) \sqrt{\frac{9}{8.625}} \right]^2$$

Assuming a constant velocity of the solid bed, the mass flow ratio G_s/G results from

$$\frac{G_{\rm s}}{G} = \frac{\overline{X}\,\overline{H}}{W\,H_1}\tag{5.60}$$

where

 $G_{\rm S}$ = mass flow rate of the solid polymer g/s

G = througput of the extruder g/s

 \overline{X} = average of X_{in} and X_{out} mm \overline{H} = average of H_{out} , and H_{in} mm

For a zone of constant depth it follows that

$$\frac{G_{\rm s}}{G} = \frac{\bar{X}}{W} \tag{5.61}$$

a) Constant depth

$$\frac{\overline{X}}{W} = 0.5 \left(\frac{X_{\text{in}}}{W} + \frac{X_{\text{out}}}{W} \right) = 0.5 \cdot 1.96 = 0.98$$

$$\frac{G_{\rm s}}{G}=0.98$$

b) Varying depth

$$\frac{\overline{X}}{W} = 0.5 \left(\frac{X_{\text{in}}}{W} + \frac{X_{\text{out}}}{W} \right) = 0.5 \cdot (0.96 \cdot 0.953) = 0.9565$$

$$\frac{\overline{H}}{H_1} = 0.5 \left(\frac{H_{\text{in}}}{H_1} + \frac{H_{\text{out}}}{H_1} \right) = 0.5 \cdot \left(\frac{9}{9} + \frac{8.625}{9} \right) = 0.9792$$

$$\frac{G_{\rm s}}{G} = \frac{\overline{X}\,\overline{H}}{W\,H_1} = 0.9366$$

The profiles of stock temperature and pressure can be calculated from the melting profile by using the width of the melt-filled part of the channel in the equations given in Section 5.2.2 [10].

5.2.4 Temperature Fluctuation of Melt

Temperature and pressure variations of the melt in an extruder serve as a measure for the quality of the extrudate and provide information as to the performance of the screw.

The temperature variation ΔT may be estimated from the following empirical relation, which was developed from the results of Squires' experiments [12] conducted with 3-zone screws:

$$\Delta T = \frac{5}{9} \left[\frac{1}{4.31 \, N_{\rm O}^2 - 0.024} \right] \tag{5.62}$$

This relation is valid for $0.11 < N_O < 0.5$.

The parameter $N_{\rm O}$ is given by

$$N_{\rm Q} = 14.7 \cdot 10^{-4} \, \frac{D_{\rm b}^2}{G} \sum_{H} \frac{L}{H} \tag{5.63}$$

where

 ΔT = temperature variation (°C)

 $D_{\rm b}$ = barrel diameter (cm)

G = extruder output (g/s)

L =length of screw zone in diameters

H = depth of the screw zone (cm)

Example

Following values are given:

$$D_b = 6 \text{ cm}$$

$$G = 15 \text{ g/s}$$

L	depth cm	L/H	
9	0.9	10	
3	0.6 (mean value)	3.33	
9	0.3	30	

Hence
$$\sum \frac{L}{H} = 43.33$$

 $N_{\rm O}$ from Equation 5.63:

$$N_{\rm Q} = 14.7 \cdot 10^{-4} \cdot \frac{36}{15} \cdot 43.33 = 0.153$$

 ΔT from Equation 5.62:

$$\Delta T = \frac{5}{9} \left[\frac{1}{4.31 \cdot 0.153^2 - 0.024} \right] = 7.22 \,^{\circ}\text{C or} \pm 3.61 \,^{\circ}\text{C}$$

The constants in the Equation 5.62 and Equation 5.63 depend on the type of polymer used. For screws other than 3-zone screws the geometry term in Equation 5.63 has to be defined in such a way that $N_{\rm O}$ correlates well with the measured temperature fluctuations.

5.2.5 Scale-up of Screw Extruders

Based on the laws of similarity, Pearson [13] developed a set of relationships to scale-up a single screw extruder. These relations are useful for the practicing engineer to estimate the size of a larger extruder from experimental data gathered on a smaller machine. The scale-up assumes equal length to diameter ratios between the two extruders. The important relations can be summarized as follows:

$$\frac{H_2}{H_1} = \left(\frac{D_2}{D_1}\right)^{(1-s)/(2-3s)} \tag{5.64}$$

$$\frac{N_2}{N_1} = \left(\frac{D_2}{D_1}\right)^{-(2-2s)/(2-3s)} \tag{5.65}$$

$$\frac{\dot{m}_2}{\dot{m}_1} = \left(\frac{D_2}{D_1}\right)^{(3-5\,s)/(2-3\,s)} \tag{5.66}$$

$$\frac{H_{\rm F_2}}{H_{\rm F_1}} = \left(\frac{D_2}{D_1}\right)^{(1-s)/(2-3s)} \tag{5.67}$$

where

 $H_{\rm F}$ = feed depth

H = metering depth

D =screw diameter

N =screw speed

Indices: 1 =screw of known geometry and 2 =screw to be determined.

The exponent s is given by

$$s = 0.5 (1 - n_{\rm R})$$

where n_R is the reciprocal of the power law exponent n. The shear rate required to determine n is obtained from

$$\dot{\gamma}_{\rm a} = \frac{\pi \cdot D_1 \cdot N_1}{60 \cdot H_1}$$

Example

Following conditions are given:

The resin is LDPE with the same constants of viscosity as in Example 1 of Section 5.1.1.4. The stock temperature is 200 °C. The data pertaining to screw 1 are:

 $D_1 = 90 \text{ mm}$; $H_F = 12 \text{ mm}$; $H_1 = 4 \text{ mm}$

feed length

 $= 9 D_1$

transition length = $2 D_1$

metering length = $9 D_1$

output \dot{m}_1

= 130 kg/h

screw speed $N_1 = 80 \text{ rpm}$

The diameter of screw 2 is $D_2 = 120$ mm. The geometry of screw 2 is to be determined.

Solution

The geometry is computed from the equations given above [3]. It follows that

 $D_2 = 120 \, \text{mm}$

 $H_{\rm E_1} = 14.41 \, \rm mm$

 $H_2^{-} = 4.8 \text{ mm}$

 $\dot{m}_2 = 192.5 \text{ kg/h}$

 $N_1 = 55.5 \, \text{rpm}$

Other methods of scaling up have been treated by Schenkel [29], Fenner [30], Fischer [31], and POTENTE [32].

Examples for calculating the dimensions of extrusion screws and dies are illustrated in the following figures:

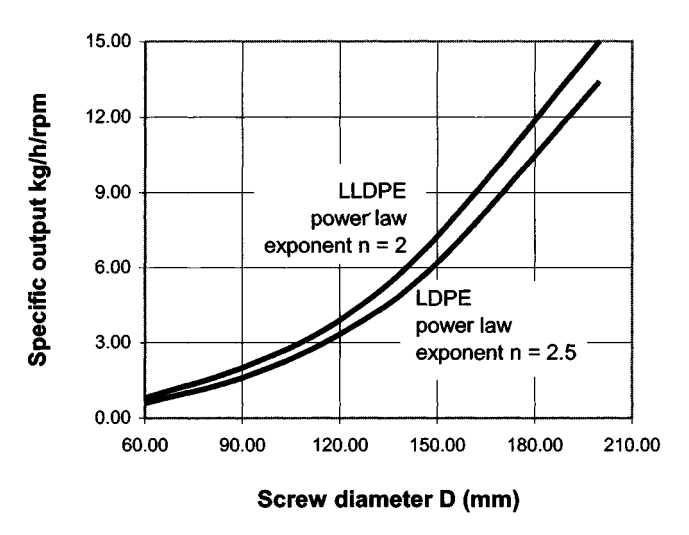


Figure 5.27 Specific output vs. screw diameter for LDPE and LLDPE (L/D = 20)

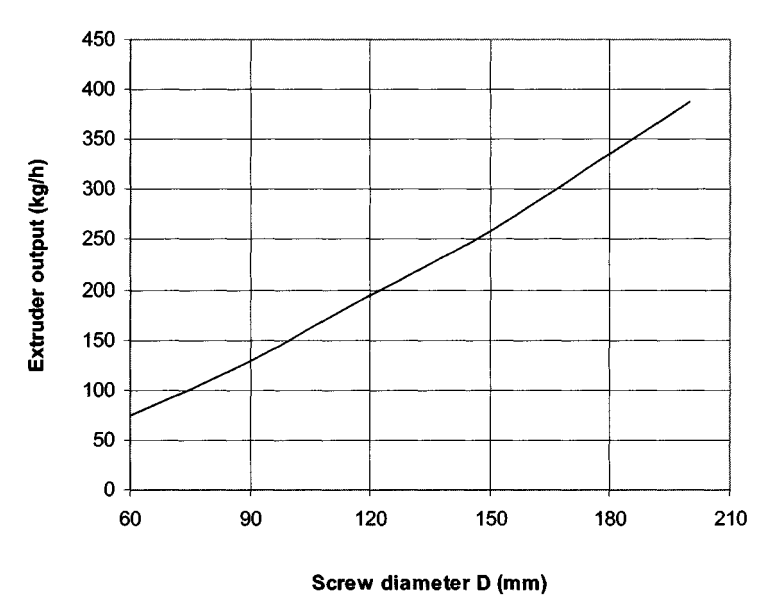


Figure 5.28 Extruder output vs. screw diameter for LDPE (L/D = 20)

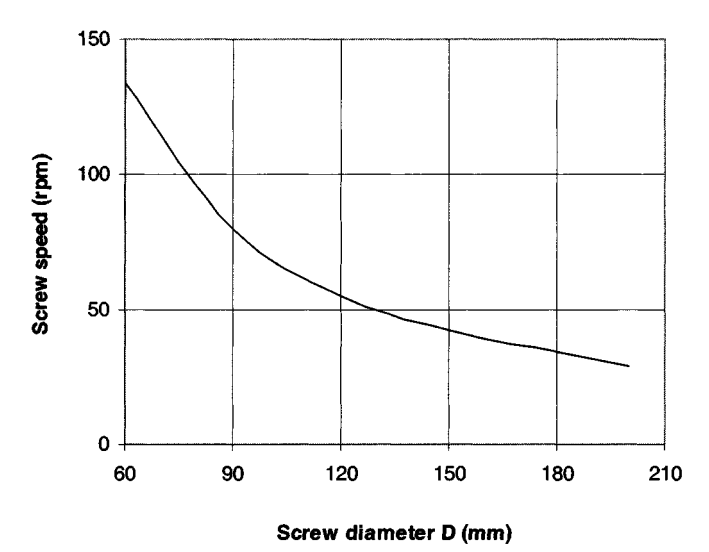


Figure 5.29 Screw speed vs. screw diameter for LDPE (L/D = 20)

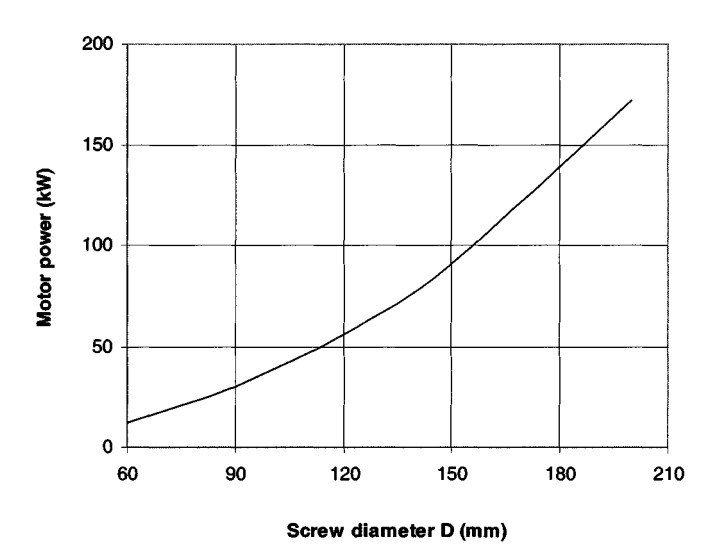


Figure 5.30 Motor power vs. screw diameter for LDPE (L/D = 20)

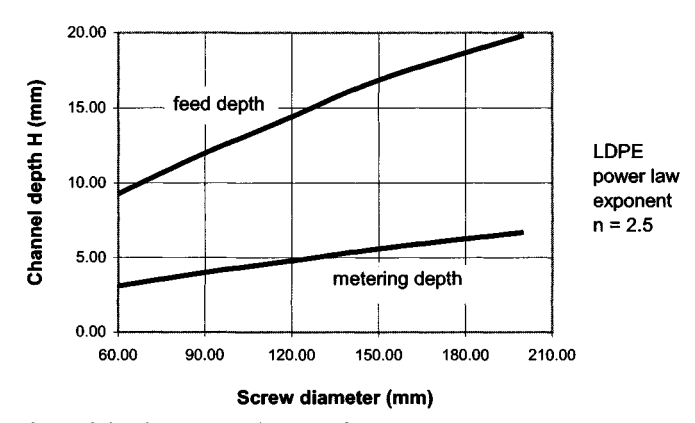


Figure 5.31 Channel depth vs. screw diameter for LDPE (L/D = 20)

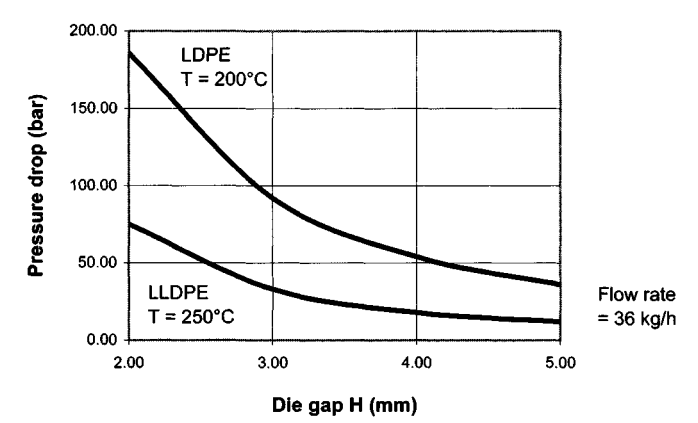


Figure 5.32 Pressure drop vs. die gap for a flat die

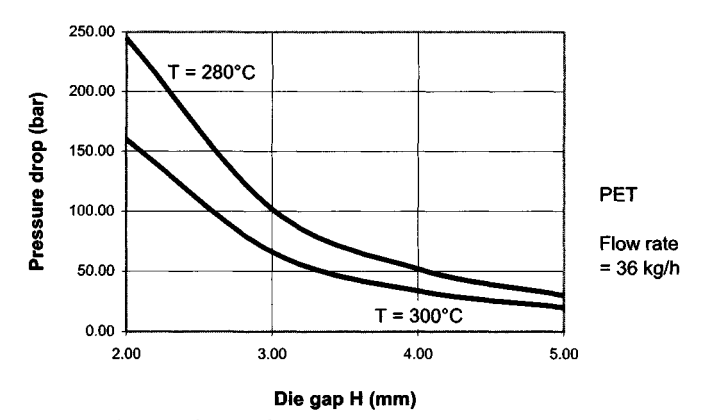


Figure 5.33 Pressure drop vs. die gap for PET

5.2.6 Mechanical Design of Extrusion Screws

5.2.6.1 Torsion

The maximum shear stress τ_{max} , which occurs at the circumference of the screw root as a result of the torque M_T , is given by [8]

$$\tau_{\text{max}} = \frac{2 \cdot M_T}{\pi \cdot R^3} \tag{5.68}$$

where R = root radius of the screw.

The maximum feed depth H_{max} can be computed from [8]

$$H_{\text{max}} = 0.5 \cdot D - \left(\frac{2 \cdot M_{\text{T}}}{\pi \cdot \tau_{\text{zul}}}\right)^{\frac{1}{3}}$$
 (5.69)

where

D = diameter

 τ_{zul} = allowable shear stress of the screw metal

Example [8]

The maximum feed depth is to be calculated for the following conditions:

$$D = 150 \text{ mm}; M_T = 17810 \text{ Nm}; \tau_{zul} = 100 \text{ MPa};$$

 H_{max} is found from Equation 5.69:

$$H_{\text{max}} = \frac{1}{2} \cdot \frac{150}{1000} - \left(\frac{2 \cdot 17810}{\pi \cdot 100 \cdot 10^6}\right)^{\frac{1}{3}}$$

= 0.075 - 0.0485 = 0.0265 m or 26.5 mm

5.2.6.2 Deflection

Lateral Deflection

The lateral deflection of the screw (Figure 5.34) caused by its own weight can be obtained from [8]

$$Y(L) = \frac{2 \cdot 1000 \cdot g \cdot \rho \cdot L^4}{F \cdot D^2}$$
 (5.70)

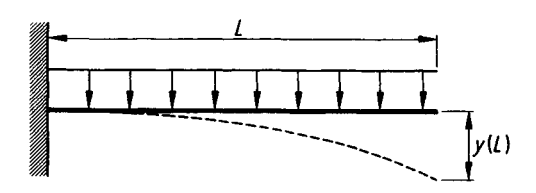


Figure 5.34 Lateral deflection of the screw as cantilever [8]

Numerical example with symbols and units [8]

 $= 9.81 \text{ m}^2/\text{s}$ acceleration due to gravity density of the screw length of the screw elastic modulus of the $\rho = 7850 \text{ kg/m}^3$ density of the screw metal L = 3 m

 $E = 210 \cdot 10^9 \, \text{Pa}$ elastic modulus of the screw metal

D = 0.15 m

Inserting these values into Equation 5.70 we get

$$Y(L) = \frac{2 \cdot 1000 \cdot 9.81 \cdot 7850 \cdot 3^4}{210 \cdot 10^9 \cdot 0.15^2} = 2.64 \text{ mm}$$

This value exceeds the usual flight clearance, so that the melt between the screw and the barrel takes on the role of supporting the screw to prevent contact between the screw and the barrel [8].

Buckling Cuased by Die Pressure

The critical die pressure, which can cause buckling, can be calculated from [8]

$$p_{K} = \frac{10^{-5} \cdot \pi^{2} \cdot E}{64 \cdot \left(\frac{L}{D}\right)^{2}}$$
 (5.71)

Numerical example [8]

 $= 210 \cdot 10^9 \, \text{Pa}$ elastic modulus of the screw metal L/D = 35length to diameter ratio of screw

 $p_{\rm K}$ from Equation 5.71:

$$p_{\rm K} = \frac{10^{-5} \cdot \pi^2 \cdot 210 \cdot 10^9}{64 \cdot 35^2} = 264.36 \, \text{bar}$$

As can be seen from Equation 5.71, the critical die pressure p_K decreases with increasing ratio L/D. This means, that for the usual range of die pressures (200-600 bar) buckling through die pressure is a possibility, if the ratio L/D exceeds 20 [8].

Screw Vibration

When the screw speed corresponds to the natural frequency of lateral vibration of the shaft, the resulting resonance leads to large amplitudes, which can cause screw deflection. The critical screw speed according to [8] is given by

$$N_{\rm K} = 0.88 \, \frac{D}{L^2} \left(\frac{E}{\rho} \right)^{\frac{1}{2}} \tag{5.72}$$

Substituting the values for steel, $E = 210 \cdot 10^9$ Pa and $\rho = 7850$ kg/m³ we get

$$N_{\rm K} = \frac{4549.5}{D \cdot \left(\frac{L}{D}\right)^2} \tag{5.73}$$

Numerical example

For D = 150 mm and $\frac{L}{D} = 30$, N_R is found from Equation 5.73

$$N_{\rm K} = \frac{4549.5}{0.15 \cdot 30^2} = 33.7 \text{ ups or } 2022 \text{ upm}$$

This result shows that at the normal range of screw speeds vibrations caused by resonance are unlikely.

Uneven Distribution of Pressure

Non-uniform pressure distribution around the circumference of the screw can lead to vertical and horizontal forces of such magnitude, that the screw deflects into the barrel. Even a pressure difference of 10 bar could create a horizontal force F_h in an extruder (diameter D=150 mm within a section of length L=150 mm)

$$F_{\rm h} = \Delta p \cdot D \cdot L = 10 \cdot 10^5 \cdot 0.15^2 = 22.5 \text{ kN}$$

According to RAUWENDAAL [8], the non uniform pressure distribution is the most probable cause of screw deflection.

5.3 Injection Molding

Other than extrusion, injection molding runs discontinuously and therefore the stages involved in this process are time-dependent [14]. The quantitative description of the important mold filling stage has been made possible by well known computer programs such as MOLDFLOW [15] and CADMOULD [16]. The purpose of this section is to present the basic formulas necessary for designing injection molding dies and screws on a rheological and thermal basis and illustrate the use of these formulas with examples.

Screw Vibration

When the screw speed corresponds to the natural frequency of lateral vibration of the shaft, the resulting resonance leads to large amplitudes, which can cause screw deflection. The critical screw speed according to [8] is given by

$$N_{\rm K} = 0.88 \frac{D}{L^2} \left(\frac{E}{\rho} \right)^{\frac{1}{2}} \tag{5.72}$$

Substituting the values for steel, $E = 210 \cdot 10^9$ Pa and $\rho = 7850$ kg/m³ we get

$$N_{\rm K} = \frac{4549.5}{D \cdot \left(\frac{L}{D}\right)^2} \tag{5.73}$$

Numerical example

For D = 150 mm and $\frac{L}{D} = 30$, $N_{\rm R}$ is found from Equation 5.73

$$N_{\rm K} = \frac{4549.5}{0.15 \cdot 30^2} = 33.7 \text{ ups or } 2022 \text{ upm}$$

This result shows that at the normal range of screw speeds vibrations caused by resonance are unlikely.

Uneven Distribution of Pressure

Non-uniform pressure distribution around the circumference of the screw can lead to vertical and horizontal forces of such magnitude, that the screw deflects into the barrel. Even a pressure difference of 10 bar could create a horizontal force F_h in an extruder (diameter D=150 mm within a section of length L=150 mm)

$$F_{\rm b} = \Delta p \cdot D \cdot L = 10 \cdot 10^5 \cdot 0.15^2 = 22.5 \text{ kN}$$

According to RAUWENDAAL [8], the non uniform pressure distribution is the most probable cause of screw deflection.

5.3 Injection Molding

Other than extrusion, injection molding runs discontinuously and therefore the stages involved in this process are time-dependent [14]. The quantitative description of the important mold filling stage has been made possible by well known computer programs such as MOLDFLOW [15] and CADMOULD [16]. The purpose of this section is to present the basic formulas necessary for designing injection molding dies and screws on a rheological and thermal basis and illustrate the use of these formulas with examples.

5.3.1 Pressure Drop in Runner

As the following example shows, the pressure drop along the runner of an injection mold can be calculated from the same relationships used for dimensioning extrusion dies.

Example

For the following conditions, the isothermal pressure drop Δp_0 and the adiabatic pressure drop Δp are to be determined:

For polystyrene with the following viscosity constants according to Equation 1.36, Section 1.3.7.3:

$$A_0 = 4.4475$$

 $A_1 = -0.4983$
 $A_2 = -0.1743$
 $A_3 = 0.03594$
 $A_4 = -0.002196$
 $c_1 = 4.285$
 $c_2 = 133.2$
 $T_0 = 190 \,^{\circ}$ C

flow rate $\dot{m} = 330.4 \text{ kg/h}$ melt density $\rho_{\text{m}} = 1.12 \text{ g/cm}^3$ specific heat $c_{\text{pm}} = 1.6 \text{ kJ/(kg} \cdot \text{K)}$ melt temperature T = 230 °Clength of the runner L = 101.6 mmradius of the runner R = 5.08 mm

Solution

a) Isothermal flow

 $\dot{\gamma}_a$ from Equation 1.19:

$$\dot{\gamma}_{a} = \frac{4 \dot{Q}}{\pi R^{3}} = \frac{4 \cdot 330.0}{3.6 \cdot \pi \cdot 1.12 \cdot 0.508^{3}} = 795.8 \text{ s}^{-1}$$

 $(\dot{Q} = \text{volume flow rate cm}^3/\text{s})$

 $a_{\rm T}$ from Equation 1.35:

$$a_{\rm T} = 10^{\frac{-c_1(T - T_0)}{c_2 + (T - T_0)}} = 10^{\frac{-4.285(230 - 190)}{133.2 + (230 - 190)}} = 10^{-0.9896} = 0.102$$

n from Equation 1.37:

$$n = 5.956$$

 η_a from Equation 1.36:

$$\eta_a = 132 \text{ Pa} \cdot \text{s}$$

 τ from Equation 1.22:

$$\tau = 105013.6 \text{ Pa}$$

K from Equation 1.26:

$$K = 9.911 \cdot 10^{-28}$$

Die constant G_{circle} from Equation 5.3:

$$G_{\text{circle}} = \left(\frac{\pi}{4}\right)^{\frac{1}{5.956}} \cdot \frac{(5.08 \cdot 10^{-3})^{\frac{1}{5.956} + 1}}{2 \cdot 0.1016} = 1.678 \cdot 10^{-3}$$

 Δp_0 with $\dot{Q} = 8.194 \cdot 10^{-5} \text{ m}^3/\text{s}$ from Equation 5.2:

$$\Delta p_0 = \frac{10^{-5} \cdot (8.194 \cdot 10^{-5})^{\frac{1}{5.956}}}{(9.911 \cdot 10^{-28})^{\frac{1}{5.956}} \cdot 1.678 \cdot 10^{-3}} = 42 \text{ bar}$$

b) Adiabatic flow

The relationship for the ratio $\frac{\Delta p}{\Delta p_0}$ is [17]

$$\frac{\Delta p}{\Delta p_0} = \frac{\ln \chi_L}{\chi_L - 1} \tag{5.74}$$

where

$$\chi_{L} = 1 + \frac{\beta \cdot \Delta p_{0}}{\rho_{m} \cdot c_{nm}} \tag{5.75}$$

Temperature rise from Equation 5.18:

$$\Delta T = \frac{\Delta p}{10 \cdot \rho_{\rm m} \cdot c_{\rm pm}} = \frac{42}{10 \cdot 1.12 \cdot 1.6} = 2.34 \text{ K}$$

For polystyrene

$$\beta = 0.026 \text{ K}^{-1}$$

$$\chi_{\rm L} = 2.34 \cdot 0.026 = 1.061$$

Finally, Δp from Equation 5.74:

$$\Delta p = \Delta p_0 \frac{\ln \chi_L}{\chi_L - 1} = \frac{42 \cdot \ln 1.061}{0.061} = 40.77 \text{ bar}$$

In the adiabatic case, the pressure drop is smaller because the dissipated heat is retained in the melt.

Examples of calculating pressure drop in runners of different geometry are shown in the following figures:

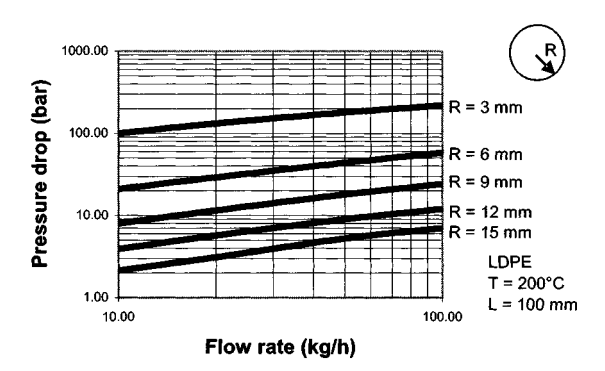


Figure 5.35 Pressure drop vs. flow rate for a circular cross-section for LDPE

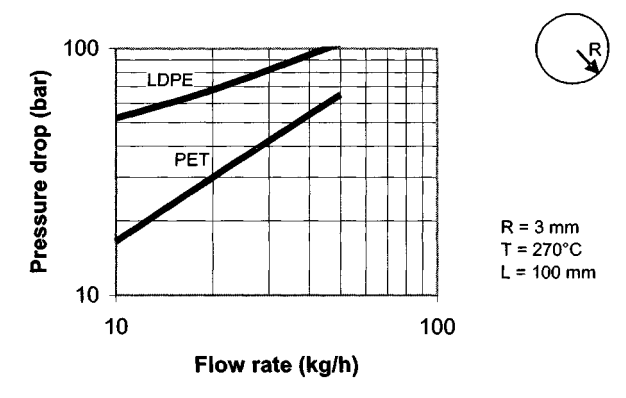


Figure 5.36 Effect of melt viscosity on pressure drop

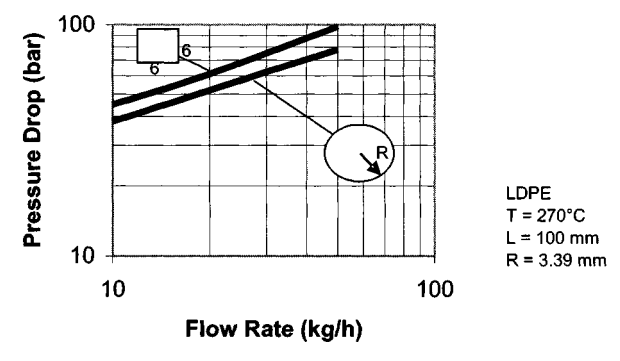


Figure 5.37 Effect of channel shape on pressure drop

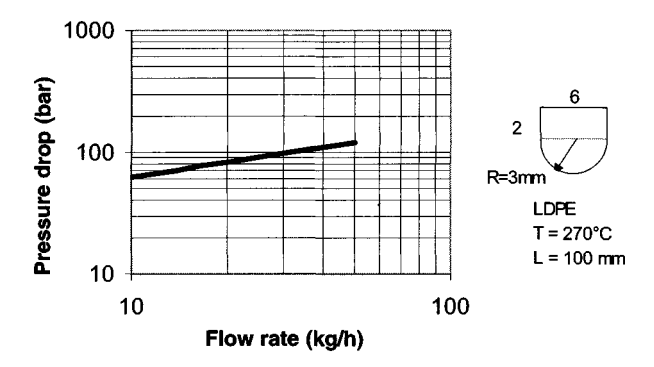


Figure 5.38 Pressure drop for a noncircular channel with $R_{\rm rh} = 2.77$ mm and n = 2.052

5.3.2 Mold Filling

As already mentioned, the mold filling process is treated extensively in commercial simulation programs [15, 16] and recently by Bangert [18]. In the following sections the more transparent method of STEVENSON [19] is given with an example.

5.3.2.1 Injection Pressure and Clamp Force

To determine the size of an injection molding machine for the production of a given part, knowledge of the clamp force exerted by the mold is important, because this force should not exceed the clamp force of the machine.

Injection Pressure

The isothermal pressure drop for a disc-shaped cavity is given as [19]

$$\Delta p_1 = \frac{K_r}{10^5 (1 - n_R)} \left[\frac{360 \cdot \dot{Q} \cdot (1 + 2 \cdot n_R)}{N \cdot \Theta \cdot 4 \pi \cdot n_R \cdot r_2 \cdot b^2} \right]^{n_R} \cdot \left(\frac{r_2}{b} \right)$$
 (5.76)

The fill time τ is defined as [19]

$$\tau = \frac{V \cdot a}{\dot{Q} \cdot b^2} \tag{5.77}$$

The Brinkman number is given by [19]

$$Br = \frac{b^2 \cdot K_r}{10^4 \cdot \lambda \cdot (T_M - T_W)} \cdot \left[\frac{\dot{Q} \cdot 360}{N \cdot \Theta \cdot 2 \,\pi \cdot b^2 \cdot r_2} \right]^{(1 + n_R)}$$
 (5.78)

Example with symbols and units

The material is ABS with $n_R = 0.2565$, which is the reciprocal of the power law exponent n. The constant K_r , which corresponds to the viscosity η_p in Equation 5.52 is $K_r = 3.05 \cdot 10^4$.

 $\dot{Q} = 160 \text{ cm}^3/\text{s}$ Constant injection rate $V = 160 \, \text{cm}^3$ Part volume $b = 2.1 \, \text{mm}$ Half thickness of the disc Radius of the disc $r_2 = 120 \text{ mm}$ N = 1Number of gates Inlet melt temperature $T_{\rm M} = 518 \; {\rm K}$ Mold temperature $T_{\rm W} = 323 {\rm K}$ $\lambda = 0.174 \, \text{W/(m} \cdot \text{K)}$ Thermal conductivity of the melt $a = 7.72 \cdot 10^{-4} \text{ cm}^2/\text{s}$ Thermal diffusivity of the polymer Melt flow angle [19]

The isothermal pressure drop in the mold Δp_1 is to be determined.

Solution

Applying Equation 5.76 for Δp_1

$$\Delta p_1 = \frac{3.05 \cdot 10^4}{10^5 (1 - 0.2655)} \left[\frac{360 \cdot 160 \cdot (1 + 2 \cdot 0.2655)}{1 \cdot 360 \cdot 4 \pi \cdot 12 \cdot 0.105^2} \right]^{0.2655} \cdot \left(\frac{12}{0.105} \right) = 254 \text{ bar}$$

Dimensionless fill time τ from Equation 5.77:

$$\tau = \frac{160 \cdot 7.72 \cdot 10^{-4}}{160 \cdot 0.105^2} = 0.07$$

Brinkman number from Equation 5.78:

Br =
$$\frac{0.105^2 \cdot 3.05 \cdot 10^4}{10^4 \cdot 0.174 \cdot 195} \cdot \left[\frac{160 \cdot 360}{1 \cdot 360 \cdot 2 \,\pi \cdot 0.105^2 \cdot 12} \right]^{1.2655} = 0.771$$

From the experimental results of STEVENSON [19], the following empirical relation was developed to calculate the actual pressure drop in the mold

$$\ln\left(\frac{\Delta p}{\Delta p_1}\right) = 0.337 + 4.7 \,\tau - 0.093 \,\mathrm{Br} - 2.6 \,\tau \cdot \mathrm{Br} \tag{5.79}$$

The actual pressure drop Δp is therefore from Equation 5.79:

$$\Delta p = 1.574 \cdot \Delta p_1 = 1.574 \cdot 254 = 400 \text{ bar}$$

Clamp Force

The calculation of clamp force is similar to that of the injection pressure. The isothermal clamp force is determined from [19]

$$F_1(r_2) = 10 \cdot \pi \, r_2^2 \left(\frac{1 - n_R}{3 - n_R} \right) \cdot \Delta p_1 \tag{5.80}$$

where $F_1(r_2)$ = isothermal clamp force (N).

 $F_1(r_2)$ for the example above is with Equation 5.80

$$F_1(r_2) = 10 \cdot \pi \, 12^2 \left(\frac{1 - 0.2655}{3 - 0.2655} \right) \cdot 254 = 308.64 \text{ kN}$$

The actual clamp force can be obtained from the following empirical relation, which was developed from the results published in [19].

$$\ln(F/F_1) = 0.372 + 7.6 \tau - 0.084 \text{ Br} - 3.538 \tau \text{ Br}$$
 (5.81)

Hence the actual clamp force F from Equation 5.81

$$F = 1.91 \cdot 308.64 = 589.5 \text{ kN}$$

The above relationships are valid for disc-shaped cavities. Other geometries of the mold cavity can be taken into account on this basis in the manner described by Stevenson [19].

5.3.3 Flowability of Injection Molding Resins

The flowability of injection molding materials can be determined on the basis of melt flow in a spiral channel. In practice, a spiral-shaped mold of rectangular crosssection with the height and width in the order of a few millimeters is often used to classify the resins according to their flowability. The length *L* of the solidified plastic in the spiral is taken as a measure of the viscosity of the polymer concerned.

Figure 5.39 shows the experimentally determined flow length L as a function of the height H of the spiral for polypropylene. A quantitative relation between L and the parameters influencing L such as type of resin, melt temperature, mold temperature, and injection pressure can be developed by using the dimensionless numbers as defined by Thorne [23] in the following manner:

The Reynolds number Re is given by [23]

$$Re = \frac{V_e^{2-n_R} \cdot \rho \cdot H^{*n_R}}{L^*}$$
 (5.82)

where

$$k^* = \eta_a \ \dot{\gamma}^{1-n_{\rm R}} \tag{5.83}$$

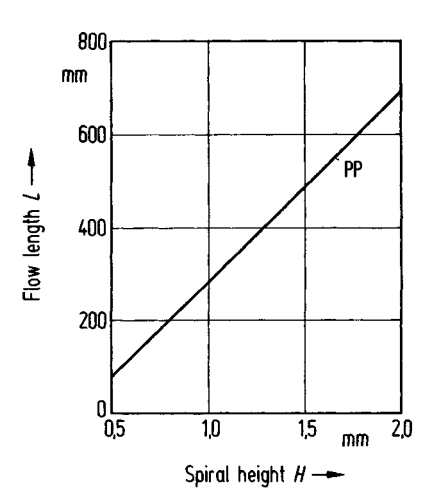


Figure 5.39 Flow length *L* as a function of the spiral height *H*

$$V_{e} = \frac{\dot{Q}}{W \cdot H}$$

$$\dot{Q} = \frac{\dot{G}}{\rho}$$

$$\dot{\gamma} = \frac{6 \cdot \dot{Q}}{W \cdot H^{2}}$$

$$H^{*} = 0.5 H$$

Prandtl number Pr [23]

$$Pr = \frac{k^* \cdot c_p \cdot H^{*(1-n_R)}}{\lambda \cdot V_a^{1-n_R}}$$
 (5.84)

and Brinkman number Br [23]

$$Br = \frac{k^* \cdot V_e^{1 + n_R} \cdot H^{*(1 - n_R)}}{\lambda \cdot (T_M - T_W)}$$
(5.85)

In addition, the Graetz number is defined by

$$Gz = \frac{G \cdot c_{p}}{\lambda \cdot L} \tag{5.86}$$

As shown in [20] and in Figure 5.40, the Graetz number correlates well with the product $Re \cdot Pr \cdot Br$

$$Gz = f(Re \cdot Pr \cdot Br)$$
 (5.87)

An explicit relationship for the spiral length L can therefore be computed from this correlation.

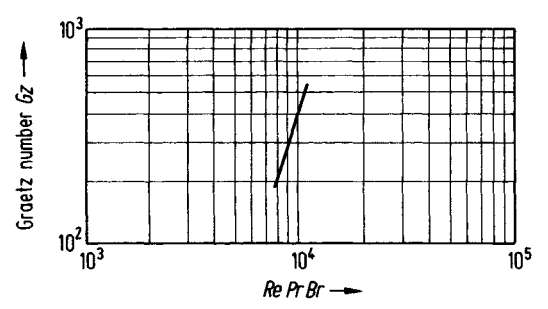


Figure 5.40 Dimensionless groups for determining the flowability of a resin [20]

Symbols and units:

Br Brinkman number

Specific heat kJ/(kg · K)

 $c_{\mathrm{p}} \ \dot{\gamma}$ Apparent shear rate s-1

Mass flow rate kg/h G

Gz Graetz number

Height of the spiral mm Η

Half height of the spiral mm Η̈́

 k^* Constant from Equation 5.83

L Length of the spiral mm

Reciprocal of the power law exponent $n_{\rm R}$

Prandtl number Pr

Ò Volume flow rate m³/s

Re Reynolds number

Melt temperature °C $T_{\mathbf{M}}$

Mold temperature °C T_{w}

Velocity of the melt front m/s $V_{\rm e}$

W Width of the spiral mm

λ Thermal conductivity $W/(m \cdot K)$

Melt density g/cm³ ρ

Melt viscosity Pa·s η_a

Example

This example illustrates the calculation of the dimensionless numbers Gz, Re, Pr and Br for:

$$W = 10 \text{ mm}; H = 2 \text{ mm}; L = 420 \text{ mm}; \rho = 1.06 \text{ g/cm}^3; c_p = 2 \text{ kJ/(kg} \cdot \text{K)}; \lambda = 1.5 \text{ W/(m} \cdot \text{K)}; T_M = 270 \text{ °C}; T_W = 70 \text{ °C}; G = 211.5 \text{ kg/h}$$

Resin-dependent constants according to Equation 1.36:

$$A_0 = 4.7649; A_1 = 0.4743; A_2 = 0.2338; A_3 = 0.081; A_4 = 0.01063;$$

 $c_1 = 4.45; c_2 = 146.3; T_0 = 190 \,^{\circ}\text{C}$

Solution

The conversion factors for the units used in the calculation of the dimensionless numbers below are

$$F_1 = 0.001; F_2 = 1000; F_3 = 3600$$

The Graetz number Gz is calculated from

$$Gz = \frac{F_2 \cdot G \cdot c_p}{F_1 \cdot F_3 \cdot \lambda \cdot L}$$

with G in kg/h and L in mm. Using the values given above, Gz = 186.51. The Reynolds number is obtained from

$$Re = \frac{F_2 \cdot V_e^{2-n_R} \cdot \rho \cdot H^{*n_R}}{L^*}$$

with V_e in m/s, H^{*} in m and ρ in g/cm³.

Using the values given above, Re = 0.03791.

With H^* in m and V_e in m/s we get from

$$\Pr = \frac{F_2 \cdot k^* \cdot c_p \cdot H^{*(1-n_R)}}{\lambda \cdot V_e^{1-n_R \delta}} = 103302.87$$

and the Brinkman number Br from

Br =
$$\frac{k^* \cdot V_e^{1+n_R} \cdot H^{*(1-n_R)}}{\lambda \cdot (T_M - T_W)} = 1.9833$$

Finally, the product Re \cdot Pr \cdot Br = 7768.06.

5.3.4 Cooling of Melt in Mold

As mentioned in Section 3.2.1, the numerical solution of the Fourier equation, Equation 3.31, is presented here for crystalline and amorphous polymers.

5.3.4.1 Crystalline Polymers

The enthalpy temperature diagram of a crystalline polymer shows that there is a sharp enthalpy rise in the temperature region where the polymer begins to melt. This is caused by the latent heat of fusion absorbed by the polymer when it is heated and has to be taken into account when calculating cooling curves of crystalline polymers.

By defining an equivalent temperature for the latent heat (Figure 5.41), GLOOR [22] calculated the temperature of a slab using the Fourier equation for the non-steady-state

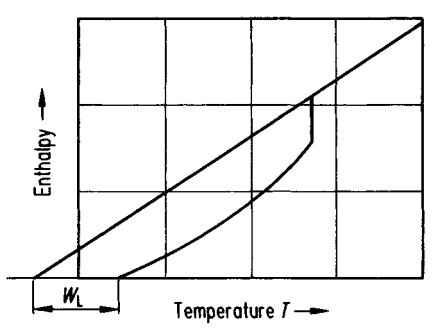


Figure 5.41 Representation of temperature correction for latent heat [22]

heat conduction. The numerical solution of Equation 3.31 using the correction introduced by Gloor [22] was given in [25] on the basis of the method of differences after Schmidt [24]. A computer program for this solution is presented in [3]. The time interval used in this method is

$$\Delta t = \frac{c_{\rm p} \cdot \rho}{\lambda} \cdot \frac{\Delta x^2}{M} \tag{5.88}$$

where

 $\Delta t = \text{time interval}$

 $\Delta x = \text{thickness of a layer}$

M = number of layers, into which the slab is devided, beginning from the mid plane of the slab (Figure 5.42)

The mold temperature and the thermodynamic properties of the polymer are assumed to be constant during the cooling process. The temperature at which the latent heat is evolved, and the temperature correction $W_{\rm L}$ (Figure 5.41) are obtained from the enthalpy diagram as suggested by Gloor [22]. An arbitrary difference of about 6 °C is assigned between the temperature of latent heat release at the mid plane and the temperature at the outer surface of the slab.

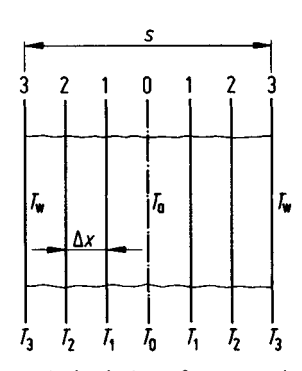


Figure 5.42 Nomenclature for numerical solution of non-steady state conduction in a slab [25]

Figure 5.43 shows a sample plot of temperature as a function of time for a crystalline polymer.

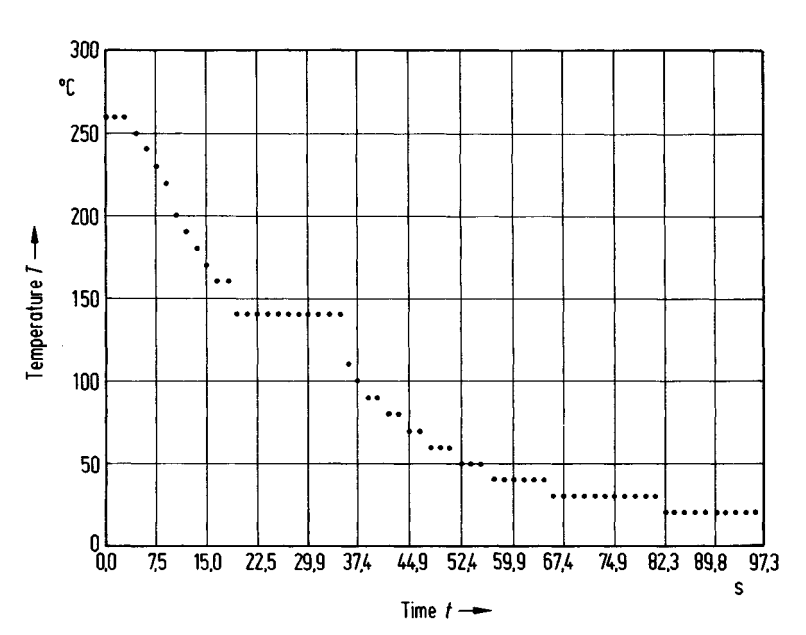


Figure 5.43 Plot of mid plane temperature vs. time for a crystalline polymer

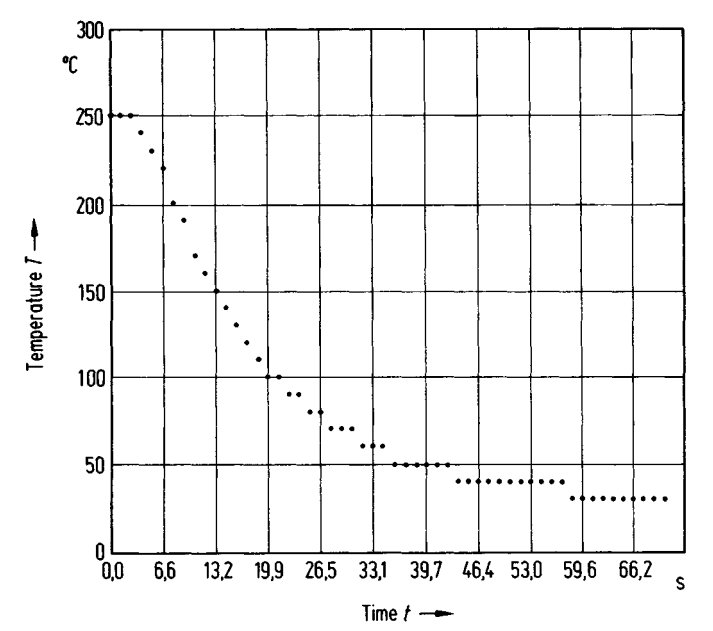


Figure 5.44 Plot of mid plane temperature vs. time for an amorphous polymer

5.3.4.2 Amorphous Polymers

Amorphous polymers do not exhibit the sharp enthalpy change as crystalline plastics when passing from liquid to solid. Consequently, when applying the numerical method of SCHMIDT [24], the correction for the latent heat can be left out in the calculation. A sample plot calculated with the computer program given in [3] is shown in Figure 5.44 for amorphous polymers.

It is to be mentioned here that the analytical solutions for non-steady heat conduction given in Section 3.2.1 serve as good approximations for crystalline as well as for amorphous polymers.

5.3.5 Design of Cooling Channels

5.3.5.1 Thermal Design

In practice, the temperature of the mold wall is not constant, because it is influenced by the heat transfer between the melt and the cooling water. Therefore, the geometry of the cooling channel lay out, the thermal conductivity of the mold material, and the velocity of the cooling water affect the cooling time significantly.

The heat transferred from the melt to the cooling medium can be expressed as (Figure 5.45)

$$Q_{ab} = 10^{-3} \cdot [(T_{M} - T_{E}) c_{ps} + i_{m}] \cdot \rho_{m} \cdot \frac{s}{2} \cdot x \text{ (kJ/m)}$$
 (5.89)

The heat received by the cooling water in the time t_K amounts to

$$Q_{\rm w} = 10^{-3} \cdot t_{\rm K} \left(\frac{1}{\lambda_{\rm st} S_{\rm e}} + \frac{1}{\alpha \cdot 10^{-3} \cdot 2 \cdot \pi \cdot R} \right)^{-1} \cdot (T_{\rm W} - T_{\rm water}) \text{ (kJ/m)}$$
 (5.90)

The cooling time $t_{\rm K}$ in this equation can be obtained from Equation 3.41. The influence of the cooling channel lay out on heat conduction can be taken into account by the shape factor $S_{\rm e}$ according to [23, 26].

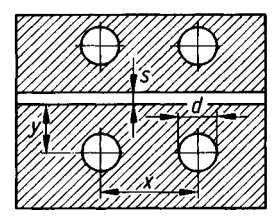


Figure 5.45 Geometry for the thermal design of cooling channels

$$S_{e} = \frac{2\pi}{\ln\left[\frac{2 \cdot X \cdot \sinh\left(\frac{2\pi y}{x}\right)}{\pi d}\right]}$$
(5.91)

With the values for the properties of water

$$c_p = 4.18 \text{ kJ/(kg} \cdot \text{K)}$$

 $\mu = 1.12 \cdot 10^{-3} \text{ Pa} \cdot \text{s}$
 $\lambda = 0.6 \text{ W/(m} \cdot \text{K)}$

the heat transfer coefficient a can be obtained from Equation 3.52

$$\alpha = \frac{0.031395}{d} \cdot \text{Re}^{0.8} \tag{5.92}$$

The mold temperature $T_{\rm w}$ in Equation 3.41 is calculated iteratively from the heat balance $\dot{Q}_{\rm ab} = \dot{Q}_{\rm w}$.

Example with symbols and units

Part thickness	S	= 2 mm
Distance	x	= 30 mm
Distance	y	= 10 mm
Diameter of cooling channel	d	= 10 mm
Melt temperature	$T_{\mathbf{M}}$	= 250 °C
Demolding temperature	$T_{\rm E}$	= 90 °C
Latent heat of fusion of the polymer	$i_{\rm m}$	= 130 kJ/kg
Specific heat of the polymer	$c_{\rm ps}$	$= 2.5 \text{ kJ/(kg} \cdot \text{K)}$
Melt density	$ ho_{ m m}^{ m r}$	$= 0.79 \text{ g/cm}^3$
Thermal diffusivity of the melt	a	$= 8.3 \cdot 10^{-4} \text{ cm}^2/\text{s}$
Kinematic viscosity of cooling water	ν	$= 1.2 \cdot 10^{-6} \text{ m}^2/\text{s}$
Velocity of cooling water	и	= 1 m/s
Temperature of cooling water	T_{wate}	_{er} = 15 °C
Thermal conductivity of mold steel	$\lambda_{\rm st}$	$= 45 \text{ W/(m} \cdot \text{K)}$

With the data above the heat removed from the melt Q_{ab} according to Equation 5.89 is

$$Q_{ab} = 10^{-3} [(250 - 90) \cdot 2.5 + 130] \cdot 0.79 \cdot \frac{2}{2} \cdot 30 = 12.56 \text{ kJ/m}$$

Shape factor S_e from Equation 5.91:

$$S_{e} = \frac{2 \pi}{\ln \left[\frac{2 \cdot 30 \sinh \left(\frac{2 \pi \cdot 10}{30} \right)}{\pi \cdot 10} \right]} = 3.091$$

Reynolds number of water:

Re =
$$10^{-3} \cdot u \cdot d/v = \frac{10^{-3} \cdot 1 \cdot 10}{1.2 \cdot 10^{-6}} = 8333$$

Using Equation 5.92 for the heat transfer coefficient α

$$\alpha_{\text{water}} = \frac{0.031395 \cdot \text{Re}^{0.8}}{10^{-3} \cdot 10} = 4300 \text{ W/(m}^2 \cdot \text{K)}$$

From Equation 5.90 we get for the heat received by the cooling water Q_w

$$Q_{\rm w} = 10^{-3} \cdot t_{\rm K} \left(\frac{1}{45 \cdot 3.091} + \frac{1}{4300 \cdot 10^{-3} \cdot 2 \,\pi \cdot 5} \right)^{-1} \cdot (T_{\rm w} - 15)$$

Cooling time t_K from Equation 3.41:

$$t_{\rm K} = \frac{(10^{-1} \cdot 2)^2}{\pi^2 \cdot 8.3 \cdot 10^{-4}} \cdot \ln \left[\frac{4}{\pi} \cdot \frac{(250 - T_{\rm w})}{(90 - T_{\rm w})} \right]$$

From the heat balance

$$Q_{ab} = Q_w = 12.56$$

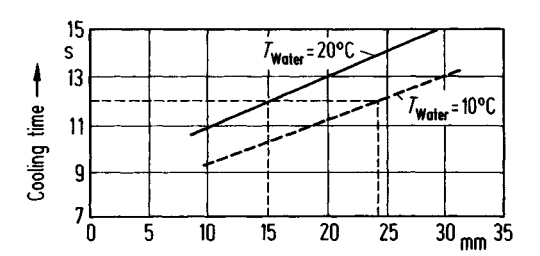
we obtain by iteration

$$T_{\rm w} = 37.83 \,{\rm ^{\circ}C}$$

Finally, the cooling time t_K with $T_w = 37.83$ is from Equation 3.41

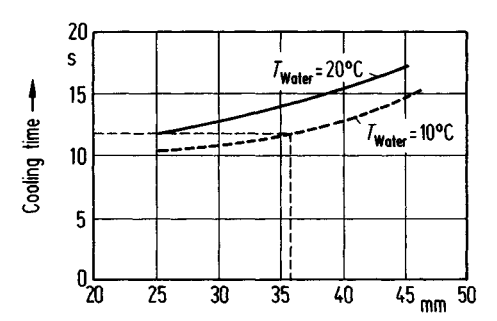
$$t_{\rm K} = 8.03 {\rm s}$$

The influence of the cooling channel lay out on cooling time can be simulated on the basis of the equations given by changing the distances x and y (Figure 5.45) as shown in Figure 5.46 and Figure 5.47. The effects of the temperature of cooling water and of its velocity are presented in Figure 5.48 and Figure 5.49, respectively. From these results it follows that the cooling time is significantly determined by the cooling channel lay out.



Distance between mold surface and cooling channel Y

Figure 5.46 Effect of cooling channel distance y on cooling time



Distance from channel to channel X --

Figure 5.47 Effect of cooling channel distance x on cooling time

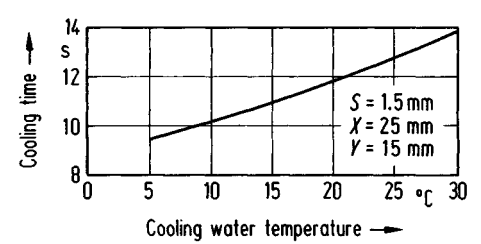


Figure 5.48 Influence of the temperature of cooling water on cooling time

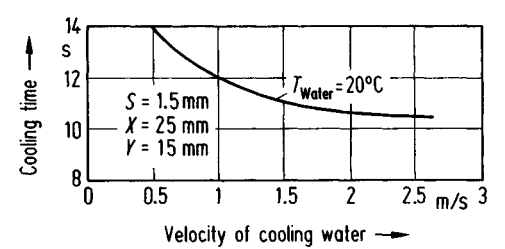


Figure 5.49 Influence of the velocity of cooling water on cooling time

5.3.5.2 Mechanical Design

The cooling channels should be as close to the surface of the mold as possible so that heat can flow out of the melt in the shortest time possible.

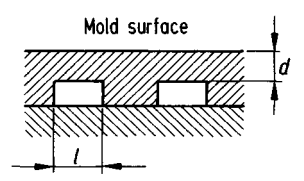


Figure 5.50 Geometry for the mechanical design of cooling channels

However, the strength of the mold material sets a limit to the distance between the cooling channel and the mold surface. Taking the strength of the mold material into account, the allowable distance d (Figure 5.50) was calculated by [27] on the basis of the following equations:

$$\sigma_{\mathbf{b}_{\text{max}}} = \frac{0.5 \cdot P \cdot l^2}{d^2} \tag{5.93}$$

$$\tau_{\text{max}} = \frac{0.75 \cdot P \cdot l}{d} \tag{5.94}$$

$$f_{\text{max}} = \frac{1000 \cdot P \cdot l^2}{d} \cdot \left(\frac{l^2}{32 \cdot E \cdot d^2} + \frac{0.15}{G} \right)$$
 (5.95)

where

 $p = \text{mold pressure N/mm}^2$

l, d = distances mm, see Figure 5.50

E = tensile modulus N/mm² G = shear modulus N/mm²

 $\sigma_{\rm b_{max}}$ = allowable tensile stress N/mm² $\tau_{\rm max}$ = allowable shear stress N/mm²

 f_{max} = max. deflection of the mold material above the cooling channel μ m

The minimization of the distance d such that the conditions

$$f \le f_{\max}$$

$$\sigma_{b} \le \sigma_{b_{\max}}$$

 $\tau \leq \tau_{\max}$

are satisfied, can be accomplished by the computer program given in [3]. The results of a sample calculation are shown Table 5.2.

		_		
Input			Output	
Mold pressure	P	= 4.9 N/mm ²	Channel distance	d = 2.492 mm
Maximum deflection	$f_{ m max}$	$= 2.5 \mu m$	Deflection	$f = 2.487 \mu \text{m}$
Modulus of elasticity	E	$= 70588 \text{ N/mm}^2$	Tensile stress	$\sigma = 39.44 \text{ N/mm}^2$
Modulus of shear	G	$= 27147 \text{ N/mm}^2$	Shear stress	$\tau = 14.75 \text{ N/mm}^2$
Allowable tensile stress	$\sigma_{ m b_{max}}$	$= 421.56 \text{ N/mm}^2$		
Allowable shear stress	$ au_{ ext{max}}^{- ext{max}}$	$= 294.1 \text{ N/mm}^2$		
Channel dimension	1	= 10 mm		

Table 5.2 Results of Optimization of Cooling Channel Distance in Figure 5.50

The equations given provide approximate values for circular channels as well. The distance from wall to wall of the channel should be approximately the channel length *l* or channel diameter, taking the strength of the mold material into account.

5.3.6 Melting in Injection Molding Screws

The plastication of solids in the reciprocating screw of an injection molding machine is a batch process and consists of two phases. During the stationary phase of the screw melting takes place mainly by heat conduction from the barrel. The melting during screw rotation time of the molding cycle is similar to that in an extrusion screw but instationary. With long periods of screw rotation, it approaches the steady state condition of extrusion melting.

5.3.6.1 Melting by Heat Conduction

According to Donovan [28], the equation describing conduction melting can be written as

$$K = \frac{-2 \cdot 10^{-6}}{i \cdot \rho_{\rm m}} \left\{ \frac{(T_{\rm m} - T_{\rm b}) \cdot \lambda_{\rm m} \cdot \exp(-K^2/4 \cdot \alpha_{\rm m})}{\sqrt{\pi \cdot a_{\rm m}} \cdot \operatorname{erf}(K/2\sqrt{a})} - \frac{(T_{\rm r} - T_{\rm m}) \cdot \lambda_{\rm s} \cdot \exp(-K^2/a_{\rm s})}{\sqrt{\pi \cdot a_{\rm s}} \cdot \operatorname{erf} c(K/2\sqrt{a})} \right\} (5.96)$$

where

 $T = \text{temperature } ^{\circ}\text{C}$

 λ = thermal conductivity W/(m·K)

 $K = \text{Parameter defined by } [28] \text{ m/s}^{0.5}$

 $a = \text{thermal diffusivity m}^2/\text{s}$

I = latent heat of fusion kJ/kg

 $\rho = \text{density g/cm}^3$

Indices:

r: middle of solid bed

s: solid m: melt b: barrel The parameter K can be determined iteratively by means of the computer program given in [9].

5.3.6.2 Melting during Screw Rotation

Analogous to the melting model of Tadmor (Section 4.2.3), Donovan [28] defines an area ratio A^*

$$A^* = \frac{A_{\rm s}}{A_{\rm T}}$$

to quantitatively describe the melting or solid bed profile of a reciprocating screw. A^* is the ratio of the cross-sectional area of solid bed A_s to the cross sectional area of screw channel A_T .

The equations according to Donovan [28] for calculating the solid bed profiles are as follows:

$$A_{f}^{*} - A_{i}^{*} = \frac{A_{f}^{*} \left[K \sqrt{t_{T} - t_{R} + \left(\frac{\delta_{i}^{2}}{K} \right)} - \delta_{i} \right]}{H}$$
 (5.97)

$$A_{\rm f}^* = A_{\rm e}^* - \left[\frac{A_{\rm f}^* - A_{\rm i}^*}{1 - \exp\left(\frac{-\beta \cdot 2 \,\pi \cdot N \cdot t_{\rm R}}{60}\right)} \right] \cdot \exp\left(-\frac{\beta \cdot 2 \,\pi \cdot N \cdot t_{\rm R}}{60}\right)$$
 (5.98)

$$A_{i}^{*} = A_{e}^{*} - \left[\frac{A_{f}^{*} - A_{i}^{*}}{1 - \exp\left(\frac{-\beta \cdot 2 \,\pi \cdot N \cdot t_{R}}{60}\right)} \right]$$
 (5.99)

where

 $t_{\rm T}$ = total cycle time s

 $t_{\rm R}$ = screw rotation time s

 $\hat{\delta_i}$ = thickness of melt film m

 \vec{H} = depth of the screw channel m

b = dimensionless parameter

N =screw speed rpm

Indices:

i: beginning of screw rotation

f: end of screw rotation

e: extrusion

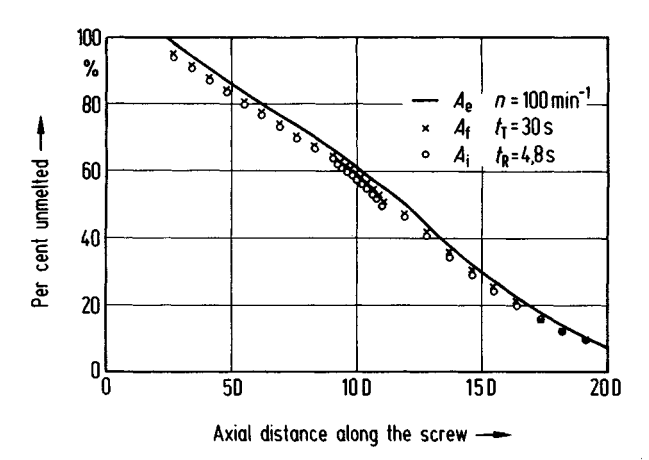


Figure 5.51 Solid bed profile of an injection molding screw

The thickness of the melt film δ_i and the solid bed profile for steady state extrusion A_e^* can be obtained from the relationships in the Tadmor model given in Section 4.2.3.

The area ratio at the start of screw rotation A_i^* and the value at the end of screw rotation A_f^* can then be obtained by using the computer program given in [9]. Figure 5.51 shows the solid bed profiles of a computer simulation [9] for a particular resin at given operating conditions.

Calculation procedure

Step 1: Calculate K using Equation 5.96.

Step 2: Calculate δ_{av} according to

$$\delta_{\text{av}} = 0.5 \left\{ \frac{\left[2 \, \lambda_{\text{m}} \, (T_{\text{b}} - T_{\text{m}}) + \eta_{\text{f}} \, v_{\text{j}}^2 \cdot 10^{-4}\right] W}{10^3 \, v_{\text{bx}} \, \rho_{\text{m}} \left[c_{\text{ps}} \, (T_{\text{m}} - T_{\text{s}}) + i_{\text{m}}\right]} \right\}^{0.5}$$

The average temperature in the melt film is obtained from

$$\overline{T}_{\rm f} = 0.5 \cdot (T_{\rm b} - T_{\rm m}) + \frac{10^{-4} \eta_{\rm f} \ v_{\rm j}^2}{12 \ \lambda_{\rm m}}$$

Substitute δ_i with δ_{av} .

Step 3: Calculate the solid bed ratio A_e^* for steady-state extrusion with the simplified model for a linear temperature profile.

Step 4: Find the solid bed ratio A_f^* at the end of the screw rotation using Equation 5.97 and Equation 5.98.

<u>Step 5:</u> Calculate A_i^* , the solid bed ratio at the start of screw rotation from Equation 5.99.

The following sample calculation shows the symbols and units of the variables occurring in the equations above.

Example

The thermal properties for LDPE and the barrel temperature are as given in the previous calculation for the parameter *K*. In addition,

Total cycle time	$t_{\rm T} = 45 \text{ s}$
Screw rotation time	$t_{\rm R}^{-} = 22 {\rm s}$
Empirical parameter for all polymers	$\hat{\boldsymbol{\beta}} = 0.005$
Screw speed	N = 56 rpm
Channel depth	H = 9.8 mm
Channel width	W = 52.61 mm
Cross-channel velocity of the melt	$v_{\rm bx} = 5.65 {\rm cm/s}$
Relative velocity of the melt	$v_i = 15.37 \text{ cm/s}$
Solids temperature	$T_{\rm s}' = 20 {\rm ^{o}C}$

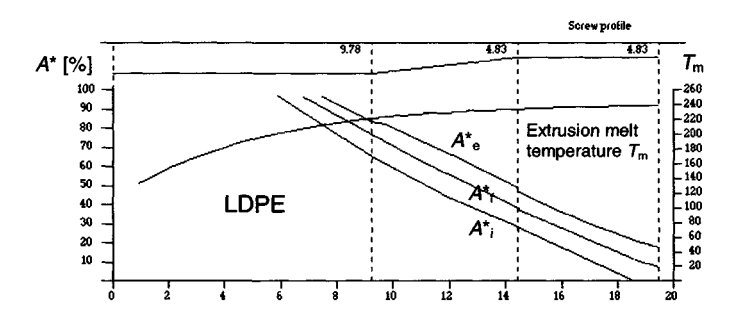
By using these values and by iteration, the following target values are obtained:

Melt viscosity in the film	$\eta_{\rm f} = 211 \mathrm{Pa} \cdot \mathrm{s}$
Average temperature of the melt in the film	$\bar{T}_{\rm f} = 172.8 {\rm ^{\circ}C}$
Average thickness of the melt film	$\delta_{av} = 7.678 \ 10^{-3} \ cm$

Using $K = 5.6 \cdot 10^{-4}$, the solid bed ratios are found to be: the solid bed ratio at the end of screw rotation, $A_{\rm f}^{\star} = 0.583$; the solid bed ratio at the start of screw rotation, $A_{\rm i}^{\star} = 0.429$. The solid bed ratio for steady-state extrusion, $A_{\rm e}^{\star}$, is calculated from the simplified melting model for extrusion. Its numerical value for the conditions above is $A_{\rm e}^{\star} = 0.75$.

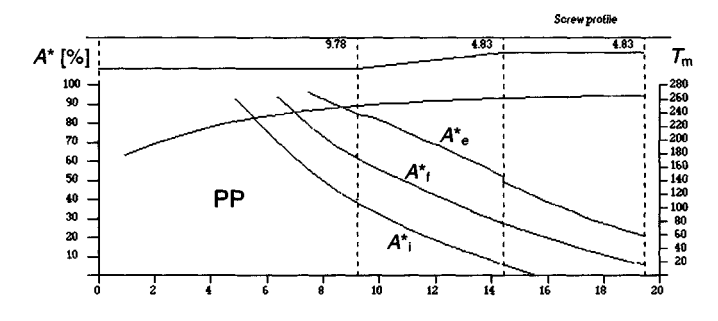
In the following figures the steady-state extrusion profile begins at the position of the stroke. The temperature of the melt refers to the temperature at the end of the screw for the case of steady-state extrusion. The solid bed ratio A^* is the ratio between the cross-sectional area of the solid bed A_s and the total cross-sectional area of the channel A_T . In Figure 5.52 the effect of the resin type on the solid bed profiles is presented. It appears that the conductivity parameter K and the melt viscosity affect these profiles significantly, even if the screw rotation and cycle times remain the same. It can be seen from Figure 5.53 that the barrel temperature has little effect on the plastication process in the screw.

As Figure 5.54 depicts, slow screw speed and a high percentage of screw rotation time compared to total cycle time favor melting strongly, which has also been found by Donovan [28]. The marked influence of screw geometry on melting becomes clear from Figure 5.55. As can be expected, melting is much faster in a shallower channel.



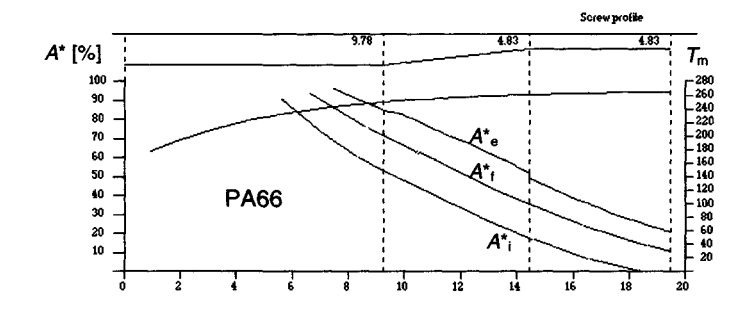
Axial length (screw diameters)

 $T_b = 232$ °C, $t_T = 45$ s, $t_R = 22$ s, G = 58.6 kg/h, N = 56 rpm



Axial length (screw diameters)

 $T_b = 260 \, ^{\circ}\text{C}$, $t_T = 45 \, \text{s}$, $t_R = 22 \, \text{s}$, $G = 48.5 \, \text{kg/h}$, $N = 56 \, \text{rpm}$



Axial length (screw diameters)

 $T_b = 300$ °C, $t_T = 45$ s, $t_R = 22$ s, G = 47.9 kg/h, N = 56 rpm

Figure 5.52 Effect of polymer on the melting profiles

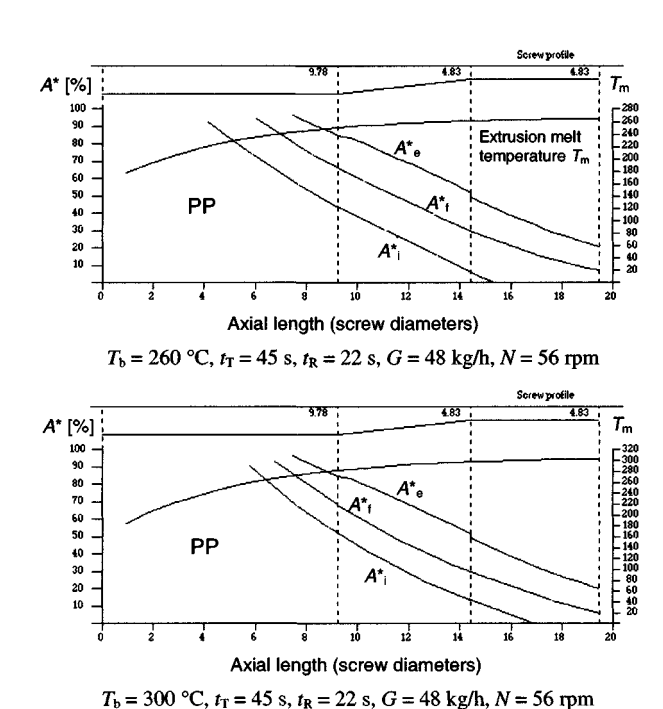


Figure 5.53 Effect of barrel temperature on the melting profile for PP

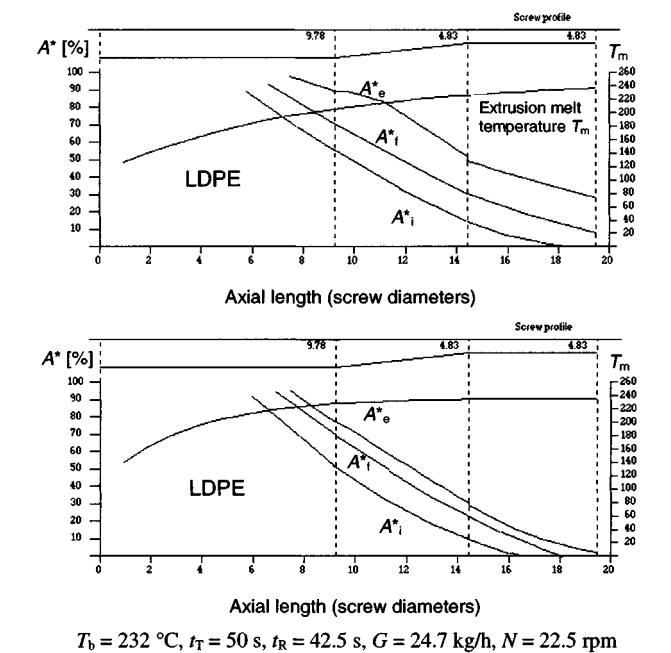


Figure 5.54 Effect of screw rotation time and screw speed on melting of LDPE

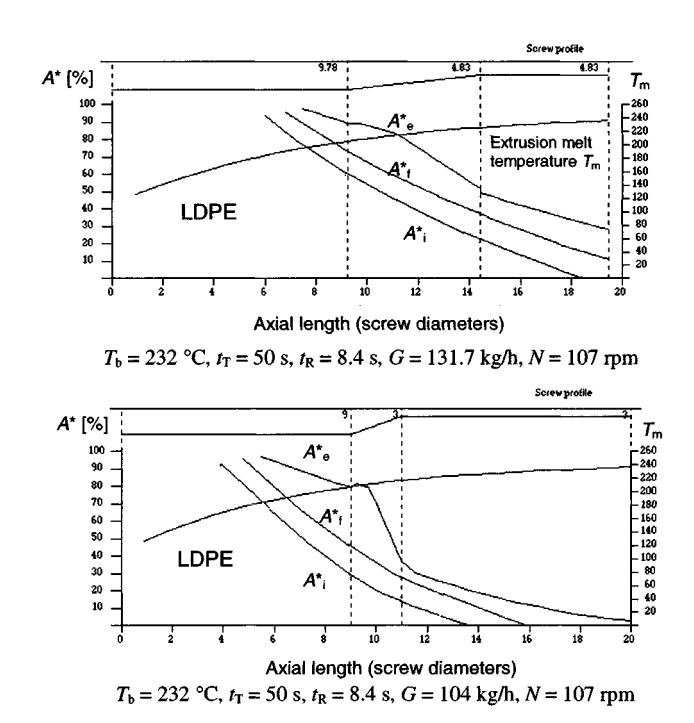


Figure 5.55 Effect of screw geometry on the melting for LDPE

5.3.7 Predicting Flow Length of Spiral Melt Flows

Injection molding is widely used to make articles out of plastics for various applications. One of the criteria for the selection of the resin to make a given part is whether the resin is an easy flowing type or whether it exhibits a significantly viscous behavior. To determine the flowability of the polymer melt, the spiral test, which consists of injecting the melt into a spiral shaped mold shown in Figure 5.56, is used. The length of the spiral serves as a measure of the ease of flow of the melt in the mold and enables mold and part design appropriate for a specific material flow behavior.

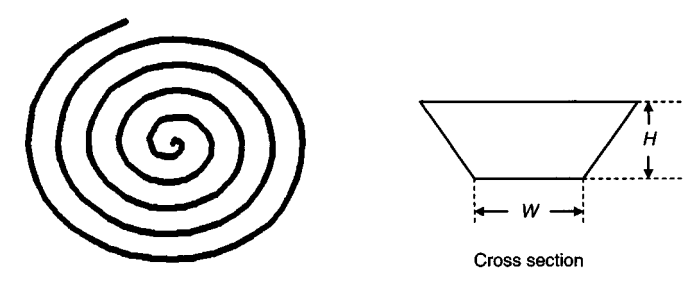


Figure 5.56 Schematic representation of spiral form

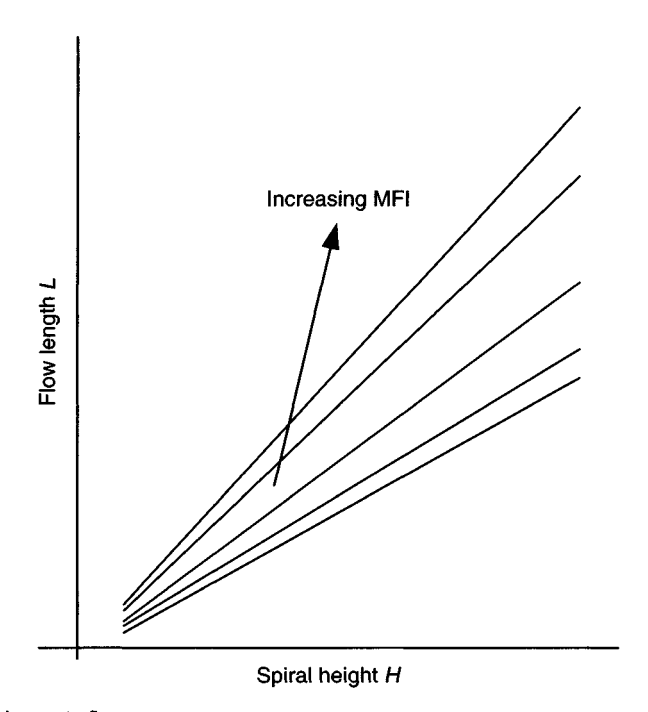


Figure 5.57 Schematic flow curves

The experimental flow curves obtained at constant injection pressure under given melt temperature, mold temperature, and axial screw speed are given schematically in Figure 5.57 for a resin type at various spiral heights with melt flow index of the polymer brand as parameter. By comparing the flow lengths with one another at any spiral height, also called wall thickness, the flowability of the resin in question with reference to another resin can be inferred.

The transient heat transfer and flow processes accompanying melt flow in an injection mold can be analyzed by state-of-the-art commercial software packages. However, for simple mold geometries, such as the one used in the spiral test, it is possible to predict the melt flow behavior on the basis of dimensionless numbers and obtain formulas useful in practice. These relationships can easily be calculated with a handheld calculator offering quick estimates of the target values. Owing to the nature of non-Newtonian flow, the dimensionless numbers used to describe flow and heat transfer processes of Newtonian fluids have to be modified for polymer melts. As already presented in Section 5.3.3, the movement of a melt front in a rectangular cavity can be correlated by Graetz number, Reynolds number, Prandtl number, and Brinkman number. Because the flow length in a spiral test depends significantly on the injection pressure (Figure 5.58), the Euler number [41] is included in the present work in order to take the effect of injection pressure on the flow length.

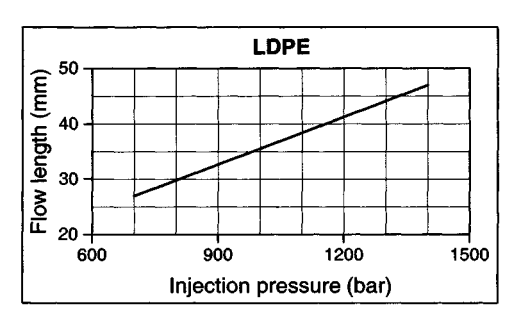


Figure 5.58 Effect of injection pressure on flow length

In addition to the dimensionless numbers Gz, Re, Pr, and Br, we consider [41] the Euler number

$$Eu = \frac{100 \cdot p_{\rm I}}{\rho \cdot V_{\rm e}^2} \tag{5.100}$$

where p_1 is the injection pressure.

Experimental flow curves for four different resins measured at constant injection pressure under different processing conditions and spiral wall thicknesses are given in Figure 5.59.

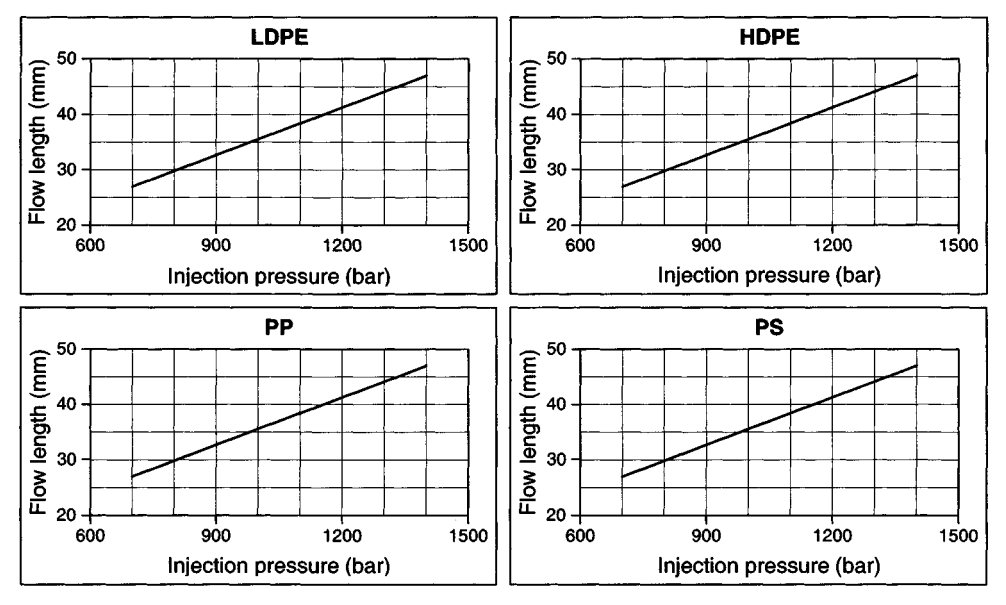


Figure 5.59 Experimental flow curves for LDPE, HDPE, PP, and PS

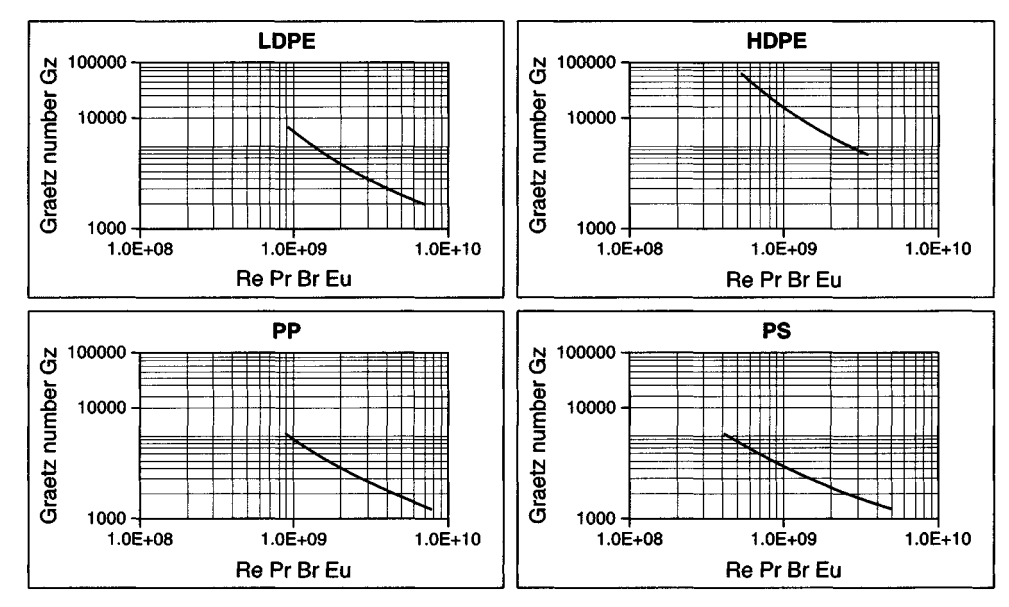


Figure 5.60 Graetz number as a function of the product of Re, Pr, Br, and Eu

The flow length as a function of injection pressure is shown in Figure 5.58 for LDPE as an example. The Graetz numbers calculated from the experimentally determined spiral lengths at different operating conditions and resins are plotted as functions of the product $Re \cdot Pr \cdot Br \cdot Eu$ as shown in Figure 5.60. As can be seen from this figure, the correlation of the Graetz number with this product is good and thus for any particular material the spiral length can be predicted from the relationship

$$Gz = f(Re \cdot Pr \cdot Br \cdot Eu) \tag{5.101}$$

Figure 5.61 shows the good agreement between measured and calculated spiral lengths for the experimentally investigated resins.

Sample Calculation

The example given below shows how the flow length of a given resin can be calculated from Equation 5.101: W=10 mm, H=2 mm, $\rho=1.06$ g/cm³, $c_{\rm p}=2$ kJ/kg · K, $\lambda=1.5$ W/K · m, $T_{\rm M}=270$ °C, $T_{\rm W}=70$ °C and G=211.5 kg/h.

The melt viscosity η_a is calculated from

$$\eta_{a} = \lg a_{T} + A_{0} + A_{1} \cdot \lg(a_{T} \cdot \dot{\gamma}) + A_{2} \cdot [\lg(a_{T} \cdot \dot{\gamma})]^{2}
+ A_{3} \cdot [\lg(a_{T} \cdot \dot{\gamma})]^{3} + A_{4} \cdot [\lg(a_{T} \cdot \dot{\gamma})]^{4}$$

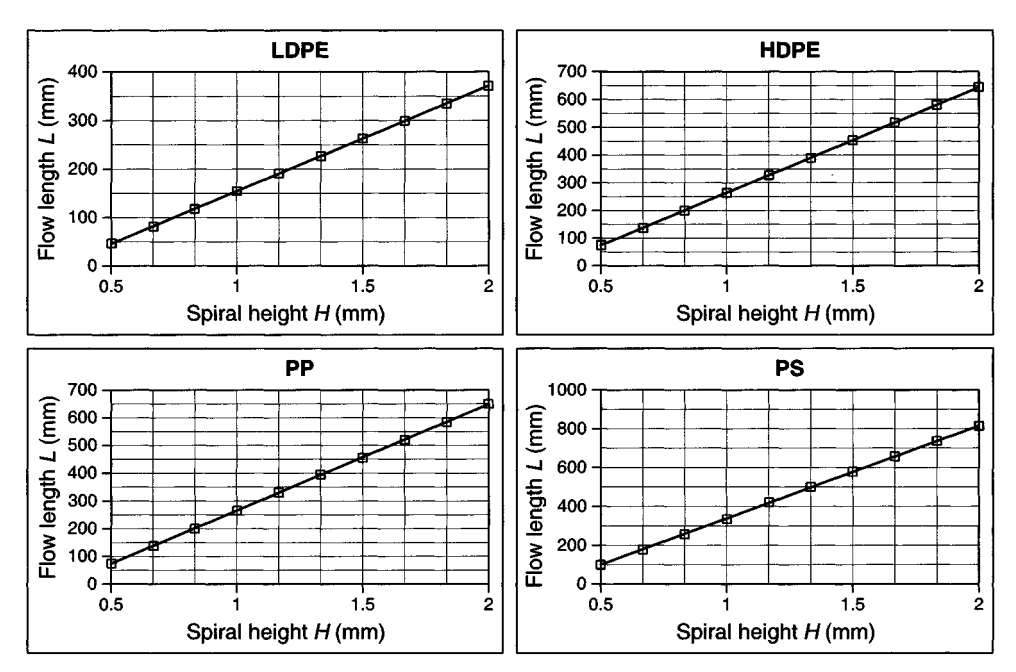


Figure 5.61 Comparison between measured and calculated flow length (—— calculated; — measured)

The shear rate $\dot{\gamma}$ is obtained from

$$\dot{\gamma} = \frac{6 \cdot Q}{W_{\text{mean}} \cdot H^2}$$

where $W_{\text{mean}} = W + H \cdot \tan \alpha$

 A_0 , A_1 , A_2 , A_3 , A_4 are material constants, and $a_{\rm T}$ the shift factor. For amorphous polymers the shift factor is obtained from

$$\lg a_{\rm T} = \frac{-c_1 \cdot (T - T_0)}{c_2 + (T - T_0)}$$

with constants c_1 , c_2 and melt and reference temperatures T and T_0 , respectively, in K. For semi-crystalline and crystalline polymers a_T is calculated from

$$a_{\rm T} = b_1 \cdot e^{b_2/T}$$

with the constants b_1 , b_2 and melt temperature T in K.

Using the values of $A_0 = 4.7649$, $A_1 = -0.4743$, $A_2 = -0.2338$, $A_3 = 0.081$, $A_4 = -0.01063$, $c_1 = 4.45$, $c_2 = 146.3$ and $T_0 = 190$ °C, the following output is obtained: Re = 0.05964, Pr = 76625.34, Br = 1.7419, and Eu = 10825.84. The Graetz number Gz for the product Re · Pr · Br · Eu follows from Figure 5.60: Gz = 217.63. Hence L = 420 mm.

References

- [1] RAO, N.: EDV Auslegung von Extrudierwerkzeugen, Kunststoffe 69 (1979) 3, p. 226
- [2] PROCTER, B.: SPE J. 28 (1972) p. 34
- [3] RAO, N.: Designing Machines and Dies for Polymer Processing with Computer Programs, Hanser Publishers, Munich (1981)
- [4] RAMSTEINER, F.: Kunststoffe 61 (1971) 12, p. 943
- [5] SCHENKEL, G.: Private Communication
- [6] Tadmor, Z., Klein, I.: Engineering Principles of Plasticating Extrusion, Van Nostrand Reinhold, New York (1970)
- [7] Bernhardt, E. C.: Processing of Thermoplastic Materials, Reinhold, New York (1963)
- [8] RAUWENDAAL, C.: Polymer Extrusion, Hanser Publishers, Munich (2001)
- [9] Rao, N.: Computer Aided Design of Plasticating Screws, Programs in Fortran and Basic, Hanser Publishers, Munich (1986)
- [10] Klein, L, Marshall, D. I.: Computer Programs for Plastics Engineers, Reinhold, New York (1968)
- [11] WOOD, S. D.: SPE 35, Antec (1977)
- [12] SQUIRES, P. H.: SPE J. 16 (1960), p. 267
- [13] Pearson, J. R. A.: Reports of University of Cambridge, Polymer Processing Research Centre (1969)
- [14] JOHANNABER, F.: Injection Molding Machines, Hanser Publishers, Munich (1994)
- [16] CADMOULD: Project Rechnergestützte Formteil- and Werkzeugauslegung, IKV, Aachen
- [17] McKelvey, J. M.: Polymer Processing, John Wiley, New York (1962)
- [18] Bangert, H.: Systematische Konstruktion von Spritzgießwerkzeugen unter Rechnereinsatz, Dissertation, RWTH Aachen (1981)
- [19] STEVENSON, J. F.: Polym. Eng. Sci. 18 (1978) p. 573
- [20] RAO, N.: Kunststoffe 73 (1983) 11, p. 696
- [21] RAO, N., HAGEN, K., KRÄMER, A.: Kunststoffe 69 (1979) 10, p. 173
- [22] GLOOR, W. E.: Heat Transfer Calculations, Technical Papers, Volume IX-I, p. 1
- [23] Throne, J. L.: Plastics Process Engineering, Marcel Dekker, New York (1979)
- [24] SCHMIDT, E.: Einführung in die Technische Thermodynamik, Springer, Berlin (1962) p. 353
- [25] Menges, G., Jurgens, W.: Plastverarbeiter 19 (1968) p. 201

- [26] VDI Wärmeatlas, VDI Verlag, Dusseldorf (1984)
- [27] LINDNER, E.: Berechenbarkeit von Spritzgießwerkzeugen, VDI Verlag, Düsseldorf (1974) p. 109
- [28] DONOVAN, R. C.: Polym. Eng. Sci. 11 (1971) p. 361
- [29] SCHENKEL, G.: Kunststoff-Extrudiertechnik. Hanser Publishers, Munich (1963)
- [30] FENNER, R. T.: Extruder Screw Design. ILiFFE Books, London (1970)
- [31] FISCHER, P.: Dissertation, RWTH Aachen (1976)
- [32] POTENTE, H.: Proceedings, 9. Kunststofftechnisches Kolloquium, IKV, Aachen (1978)
- [33] RAO, N. S.: Practical Computational Rheology Primer, Proc., TAPPI PLC (2000)
- [34] SAMMLER, R. L., KOOPMANS, R. J., MAGNUS, M. A. and BOSNYAK, C. P.: Proc. ANTEC 1998, p. 957 (1998)
- [35] ROSENBAUM, E. E. et al.: Proc., ANTEC 1998, p. 952 (1998)
- [36] BASF Brochure: Blow molding (1992)
- [37] Rao, N. S. and O'Brien, K.: Design Data for Plastics Engineers, Hanser Publishers, Munich (1998)
- [38] BASF Brochure: Kunststoff Physik im Gespräch (1977)
- [39] AGASSANT, J. F., AVENAS, P., SERGENT, J.Ph. and CARREAU, P. J.: Polymer Processing, Hanser Publishers, Munich (1991)
- [40] KAMAL, M. R., KERNIG, S.: Polym. Eng. Sci. 12 (1972)
- [41] Perry, R. H., Green, D.: Perry's Chemical Engineer's Handbook, Sixth Edition, p. 2–116 (1984)
- [42] CARLEY, J. F., SMITH W. C.: Polym. Eng. Sci. 18 (1978)
- [43] Brochure of BASF AG, 1992

A Final Word

The aim of this book is to present the basic formulas of rheology, thermodynamics, heat transfer, and strength of materials applicable to plastics engineering and to show how, starting from these formulas, models for designing polymer processing equipment can be developed.

Thoroughly worked out examples in metric units illustrate the use of these formulas, which have been successfully applied by well known machine manufacturers time and again in their design work. However, owing to the ever increasing growth of knowledge brought forth by research and development in the plastics field, a book of this kind needs to be renewed often and as such cannot claim to be an exhaustive work.

Biography

Natti S. Rao obtained his B.Tech(Hons) in Mechanical Engineering and M.Tech. in Chemical Engineering from the Indian Institute of Technology, Kharagpur, India. After receiving his Ph. D. in Chemical Engineering from the University of Karlsruhe, Germany, he worked for the BASF AG for a number of years. Later, he served as a technical advisor to the leading machine and resin manufacturers in various countries.

Natti has published over 60 papers and authored four books on designing polymer machinery with the help of computers. Prior to starting his consulting company in 1987, he worked as a visiting professor at the Indian Institute of Technology, Chennai, India. Besides consultating, he also holds seminars, teaching the application of his software for designing extrusion and injection molding machinery.

He is currently giving lectures in polymer engineering at the University of Texas, in Austin and at the University of Massachusetts in Lowell, USA. Natti is a member of SPE and TAPPI, and has been presenting papers at the annual conferences of these societies for the last 10 years.

Guenter Schumacher obtained his Ph. D. in Applied Mathematics from the University of Karlsruhe and worked as a lecturer there for a number of years. He contributed significantly to the improvement of the software for robotics and quality control. He is presently working at the innovation center of the European Commission in Brussels, Belgium.

Index

Index terms	<u>Li</u>	<u>nks</u>	<u>Index terms</u>	<u>Li</u>	<u>inks</u>
A					
Absorption	70		crystalline polymers	142	
1			in mold	142	
В			Cooling time	52	145
Bagley plot	6		Correction factor	111	
Biot number	54	55	Critical strain	77	
	57	60			
Brinkman number	60	140	D		
	142		Deborah number	60	
Buckling	132		Deflection	131	
			Desorption	69	70
C			Die geometry	81	
Clamp force	139		Die swell	31	
Conduction	43		Dielectric heating	67	
composite walls	46		Diffusion coefficient	69	
cylinder	44		Dimensionless numbers	60	
dissipation, with	59				
hollow sphere	45		\mathbf{E}		
plane wall	43		Engineering strain	1	
sphere	45		Enthalpy	38	
Contact temperature	57		Entrance loss	5	
Convection resistance	49		Extensional flow	31	
Cooling channel	145		Extrusion die	81	
mechanical design	149		Extrusion screws	105	
Cooling of melt	142				
amorphous polymers	145				

Index terms	Links	Index terms	<u>Li</u> ı	<u>nks</u>
F		Linear Viscoelastic		
Fick's Law	69	Behavior	19	25
Findley function	77	creep	26	
Flight diameter	112	tensile extensional flow	25	
Flow curves	6			
Flow length	156	M		
Flowability	139	Maxwell		
Fourier number	51 60	fluid	30	
		model	29	
G		Mechanical design of		
Glass transition		cooling channels	149	
temperature	41	Mechanical design of	4.4.4	
Graetz number	60 140	extrusion screws	131	
	142	Melt conveying	109	
Grashof number	60	Melt film	118	
		Melt pressure	116	
Н		Melt temperature	115	
Half-life	70	Melting		
Heat penetration	57	injection molding		
Heat transfer	43	screws	150	
Hencky strain	1	parameter	121	
Hookean solid	2	profile	122	
Hooke's Law	3	rate	121	
Hyperbolic Function	8	screw rotation	151	
71		Modulus of elasticity	3	
I		N T		
Ideal solid	1	N		
		Nahme number	60	
\mathbf{L}		Newtonian Fluids	3	
Lambert's law	65	Non-Newtonian fluids	4	
Lewis number	60			
			_	

This page has been reformatted by Knovel to provide easier navigation.

Index terms	<u>Li</u>	<u>nks</u>	Index terms	<u>Links</u>
Nonlinear Viscoelastic			Screw extruders	
Behavior	23	28	mechanical design	131
tensile compliance	28		scale-up	126
tensile extensional flow	28		Shear	19
tensile relaxation			compliance	23
modulus	28		time-dependent behavior	20
transient state	24		Shear flow	4
Nusselt number	60		steady	19
n.			Shear rate	5
P			apparent	5
Part failure	74		Shear Stress	6
Peclet number	60		Sherwood number	60
Permeability	69		Shift factor	12
Plastics parts	73		Solids	
Poisson ratio	2		conveying	105
Prandtl number	60	140	conveying efficiency	106
			Specific heat	36
R			Spiral melt flows	156
Radiation	64		Stefan-Boltzmann	
Recoverable shear strain	19		constant	64
Reference area	2		Stokes number	60
Relative velocity	120			
Retardation	20		T	
Reynolds number	60	142	Temperature fluctuation	125
Runner	134		Tensile creep compliance	26
			Tensile stress	1
S			Thermal conductivity	40
Scale-up of screw			Torsion	131
extruders	126		Trouton viscosity	4
Schmidt number	60			

Index terms	<u>Links</u>	Index terms	Links
\mathbf{V}		Muenstedt	11
Viscosity		power law	9
apparent	7	Viscosity, influence of	
true	8	mixture	18
Viscosity function		molecular weight	17
Carreau	14	pressure	16
Klein	16	shear rate	8